Supporting Information

Merging Platinahelicene and Nanographene: A Strategy for Circularly Polarized Phosphorescence in the Near-Infrared (NIR)

Wenying Cui,[a,b] Huimin Zhou,[b] Thierry Roisnel,[a] Nicolas Vanthuyne,[c] Chengshuo Shen,[b] Joachim Grzybowski,[d] J. A. Gareth Williams,[e] Monika Srebro-Hooper,[*d] Yohan Gisbert,[*a] Jeanne Crassous[*a]

a) Univ Rennes, CNRS, ISCR (Institut des Sciences Chimiques de Rennes) − UMR 6226, F-35000 Rennes, France.
b) School of Chemistry and Chemical Engineering, Zhejiang Sci-Tech University, Hangzhou 310018, China.
c) Aix Marseille Univ, CNRS, Centrale Med, FSCM, Marseille 13013, France.
d) Faculty of Chemistry, Jagiellonian University, Gronostajowa 2, 30-387 Krakow, Poland.
e) Department of Chemistry, University of Durham, Durham, DH1 3LE, United Kingdom.

Table of contents

1. Comparison of NG1 and reported chiral platinum complexes

Table S1. Comparison of the emission properties of **NG1** and other reported chiral platinum(II) complexes.

Structure	λ_{em} (nm)	$\lvert g_{lum} \rvert$	ϕ (%)	$\tau_{295\ K}$ (μs)	Ref
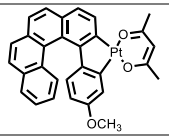	644	3.0×10^{-3}	10	21	1,2
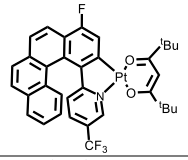	612	3.7×10^{-3}	27	15.7 (298 K)	3
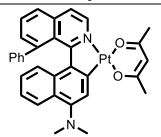	757	2.0×10^{-3}	< 1	2.1	4
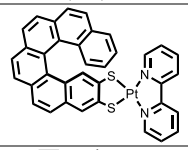	720	3.0×10^{-4}	0.15	0.124	5
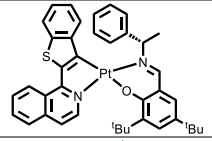	731	2.8×10^{-3}	14	0.85	6
NG1 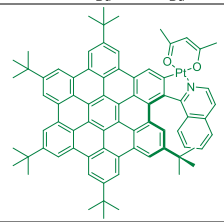	**751**	**4.0×10^{-3}**	**0.33**	**0.71**	**This work**

2. Supplementary experimental procedures

1.1. General Methods

Materials and methods. Experiments were performed using standard Schlenk techniques. Column chromatography purifications were performed in air over silica gel (Macherey Nagel 60 M, 0.04-0.063 mm). “Petroleum ether” stands for the 40-60 °C fraction of petroleum distillate, purchased from Fischer Scientific. All reactions were monitored by TLC analysis and visualizations were accomplished by irradiation with a UV light at 254 nm and 356 nm. Dry toluene and CH_2Cl_2 were obtained from an MB-SPS-800 and were degassed by argon bubbling. Other reagents or solvents were purchased from Sigma-Aldrich, Alfa Aesar, ABCR, Fluorochem, and BLDpharm, and were used as received unless otherwise noted. 4-*tert*-butylphenylacetylene[7] and 2,3,4,5-tetrakis(4-*tert*-butylphenyl)cyclopentadienone[8] were synthesized according to reported literature procedures and characterized using routine characterization techniques.

NMR spectroscopy. ^{1}H, $^{13}C\{^{1}H\}$ and ^{195}Pt NMR spectra were recorded at room temperature on Bruker Avance III 300, 400 and 500 MHz spectrometers equipped with a tunable BBFO probe. ^{11}B spectrum was acquired in a quartz NMR tube using a modified gradient echo sequence in order to suppress background signal from probe and tube. Gradients pulses were +1% and -1% sine shaped, 100ms long and were followed by a 100ms recovery delay, so the overall echo duration was 400ms. ^{1}H Waltz16 decoupling was applied during acquisition (0.17s) and relaxation delay was 0.5s. Chemical shifts δ are given in ppm, and coupling constants J in Hz. ^{1}H and ^{13}C NMR chemical shifts were determined using residual signals of the deuterated chloroform (^{1}H δ = 7.26 ppm, ^{13}C δ = 77.2 ppm). The terms s, d, t, m, dd indicate respectively singlet, doublet, triplet, multiplet, and doublet of doublets.

Chiral high-performance liquid chromatography (HPLC). The analytical and preparative separations of enantiomers were performed at Chiropole (Aix Marseille University), with Agilent Technologies 1260 Infinity units, on Chiralpak IE and Chiralpak IC (250 x 4.6 mm and 250 x 10 mm) columns.

High-resolution mass spectrometry (HR-MS). HRMS measurements were performed at the CRMPO, University of Rennes using electrospray ionization (ESI) or atmospheric solids analysis probe (ASAP).

UV-Vis spectroscopy and electronic circular dichroism (ECD). UV-Vis spectroscopy measurements were conducted on a Jasco-V630 spectrometer. Electronic circular dichroism (in $M^{-1}\cdot cm^{-1}$) was measured on a Jasco J-1700 Circular Dichroism Spectrometer.

Luminescence spectroscopy. Solution-state emission measurements were carried out in respective UV-grade solvent within quartz cuvettes of 1 cm path length. Spectra were recorded on a Jobin Yvon Fluoromax-2 spectrofluorimeter with an R928 PMT detector and corrected for the wavelength dependence of the monochromator and detector.

Circularly polarized luminescence (CPL). Circularly polarized luminescence measurements were performed using a home-built CPL spectrofluoropolarimeter (constructed with the help of the JASCO company). The samples were excited using a 90° geometry with a xenon ozone-free lamp (150 W LS).

1.2. Synthetic Procedures

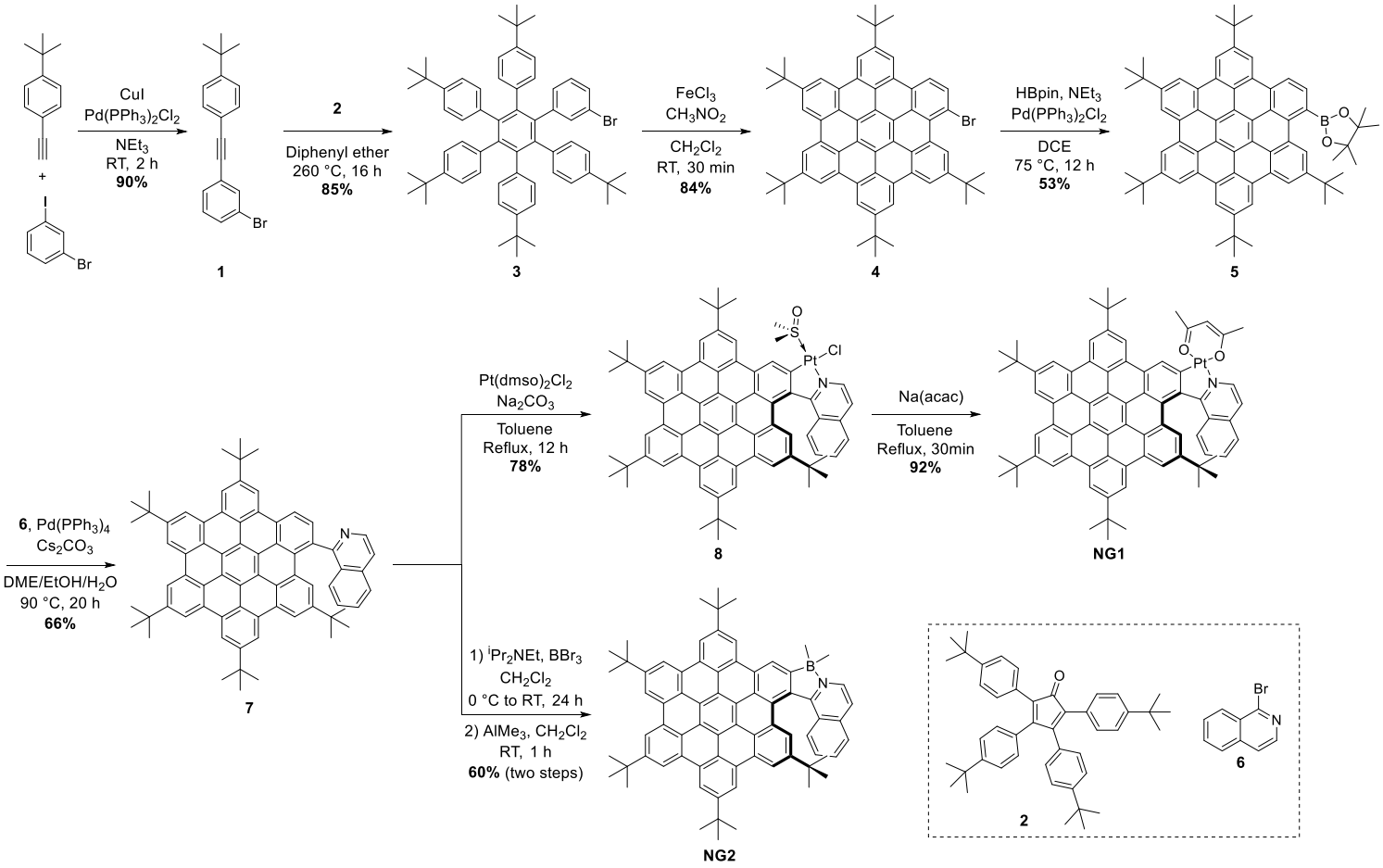

Figure S1. Overview of the synthetic pathway to nanographenes **NG1** and **NG2**. Reproduced from the main text for convenience.

1-Bromo-3-((4-(*tert*-butyl)phenyl)ethynyl)benzene (1)

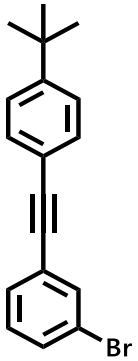

4-*Tert*-butylphenylacetylene[7] (158 mg, 1 mmol, 1 equiv.), 3-bromoiodobenzene (283 mg, 1 mmol, 1 equiv.), $Pd(PPh_3)_2Cl_2$ (35 mg, 50 µmol, 5 mol%), and CuI (19 mg, 0.1 mmol, 10 mol%) were suspended in 5 mL of degassed NEt_3 under an argon atmosphere. The mixture was stirred at 25 °C for 2 h. CH_2Cl_2 was added to the resulting solution, which was then washed twice with water, once with brine, and dried over $MgSO_4$. The solvent was removed in vacuum, and the residue was purified by column chromatography (SiO_2, petroleum ether) to obtain 1-bromo-3-((4-(*tert*-butyl)phenyl)ethynyl)benzene **1** as white solid in 90% yield (282 mg, 0.90 mmol).

^{1}H NMR (300 MHz, $CDCl_3$, 298 K): δ = 7.68 (m, 1H), 7.49-7.42 (m, 2H), 7.48 (AA'BB' pattern, ^3J = 8.6 Hz, 2H), 7.38 (AA'BB' pattern, ^3J = 8.6 Hz, 2H), 7.20 (t, ^3J = 7.9 Hz, 1H), 1.33 (s, 9H) ppm.

^{13}C{^{1}H} NMR (75 MHz, $CDCl_3$, 298 K): δ = 152.2, 134.4, 131.6, 131.3, 130.3, 129.9, 125.8, 125.6, 122.3, 119.9, 91.1, 87.3, 35.0, 31.3 ppm.

HRMS (ASAP$^+$) for $C_{18}H_{17}Br^+(M^+)$: *m/z* 312.0508 (found), 312.0508 (calculated).

Hexaarylbenzene 3

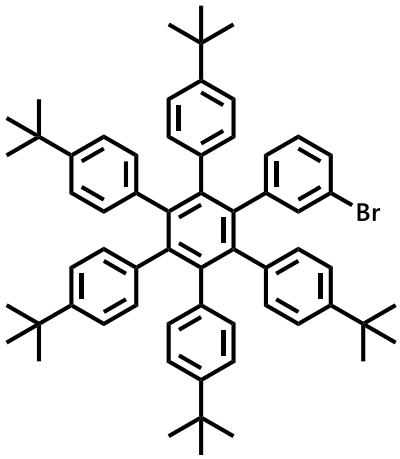

1-Bromo-2-((4-(*tert*-butyl)phenyl)ethynyl)benzene **1** (313 mg, 1 mmol, 1 equiv.) and 2,3,4,5-tetrakis(4-*tert*-butylphenyl)cyclopentadienone[8] (609 mg, 1 mmol, 1 equiv.) were mixed with 8 mL of molten diphenyl ether under an argon atmosphere. After stirring at 260 °C for 16 h, the resulting brown mixture was then cooled to room temperature and added to 50 mL of cold methanol, inducing precipitation. The precipitate was filtered out and washed with 15 mL of cold methanol, and dried *in vacuo* to yield hexaarylbenzene **3** as a beige solid in 85% yield (763 mg, 0.85 mmol).
^{1}H NMR (400 MHz, $CDCl_3$, 298 K): δ = 6.98-6.60 (m, 24H), 1.13 (s, 18H), 1.10 (s, 27H) ppm.
^{13}C{^{1}H} NMR (100 MHz, $CDCl_3$, 298 K): δ = 148.1, 147.7, 143.4, 141.2, 140.8, 140.3, 138.5, 137.9, 137.9, 137.6, 134.8, 131.4, 131.1, 131.2, 130.5, 128.0, 127.9, 123.6, 123.4, 123.2, 120.7, 34.3, 34.2, 31.3 ppm.
HRMS (ASAP^{+}) for $C_{62}H_{69}Br^{+}$ (M^{+}): *m/z* 892.4577 (found), 892.4577 (calculated).

Brominated hexabenzocoronene 4

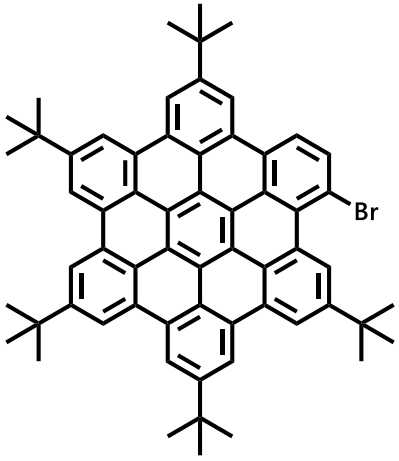

Hexaarylbenzene **3** (89 mg, 0.1 mmol, 1 equiv.) was dissolved in 100 mL of anhydrous CH_2Cl_2. The solution was stirred at room temperature for 10 min while degassing by argon bubbling. Then, a solution of $FeCl_3$ (373 mg, 23 mmol, 23 equiv.) in CH_3NO_2 (1.2 mL) was added via a syringe, and the resulting solution was stirred for a further 30 min under argon bubbling. The mixture was then quenched by addition of 20 mL of CH_3OH and was extracted with CH_2Cl_2. The organic layer was washed twice with water, once with brine, and dried over $MgSO_4$. The solvent was removed in vacuum, and the residue was purified by column chromatography (SiO_2, CH_2Cl_2) to yield pure brominated hexabenzocoronene **4** as a yellow solid in 84% yield (74 mg, 0.084 mmol).

^{1}H NMR (400 MHz, $CDCl_3$, 298 K): δ = 10.06 (d, ^4J = 1.7 Hz, 1H), 9.33-9.25 (m, 8H), 9.17-9.15 (m, 1H), 8.92 (d, ^3J = 8.8 Hz, 1H), 8.42 (d, ^3J = 8.8 Hz, 1H), 1.84 (s, 18H), 1.83 (s, 9H), 1.79 (s, 18H) ppm.

^{13}C{^{1}H} NMR (100 MHz, $CDCl_3$, 298 K): δ = 149.4, 149.3, 149.2, 147.3, 134.0, 130.7, 130.6, 130.5, 130.5, 130.3, 130.2, 130.3, 129.8, 129.7, 129.6, 129.4, 128.7, 128.7, 125.5, 124.7, 123.9, 123.8, 123.5 123.3, 122.5, 121.1, 120.6, 120.0, 119.8, 119.7, 119.2, 119.1, 119.0, 118.9, 118.9, 118.7, 118.5, 35.8, 35.8, 35.7, 35.7, 32.0, 32.0, 31.9 ppm.

HRMS (ASAP$^+$) for $C_{62}H_{57}Br^+$ (M^+): *m/z* 880.3635 (found), 880.3638 (calculated).

Bpin-hexabenzocoronene 5

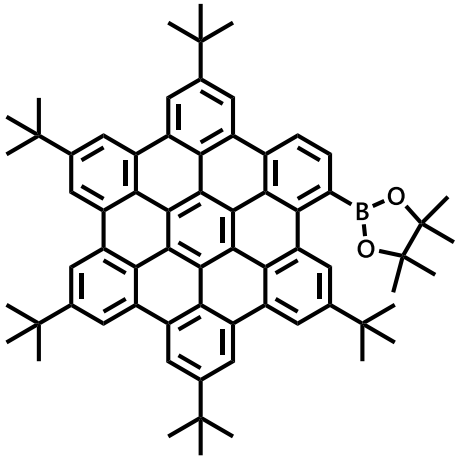

Brominated hexabenzocoronene **4** (882 mg, 1 mmol, 1 equiv.) and $Pd(PPh_3)_2Cl_2$ (70 mg, 0.1 mmol, 10 mol%) were suspended in 70 mL of anhydrous 1,2-dichloroethane under argon. The mixture was stirred for 10 min before 1.8 mL of NEt_3 was added dropwise to the suspension. After stirring for a further 5 min, pinacolborane was added dropwise. The mixture was then stirred for 16 hours at 75 °C. After cooling to room temperature and quenching with water, the mixture was extracted with CH_2Cl_2. The organic layer was washed twice with water, once with brine, and dried over $MgSO_4$. The solvent was removed in vacuum, and the residue was purified by column chromatography (SiO_2, petroleum ether / CH_2Cl_2 3:1) to afford Bpin-hexabenzocoronene **5** as a yellow solid in 53% yield (492 mg, 0.53 mmol).

^{1}H NMR (400 MHz, $CDCl_3$, 298 K): δ = 9.37-9.20 (m, 10H), 8.90 (d, ^4J = 1.6 Hz, 1H), 8.60 (d, ^3J = 8.0 Hz, 1H), 1.84 (s, 18H), 1.83 (s, 9H), 1.82 (s, 9H), 1.80 (s, 9H), 1.51 (s, 12H) ppm.

^{13}C{^{1}H} NMR (100 MHz, $CDCl_3$, 298 K): δ = 149.3, 149.3, 149.2, 148.3, 136.8, 133.8, 132.2, 131.5, 130.8, 130.8, 130.7, 130.6, 130.6, 130.5, 130.2, 130.0, 126.5, 125.6, 124.5, 124.3, 124.2, 124.0, 121.0, 120.9, 120.8, 120.8, 120.7, 120.6, 120.5, 120.2, 119.7, 119.4, 119.3, 119.1, 119.1, 119.1, 118.8, 35.9, 35.9, 35.9, 35.9, 32.3, 32.2, 25.4 ppm.

HRMS (ASAP$^+$) for $C_{68}H_{69}BO_2^+$ (M^+): *m/z* 928.5392 (found), 928.5385 (calculated).

Quinoline-hexabenzocoronene 7

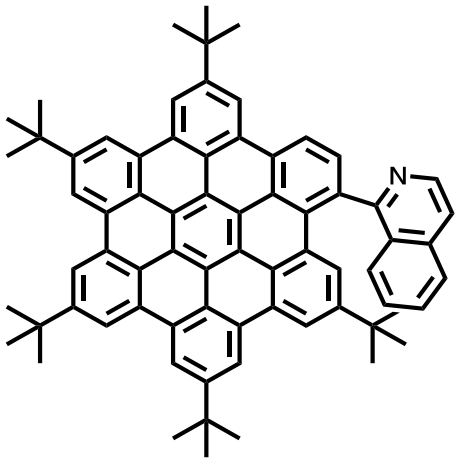

Bpin-hexabenzocoronene **5** (93 mg, 0.1 mmol, 1 equiv.) was added to a degassed solution of $Pd(PPh_3)_4$ (12 mg, 0.01 mmol, 10 mol%) in 1,2-dimethoxyethane (DME, 1 mL) under an argon atmosphere. Subsequently, a degassed solution of 1-bromoisoquinoline (104 mg, 0.5 mmol, 5 equiv.) in ethanol (0.5 mL) and a degassed solution of Cs_2CO_3 (228 mg, 0.7 mmol, 7 equiv.) in water (0.5 mL) were added to the mixture. After heating at 90 °C for 20 h, the reaction mixture was cooled to room temperature and extracted three times with CH_2Cl_2. The combined organic layers were washed with brine, dried over $MgSO_4$, filtered, and the solvent was removed by rotary evaporation. The crude product was purified by column chromatography (SiO_2, petroleum ether / CH_2Cl_2 1:1) to afford product **7** as a yellow solid in 66% yield (61 mg, 0.066 mmol).

^{1}H NMR (400 MHz, $CDCl_3$, 298 K): δ = 9.43-9.29 (m, 8H), 9.18 (s, 1H), 8.98 (d, ^4J = 1.5 Hz, 1H), 8.93 (d, ^3J = 5.8 Hz, 1H), 8.26 (dd, ^3J = 5.0 Hz, ^4J = 3.3 Hz, 2H), 7.91 (d, J = 8.2 Hz, 1H), 7.84 (d, J = 5.8 Hz, 1H), 7.59-7.49 (m, 2H), 7.09 (t, J = 7.7 Hz, 1H), 1.85 (s, 9H), 1.85 (s, 18H), 1.79 (s, 18H) ppm.

^{13}C{^{1}H} NMR (100 MHz, $CDCl_3$, 298 K): δ = 165.4, 149.5, 149.4, 149.4, 149.3, 148.0, 143.6, 137.3, 135.9, 131.3, 131.1, 130.8, 130.8, 130.7, 130.6, 130.6, 130.4, 130.2, 129.8, 129.6, 127.7, 127.5, 127.1, 127.1, 127.0, 126.4, 124.7, 124.3, 124.1, 124.0, 123.9, 122.0, 121.2, 121.1, 121.1, 121.0, 120.9, 120.5, 119.7, 119.5, 119.2, 119.1, 119.1, 118.9, 118.9, 36.0, 35.9, 35.9, 34.9, 32.2, 32.2, 32.2, 31.3 ppm.

HRMS (ASAP$^+$) for $C_{71}H_{63}N^+$ (M^+): *m/z* 929.4954 (found), 929.4955 (calculated).

Precursor nanographene 8

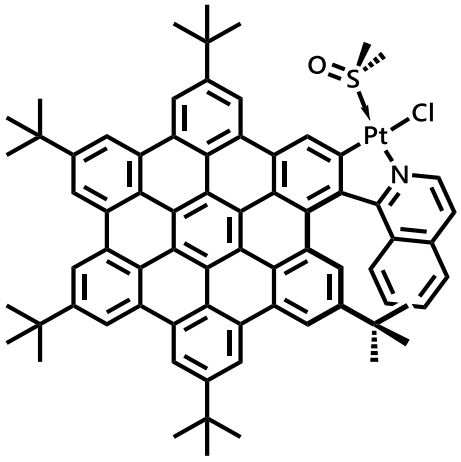

Quinoline-hexabenzocoronene **7** (93 mg, 0.1 mmol, 1 equiv.), $Pt(DMSO)_2Cl_2$ (422 mg, 1 mmol, 10 equiv.), and Na_2CO_3 (106 mg, 1 mmol, 10 equiv.) were suspended in 8 mL of anhydrous toluene under argon. The reaction mixture was stirred at 110 °C for 15 h. After cooling to room temperature, the suspension was extracted with EtOAc, and the organic layer was washed twice with water, once with brine, and dried over $MgSO_4$. The solvents were removed by rotary evaporation, and the crude residue was purified by column chromatography (SiO_2, petroleum ether / EtOAc 3:1) to yield compound **8** as a red solid in 78% yield (96 mg, 0.078 mmol).

^{1}H NMR (400 MHz, $CDCl_3$, 298 K): δ = 10.37 (s, 1H), 9.72 (d, ^3J = 6.6 Hz, 1H), 9.57 (s, 1H), 9.39-9.31 (m, 6H), 9.20 (s, 1H), 8.91 (s, 1H), 8.10 (d, ^4J = 1.5 Hz, 1H), 7.69 (d, ^3J = 8.1 Hz, 1H), 7.62 (d, ^3J = 8.2 Hz, 1H), 7.57 (d, ^3J = 8.6 Hz, 1H), 7.35 (t, ^3J = 7.6 Hz, 1H), 6.68 (t, ^3J = 7.4 Hz, 1H), 3.94 (s, 3H), 3.84 (s, 3H), 1.85 (s, 9H), 1.85 (s, 9H), 1.85 (s, 9H), 1.82 (s, 9H), 0.98 (s, 9H) ppm.

^{13}C{^{1}H} NMR (100 MHz, $CDCl_3$, 298 K): δ = 171.3, 149.8, 149.4, 149.3, 149.3, 147.9, 141.5, 140.4, 139.4, 138.2, 132.3, 131.9, 131.0, 130.8, 130.8, 130.8, 130.7, 130.7, 130.5, 130.4, 130.3, 130.2, 130.1, 127.7, 126.6, 125.5, 125.3, 124.6, 124.3, 124.2, 124.2, 124.1, 123.9, 121.7, 121.3, 120.6, 120.5, 120.3, 120.0, 119.8, 119.2, 119.1, 119.0, 47.6, 47.5, 36.0, 35.9, 35.9, 34.9, 32.2, 32.2, 31.3 ppm.

^{195}Pt NMR (107 MHz, $CDCl_3$, 298 K): δ = -3697.71 ppm.

HRMS (ESI^+) for $C_{73}H_{68}ClNO^{195}PtS^+$ (M^+): *m/z* 1236.4352 (found), 1236.4353 (calculated).

Nanographene NG1

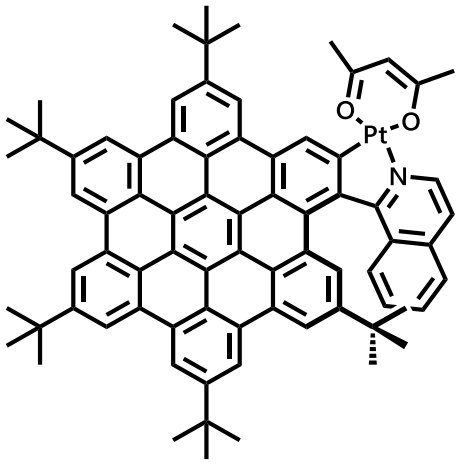

Precursor **8** (44 mg, 0.036 mmol, 1 equiv.) and Na(acac) (44 mg, 0.36 mmol, 10 equiv.) were added to 3 mL of degassed anhydrous toluene under argon. The reaction medium was refluxed for 30 min. The mixture was then extracted with CH_2Cl_2 and the organic layer was washed twice with water, once with brine, and dried over $MgSO_4$. The solvent was removed in vacuum, and the residue was purified by column chromatography (SiO_2, petroleum ether / CH_2Cl_2 1:1) to afford nanographene **NG1** as a red solid in 92% yield (40 mg, 0.033 mmol).

^{1}H NMR (500 MHz, $CDCl_3$, 298 K): δ = 9.54 (s, 1H), 9.47 (s, 1H), 9.38-9.30 (m, 6H), 9.19 (s, 1H), 9.09 (d, ^3J = 6.4 Hz, 1H), 8.90 (s, 1H), 8.20 (d, ^4J = 1.7 Hz, 1H), 7.62 (d, ^3J = 8.0 Hz, 1H), 7.59 (d, ^3J = 8.8 Hz, 1H), 7.51 (d, ^3J = 6.5 Hz, 1H), 7.29 (t, ^3J = 7.1 Hz, 1H), 6.65 (t, ^3J = 7.8 Hz, 1H), 5.67 (s, 1H), 2.28 (s, 3H), 2.19 (s, 3H), 1.85 (s, 9H), 1.85 (s, 9H), 1.84 (s, 9H), 1.82 (s, 9H), 0.99 (s, 9H) ppm.

^{13}C{^{1}H} NMR (125 MHz, $CDCl_3$, 298 K): δ = 186.4, 184.6, 172.6, 149.2, 149.0, 147.6, 140.1, 139.9, 139.5, 137.3, 131.1, 131.0, 130.8, 130.8, 130.8, 130.7, 130.7, 130.6, 130.6, 130.4, 130.4, 130.1, 130.0, 129.0, 128.8, 127.1, 126.5, 125.4, 125.1, 124.8, 124.4, 124.3, 124.3, 124.1, 123.7, 121.7, 121.2, 121.0, 120.6, 120.1, 120.1, 119.8, 119.7, 119.6, 119.2, 119.1, 119.1, 119.0, 118.9, 118.8, 102.8, 35.9, 35.9, 35.9, 34.9, 32.2, 32.2, 32.1, 31.2, 29.9, 28.6, 27.5 ppm.

^{195}Pt NMR (107 MHz, $CDCl_3$, 298 K): δ = -2790.32 ppm.

HRMS (ESI$^+$) for $C_{76}H_{69}NO_2{}^{195}Pt^+$ (M^+): *m/z* 1222.4971 (found), 1222.4971 (calculated).

Nanographene NG2

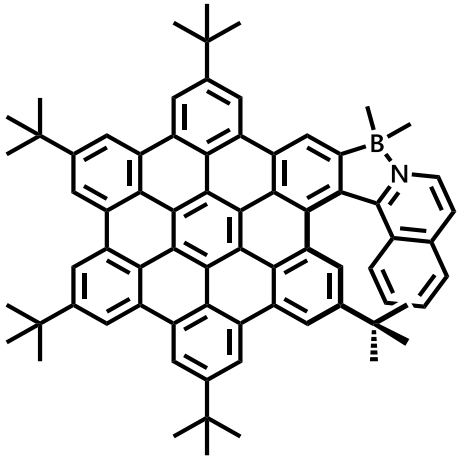

Quinoline-hexabenzocoronene **7** (46 mg, 0.05 mmol, 1 equiv.) was dissolved in 0.4 mL of degassed anhydrous CH_2Cl_2 under argon, and 11 µL of DIPEA (0.065 mmol, 1.3 equiv.) was added. The mixture was then cooled to 0 °C and 0.3 mL of BBr_3 (1 M in CH_2Cl_2, 0.3 mmol, 6 equiv.) was added dropwise to the suspension, under vigorous stirring. The reaction mixture was allowed to warm to room temperature and stirred for 24 h. The solvent was then removed in vacuum using an external cold trap. The residue was dissolved in a solution of 0.3 mL of $AlMe_3$ (2 M in hexanes, 0.6 mmol, 12 equiv.) diluted in 0.8 mL of anhydrous CH_2Cl_2. The reaction mixture was stirred at room temperature for 30 min and quenched by addition of ice-cold water. The mixture was extracted with CH_2Cl_2, the organic layer was washed twice with water, once with brine, and dried over $MgSO_4$. The solvent was removed in vacuum, and the residue was purified by column chromatography (SiO_2, petroleum ether / CH_2Cl_2 7:2) to afford **NG2** as a bright orange solid in 60% yield (29 mg, 0.03 mmol).

^{1}H NMR (400 MHz, $CDCl_3$, 298 K): δ = 9.55 (s, 1H), 9.47 (s, 1H), 9.39 (s, 1H), 9.38-9.34 (m, 5H), 9.29 (s, 1H), 9.06 (s, 1H), 8.55 (d, *J* = 6.2 Hz, 1H), 8.34 (d, *J* = 1.7 Hz, 1H), 7.90 (t, *J* = 8.9 Hz, 2H), 7.80 (d, *J* = 6.2 Hz, 1H), 7.60 (t, *J* = 7.7 Hz, 1H), 7.04 (t, *J* = 8.0 Hz, 1H) , 1.87 (s, 9H), 1.86 (s, 9H), 1.86 (s, 9H), 1.85 (s, 9H), 1.04 (s, 9H), 0.61 (s, 3H), 0.39 (s, 3H) ppm.

^{13}C{^{1}H} NMR (100 MHz, $CDCl_3$, 298 K): δ = 159.8, 149.4, 149.3, 149.3, 149.2, 147.3, 137.6, 134.6, 132.0, 131.7, 130.9, 130.8, 130.7, 130.7, 130.6, 130.6, 130.6, 130.4, 130.4, 130.3, 130.2, 129.1, 128.3, 127.4, 127.0, 126.2, 124.5, 124.5, 124.4, 124.3, 124.2, 124.2, 123.8, 121.2, 120.9, 120.7, 120.7, 120.5, 120.5, 120.4, 120.4, 120.4, 120.2, 119.7, 119.3, 119.2, 119.1, 119.1, 119.1, 119.0, 36.0, 35.9, 35.9, 35.9, 35.0, 32.3, 32.2, 32.2, 31.1, 9.8 ppm.

^{11}B{^{1}H} NMR (193 MHz, $CDCl_3$, 300K): δ = 1.9 ppm.

HRMS (ASAP$^+$) for $C_{73}H_{68}BN^+$ (M^+): *m/z* 969.5441 (found), 969.5439 (calculated).

3. Photophysical studies

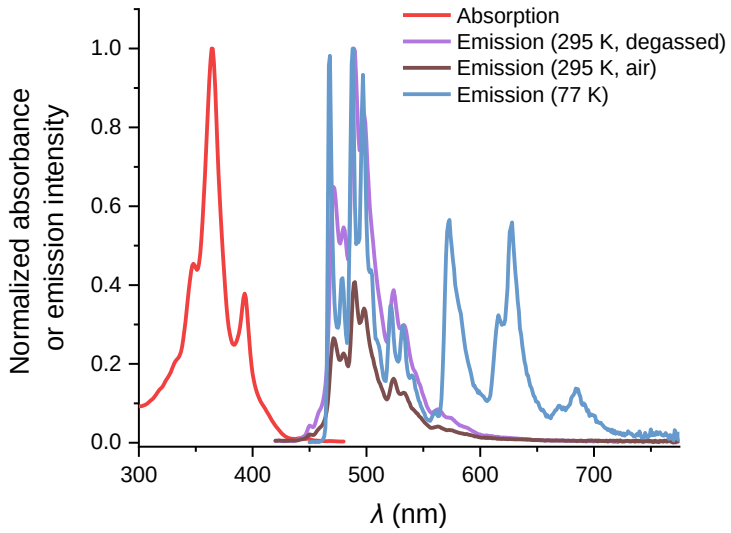

Figure S2. Normalized absorption spectrum (red) and emission spectra of ligand **7** in deoxygenated and air-equilibrated toluene at 295 K (purple and brown lines respectively, plotted on the same intensity scale, λ_{ex} = 405 nm) and in a diethyl ether / isopentane / ethanol (2:2:1 v/v) mixture at 77 K (blue).

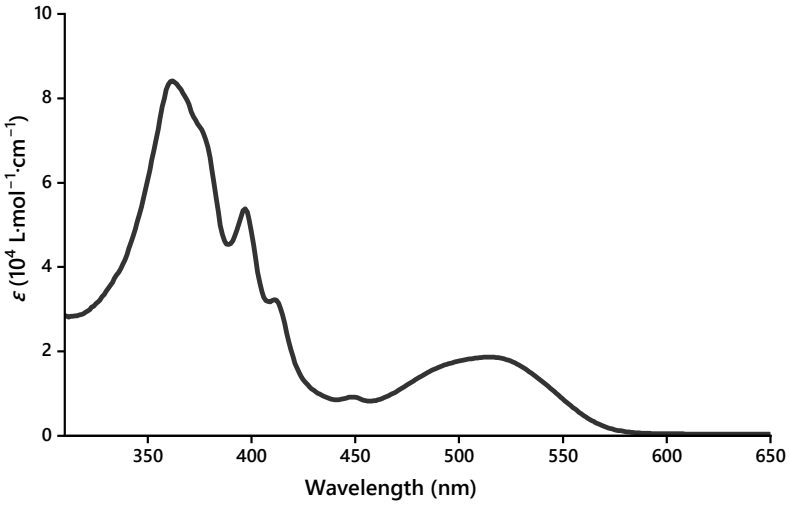

Figure S3. UV-Vis spectrum of compound **8** in toluene ($c \approx 3 \times 10^{-5}$ mol·L^{-1}, 25 °C).

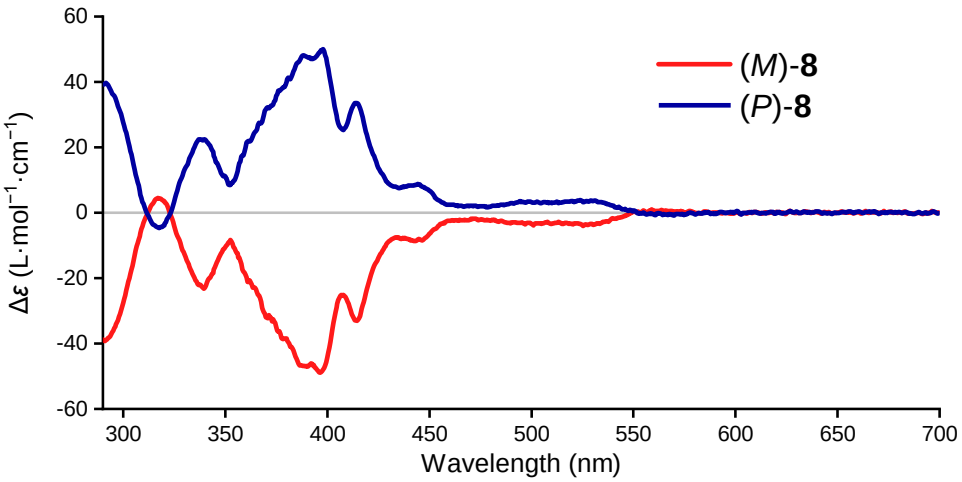

Figure S4. Electronic circular dichroism (ECD) spectra of the enantiomers of compound **8** in toluene ($c \approx 3 \times 10^{-5}$ mol·L^{-1}, 25 °C).

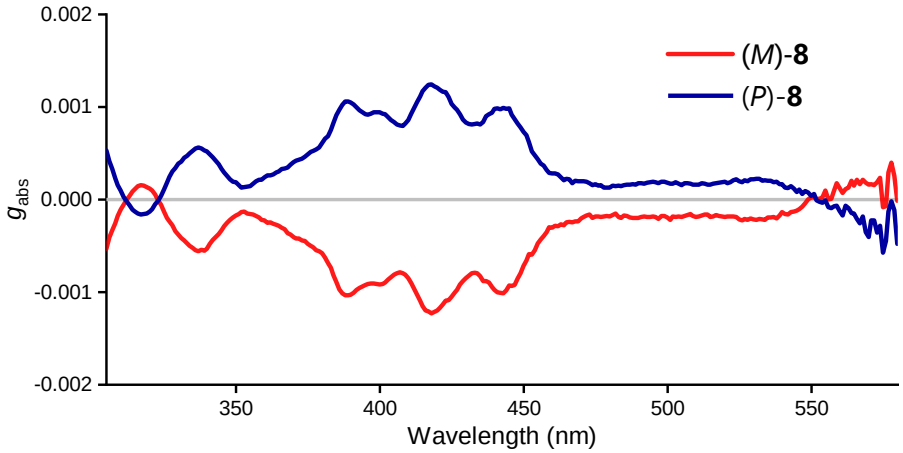

Figure S5. Absorption dissymmetry factor (g_{abs}) plots for the enantiomers of compound **8** in toluene ($c \approx 3 \times 10^{-5}$ mol·L^{-1}, 25 °C).

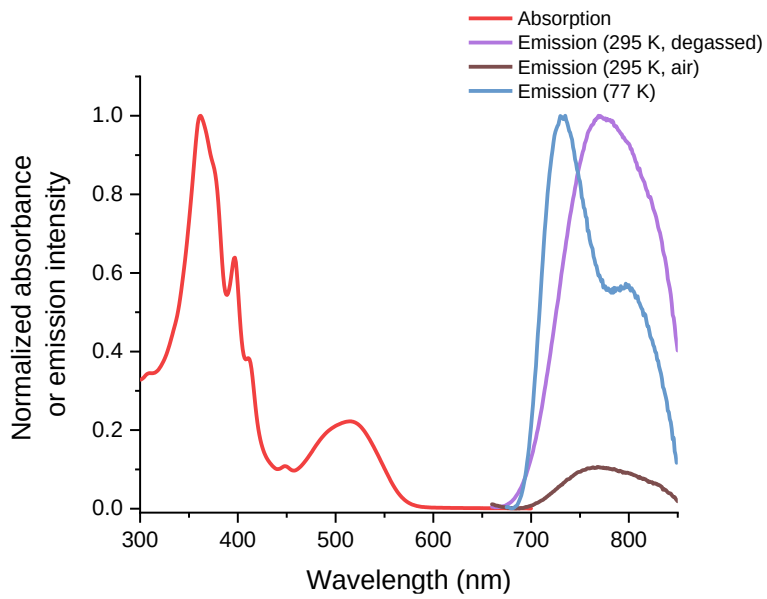

Figure S6. Normalized absorption spectrum (red) and emission spectra of **8** in deoxygenated and air-equilibrated toluene at 295 K (purple and brown lines respectively, plotted on the same intensity scale, λ_{ex} = 442 nm) and in a diethyl ether / isopentane / ethanol (2:2:1 v/v) mixture at 77 K (blue).

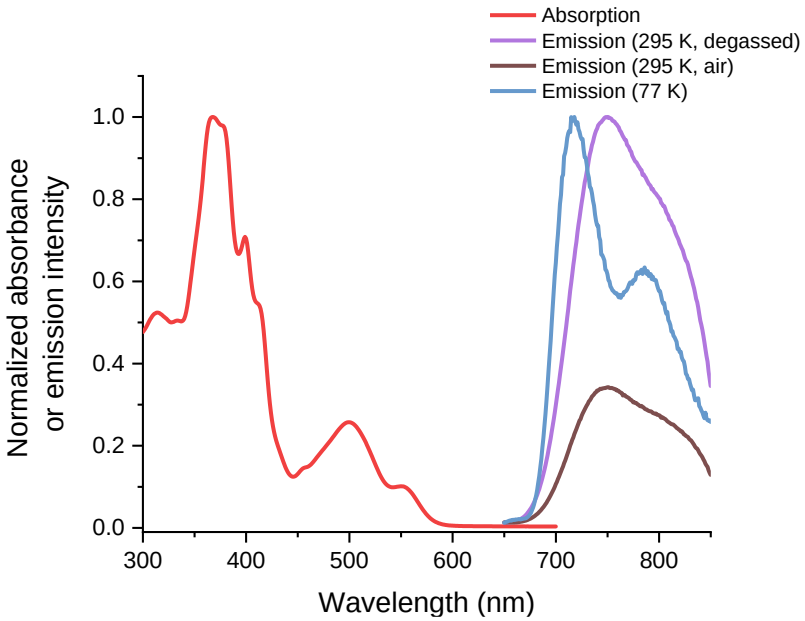

Figure S7. Normalized absorption spectrum (red) and emission spectra of **NG1** in deoxygenated and air-equilibrated toluene at 295 K (purple and brown lines respectively, plotted on the same intensity scale, λ_{ex} = 405 nm) and in a diethyl ether / isopentane / ethanol (2:2:1 v/v) mixture at 77 K (blue).

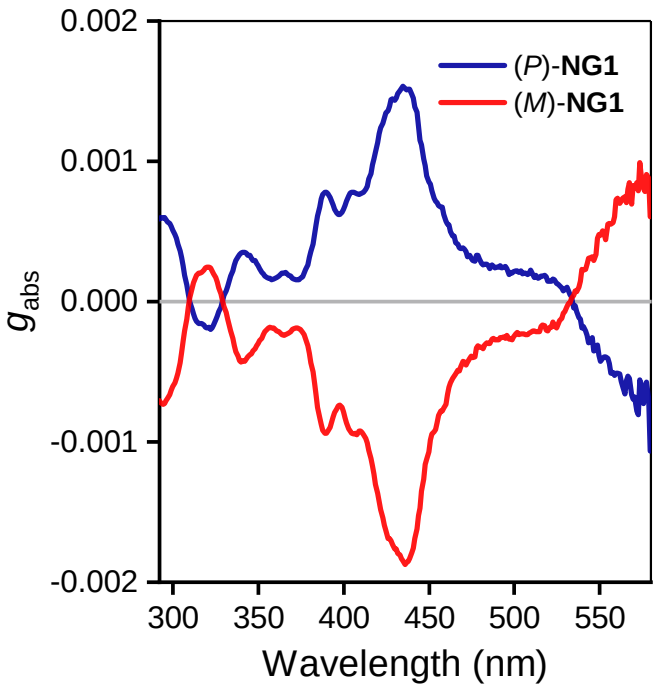

Figure S8. Absorption dissymmetry factor (g_{abs}) plots for the enantiomers of **NG1** in toluene ($c \approx 1 \times 10^{-5}$ mol·L^{-1}).

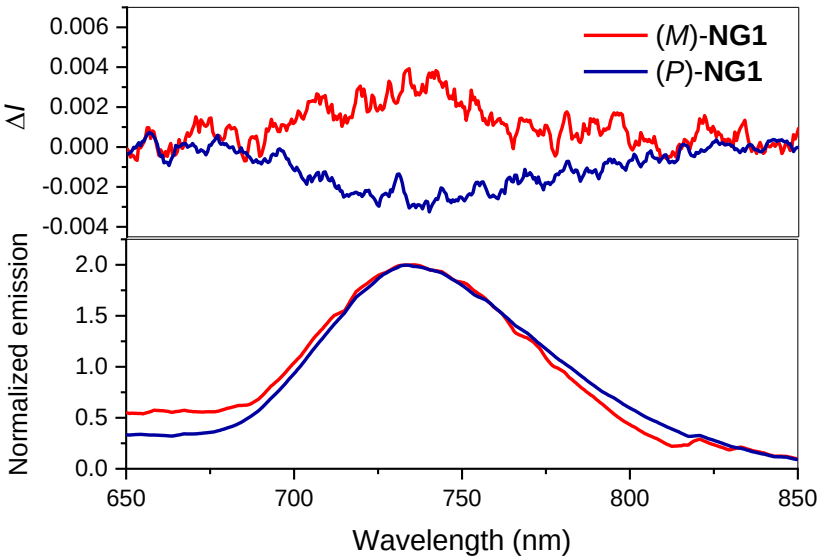

Figure S9. Circularly polarized emission (CPL) spectra (upper panel) and normalized luminescence intensity recorded while measuring CPL (lower panel) for the enantiomers of **NG1** in toluene ($c \approx 1 \times 10^{-5}$ mol·L^{-1}).

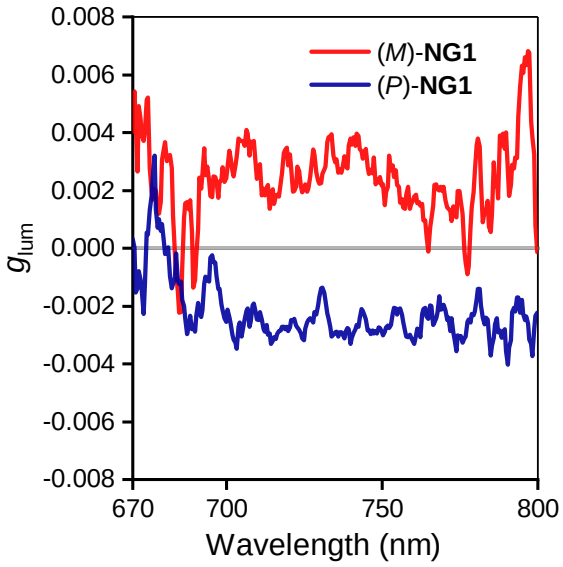

Figure S10. Emission dissymmetry factor (g_{lum}) plots for the enantiomers of **NG1** in toluene (λ_{ex} = 500 nm, $c \approx 1 \times 10^{-5}$ mol·L^{-1}).

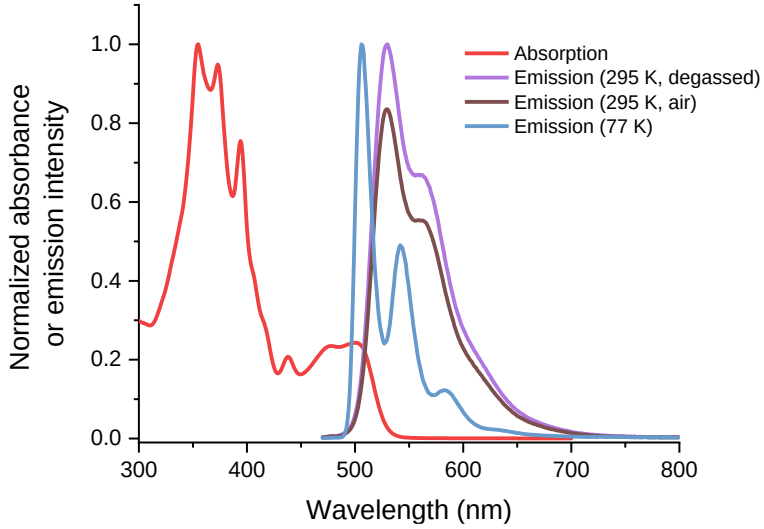

Figure S11. Normalized absorption spectrum (red) and emission spectra of **NG2** in deoxygenated and air-equilibrated toluene at 295 K (purple and brown lines respectively, plotted on the same intensity scale, λ_{ex} = 405 nm) and in a diethyl ether / isopentane / ethanol (2:2:1 v/v) mixture at 77 K (blue).

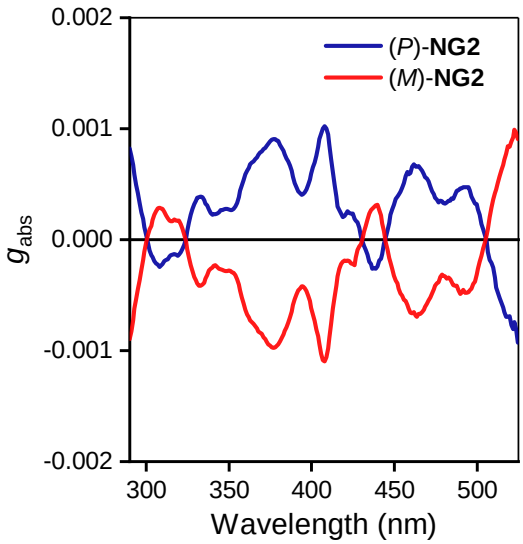

Figure S12. Absorption dissymmetry factor (g_{abs}) plots for the enantiomers of **NG2** in toluene ($c \approx 1 \times 10^{-5}$ mol·L^{-1}).

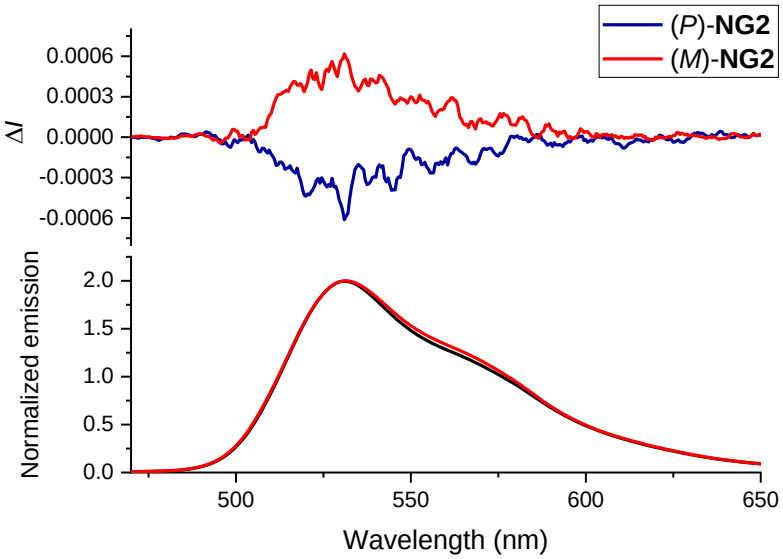

Figure S13. Circularly polarized emission (CPL) spectra (upper panel) and normalized luminescence intensity recorded while measuring CPL (lower panel) for the enantiomers of **NG2** in toluene ($c \approx 1 \times 10^{-5}$ mol·L^{-1}).

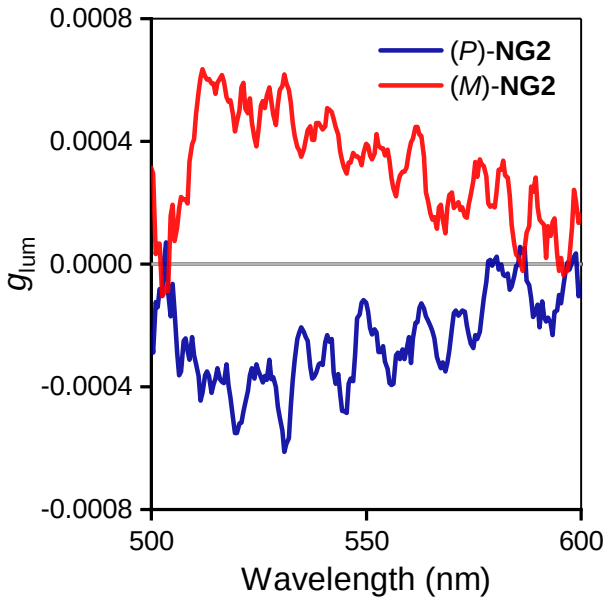

Figure S14. Emission dissymmetry factor (g_{lum}) plots for the enantiomers of **NG2** in toluene (λ_{ex} = 353 nm, $c \approx 1 \times 10^{-5}$ mol·L^{-1}).

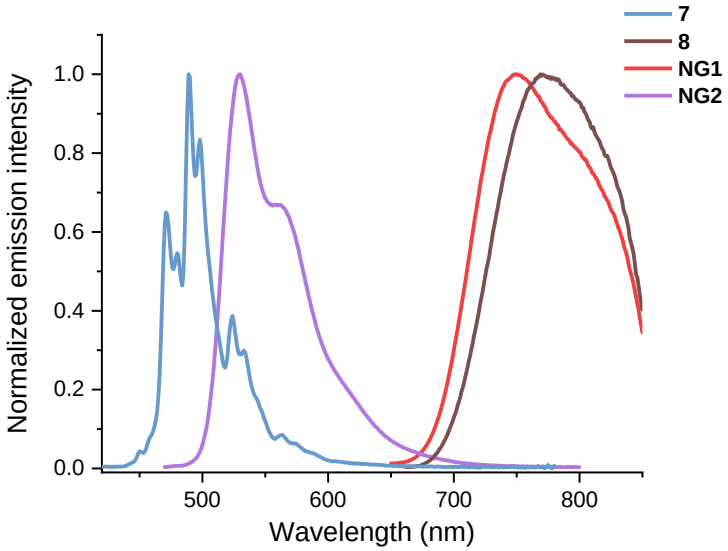

Figure S15. Comparison of the emission spectra of **7**, **8**, **NG1** and **NG2**. All spectra were recorded at 295 K in toluene. λ_{ex} = 405 nm for all compounds except **8** (λ_{ex} = 442 nm).

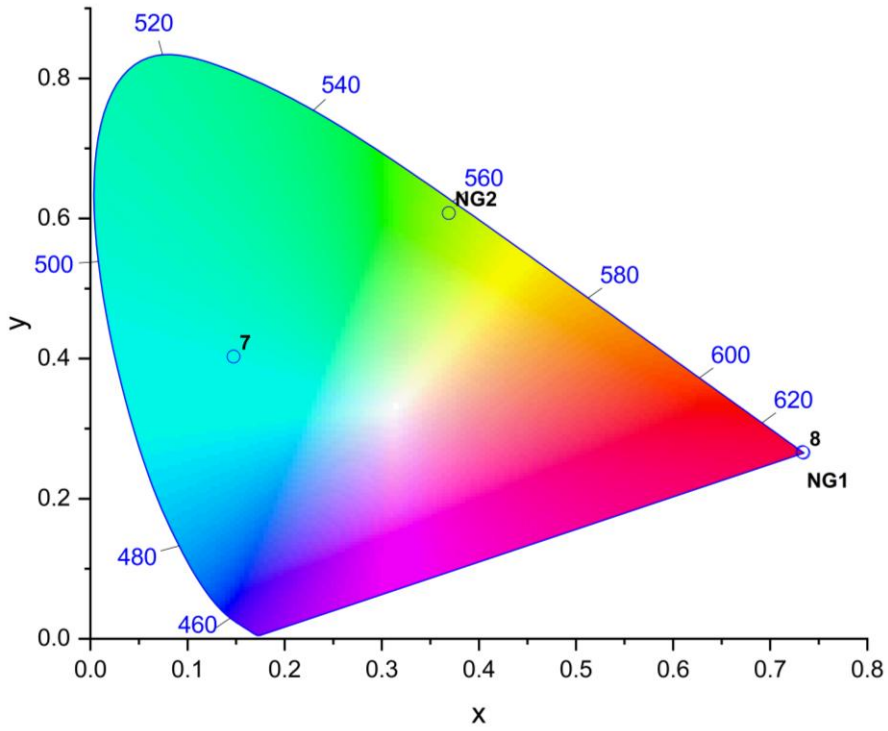

Figure S16. CIE 1931 diagram calculated from the emission spectra of **7**, **8**, **NG1** and **NG2** (toluene, 295 K, *vide supra* for more details). Platinum(II) complexes **NG1** and **8** also emit up to the NIR and are thus placed at the extreme red corner of the diagram.

Table S2. Summary of the measured photophysical properties for **7**, **8**, **NG1** and **NG2**.

Compound	Absorption [(a)] λ_{max} (nm)	Emission at 295 K [(a)] λ_{max} (nm)	τ (ns) [(c)]	Φ_{lum} [(d)] %	k_r [(e)] (x 10^6 s^{-1})	Σk_{nr} [(e)] (x 10^6 s^{-1})	k_Q^{O2} [(f)] (x 10^9 M^{-1} s^{-1})	Emission at 77 K [(b)] λ_{max} (nm)	τ (ns) [(c)]
Ligand **7**	349, 365, 393, [442, 449 (weak)]	472, 480, 489, 498, 524, 533, 563, 573	48 [18]	25 [10]	5.2	15	19	Fluorescence: 468, 478, 488, 497, 504, 511, 521, 532, 540	66
								Phosphorescence: 573, 616, 628, 669, 686	4.5 x 10^9
Precursor **8**	362, 397, 411, 449, 515	774	2300 [340]	0.14	0.00061	0.43	1.4	732, 798	4500
NG1	315, 367, 398, 457sh, 499, 549	749, 807sh	710 [230]	0.33 [0.11]	0.0046	1.4	1.6	718, 786	1200
NG2	354, 375, 395, 439, 482, 501	529, 561	9.3 [7.6]	53 [44]	57	51	13	507, 543, 583	12

(a) In toluene. *(b)* In diethyl ether / isopentane / ethanol (2:2:1 v/v). *(c)* Lifetimes in degassed solution; values in air-equilibrated solution are given in parenthesis. Measured by time-correlated single photon counting following excitation at 405 nm; estimated uncertainty is ±10%. *(d)* Quantum yield in degassed solution; values in air-equilibrated solution are given in parenthesis. Estimated uncertainty is around ±20% of the value. *(e)* k_r and Σk_{nr} are the radiative and non-radiative rate constants, respectively, estimated by assuming that the emissive state is formed with unit efficiency, such that $k_r = \Phi / \tau$ and $\Sigma k_{nr} = (1-\Phi_{lum}) / \tau$. *(f)* $k_Q^{O_2}$ is the bimolecular rate constant for quenching by oxygen, based on the lifetimes in degassed and air-equilibrated solutions, and taking $[O_2]$ = 1.8 mM in toluene at atmospheric pressure.

We note that intermediate 8 – the direct precursor to **NG1** bearing S-DMSO and Cl ligands instead of O^O-acac – also phosphoresces in the same spectral region. Its quantum yield is yet lower than **NG1** and its lifetime longer, implying a somewhat lower k_r and an influence of the ancillary ligands on the energies of the pertinent metal orbitals.

4. Computational analysis

Computational details

All calculations were carried out employing density functional theory (DFT) methods and its time-dependent variant (TDDFT) with no symmetry explicitly imposed. For all the examined structures, (*P*) helical stereochemistry was considered; in the case of the pristine ligand, axial conformational chirality was additionally taken into account.

DFT geometry optimizations were performed using the ORCA program, version 6.1,[9,10] with accounting for dispersion effects *via* the fourth-generation Grimme's set of semiempirical dispersion corrections D4,[11] and accounting for solvent effects (toluene, ε = 2.387) *via* the conductor-like polarizable continuum model (CPCM) with the default parameters of the ORCA/CPCM implementation.[12,13] The B3LYP[14–16] hybrid exchange-correlation functional was used along with a split-valence basis set including one set of polarization functions for non-hydrogen atoms, SV(P),[17–19] and a 60-electron scalar relativistic effective core potential (ECP) for Pt atom.[20]

The subsequent TDDFT linear response UV-Vis/ECD calculations[21–23] were performed with the Gaussian 16, version C.01 (G16),[24] employing the PBE0[25,26] density functional and the SV(P)(-ECP) basis set. Solvent (toluene, ε = 2.374) effects were modelled with the polarizable continuum model (PCM) using the default parameters of the Gaussian 16 implementation.[27,28] These computations covered the 200 lowest singlet excited states for each system to assure that all transitions with a significant dipole and rotatory strengths in the experimentally observed energy range are included. The presented spectra were simulated as the sums of Gaussian functions centered at the vertical excitation energies and scaled using the calculated oscillator / rotatory strengths with a broadening parameter of σ = 0.2 eV.[29]

Insight into electronic emission spectra was provided *via* S_1 excited-state and / or T_1 excited-state geometry optimizations that were performed using the TDDFT method, with the Tamm-Dancoff approximation (TDA) in the latter (T_1) case,[30–35] with the PBE0 functional, the SV(P)(-ECP) basis set, and PCM[36,37] to account for the solvent (toluene) effects. As starting points in T_1 excited-state optimizations, structures optimized with unrestricted ground-state DFT approach and a spin multiplicity of 3, $T_1^{\{DFT\}}$, were used since they are supposed to give a good description of the lowest-energy electronic triplet states. All these calculations were carried out with the Gaussian 16 program.

Luminescence dissymmetry factor g_{lum} for triplet excited state of **NG1** was obtained based on TDDFT-TDA calculations of excitation energies and magnetic transition dipole moments and rotatory strengths for the triplet-singlet transitions performed at the respective G16-optimized T_1 structure using the Amsterdam Density Functional (ADF) package from Amsterdam Modeling Suite, version 2024.106.[38–40] In this part of the studies, the PBE0 functional, Slater-type all-electron triple-zeta doubly polarized TZ2P basis set for the metal, double-zeta DZ for hydrogens, and DZP for other atoms,[41] conductor-like screening model of solvation (COSMO)[42] (toluene, ε = 2.38), and the zeroth-order regular approximation (ZORA)[43–46] two-component relativistic Hamiltonian were employed (ZORA-SOC: ZORA with spin-orbit coupling). Some test calculations also utilized the TZP (triple-zeta polarized) and QZ4P (core triple-zeta, valence quadruple-zeta,

with four sets of polarization functions) basis sets for Pt to assess the sensitivity of the computed g_{lum} to the choice of basis set for the metal.[47] Center-of-nuclear-charge coordinates for excited-state structures were used to minimize origin-dependence problem of the length-gauge results.[48] Up to 2 lowest-energy singlet states and 3 lowest-energy triplet states were cover in these computations to include as many as possible singlet states of sizable rotatory strength value; the energetic order of the excited states was thus first determined based on the corresponding excitation energies calculations with ZORA applied as scalar correction (ZORA-SC: scalar ZORA).

NMR calculations for nucleus independent chemical shifts (NICS)[49,50] and anisotropy of the induced current density (AICD)[51,52] analyses were performed at the B3LYP+D4/SV(P)(-ECP)/PCM(toluene)-optimized structures of **NG1**, **NG2**, **7**, and – for a comparison – 'pure' nanographene ligand, using the same level of theory as employed in the geometry optimizations. In these computations, the G16 and AICD (version 3.0.4)[51] softwares were used, respectively. Since the examined molecules are not fully planar, NICS(1) values were calculated for probes positioned 1 Å above the molecular surface (toward the viewer) and 1 Å below it (away from the viewer), and the results are presented as averages.

Additional calculated data and analyses

Aromaticity examination

To provide some insight into the π-electron delocalization and aromaticity distribution in the considered helicenic Pt(II)- and B(III)-based nanographene complexes **NG1** and **NG2** and their parent ligand **7**, the nucleus-independent chemical shift (NICS) values and anisotropy of the induced current density (AICD) isosurfaces were studied and analyzed in comparison with the corresponding data obtained for unsubstituted nanographene ligand (**reference**).

Let us start with the NICS analysis, focusing on $NICS(0)_{zz}$ and $NICS(1)_{zz}$ values (the negatives of the ZZ components of the shielding tensors), which were selected over $NICS_{iso}$ (the negatives of the isotropic absolute shieldings) as they reduce σ-contamination arising from induced currents generated by σ-electrons; see Table S3 and Figure S18. Assuming the molecule lies in the *xy*-plane, the external magnetic field is oriented along the *z*-axis, and the induced currents from π-electrons occur above and below this plane,[50] making the ZZ component of the shielding tensor the most relevant.[53,54] Although $NICS_{zz}$ values are not entirely free from σ-contamination (particularly in the case of NICS(0)), they provide a reasonable approximation and are easily obtainable.[55]

As shown in Table S3 and Figure S18, for all four structures considered, the central ring of the nanographene moiety (no. 10) as well as the peripheral rings (nos. 4–9) exhibited negative NICS values, indicating aromatic character.[50] In contrast, the rings adjacent to the central one (nos. 11–16) displayed values suggesting either antiaromaticity or non-aromaticity, as they ranged from highly positive for $NICS(0)_{zz}$ in **NG1** and **NG2** complexes, through near-zero for $NICS(0)_{zz}$ in both the ligand structures, to (mostly) negative (although noticeably less negative than those assigned to the previously mentioned rings) for $NICS(1)_{zz}$ in all the systems. Such aromaticity distribution is indicative of the localized benzenoid electronic structure of the NG inner core.

Comparison of the two ligand structures (**7** and the unsubstituted **reference**) revealed that substitution of ring no. 4 with quinoline led to a reduction in its aromaticity, as evidenced by an increase in its NICS values (i.e., becoming less negative), accompanied by an increase in aromaticity of ring no. 5 (reflected by a decrease in its NICS values, becoming more negative). These changes were modest for $NICS(0)_{zz}$ but more pronounced for $NICS(1)_{zz}$. The remaining nanographene rings were only slightly affected, although a minor increase in aromaticity can be observed. In contrast, the newly introduced quinoline rings exhibited strongly negative NICS values. Regarding the effect of complexation on the aromaticity of individual rings, changes in NICS values (aromaticity) were observed across the entire molecule in both **NG1** and **NG2** complexes, which overall demonstrated similar characteristics. In particular, the aromaticity of both quinoline rings decreased upon nanographene–quinoline ring closure, with a more pronounced effect observed for the pyridine moiety. As expected, the newly introduced five-membered ring was non-aromatic. For the nanographene core, the results indicated that π-aromaticity increased for the central (no. 10) and peripheral rings (nos. 4–9) in **NG1** and **NG2** compared to **7** (as shown by more negative values of $NICS(1)_{zz}$), while it generally decreased for mid-molecule rings (nos. 11–16), except for no. 11, which showed an increase, reflecting its incorporation into the helicenic skeleton. These changes in $NICS(1)_{zz}$ were accompanied by an overall increase in $NICS(0)_{zz}$ values, particularly strong for the mid-molecule rings, which became strongly positive. This is indicative of a decrease in aromaticity at the center of the ring or an increased influence of σ-electrons.

To complement the NICS analysis, AICD calculations were performed. The resulting plots for all compounds revealed similar patterns (Figure S19): neither the introduction of an aromatic substituent to the ligand nor its subsequent complexation caused noticeable changes in the nanographene's ring currents. Diatropic (clockwise) currents, indicated by blue arrows in Figure S19, were observed in the central and peripheral rings (nos. 4–10), whereas the mid-molecule rings (nos. 11–16) showed paratropic (counterclockwise) currents, marked by red arrows. These findings were consistent with the NICS results (as expected, particularly well with $NICS(1)_{zz}$), with diatropic ring currents (indicative of aromaticity)[51] corresponding to strongly negative NICS values and paratropic currents (indicative of antiaromaticity) corresponding to either positive or near-zero NICS values. Notably, the induced ring current in **NG1** shows involvement of Pt(II) lone-pair electrons, suggesting (more effective than in **NG2**) electronic π-conjugation across the formed helicenic framework.

Overall, these results align well with previously reported data for similar nanographenes with the character of the ring currents and the qualitative trends in NICS values reported therein closely matching those observed in this study.[56–58]

Analysis of absorption properties

The TDDFT-simulated UV-Vis spectra agree quite well with the experimental data in terms of energetic positions of the main bands (Figure S20). An additional absorption intensity that appears at wavelengths longer than ca. 400 nm for the helicenic Pt(II)- and B(III)-based nanographene complexes **NG1** (and its corresponding precursor **8**) and **NG2** compared to their parent ligand **7** originates – in both cases – from the lowest-energy excitations nos. 1 and 2

(Tables S4, S5, and S8; Figures S22, S23, and S26). The excitations can be jointly assigned as of mixed nanographene→quinoline intraligand charge-transfer (ILCT) and ππ* character, accompanied by some metal-to-ligand CT (MLCT) in the case of **NG1** and **8**. They involve highest-energy occupied molecular orbitals HOMO-1 and HOMO representing the π-electron system of nanographene ligand, partially extended onto helically closed Pt- / B-quinoline fragment, and lowest-energy unoccupied MO LUMO localized mostly at [6]helicenic moiety with some spread across adjacent nanographene rings; for **NG1** and **8** all these MOs include Pt(II) metal orbitals. The red-shift of these excitations and the increase of their oscillator strengths comparing to **7** (Tables S6-S7, Figures S24-S25) appear to stem from the formation of a helicenic structure due to the nanographene–quinoline ring closure that results in the polarization of the electron density visible in LUMO (and thus increase in the CT character of these low-energy excitations) accompanied with its significant energetic stabilization (and thus decrease in the energetic gaps between the highest-energy occupied MOs and LUMO). The red-shift of these lowest-energy excitations observed for **NG1** (and **8**) vs. **NG2** can be linked to the involvement of the Pt(II) metal orbitals in the π-conjugated helicenic electron system. In the higher-energy UV-Vis region (wavelengths shorter than 400 nm), the examined systems (in line with the experimental data) show similar intense spectral envelopes, dominated – in all the cases – by nanographene-localized ππ* transitions with some nanographene→quinoline ILCT components (see for example excitations nos. 9–11 for **NG1**, nos. 6–7 for **NG2**, and nos. 5–6 for **7**).

A satisfactory agreement between the calculated and experimental results can also be seen for ECD spectra (Figure S21). As the broadened vertical excitation spectra in the calculations display far less substructure, the experimental spectral envelopes, in particular at wavelengths longer than 400 nm, and especially for **NG2** and **8**, seem to be vibronic in nature. The main excitations responsible for the low-energy part of the spectra are the aforementioned nos. 1 and 2 of mixed ILCT / ππ* (and MLCT) character. For the Pt(II) complexes considered, the *P* enantiomers display a sizable negative rotatory strength (*R*) for the excitation no. 1 and a modest positive *R* value for the excitation no. 2 (Tables S4 and S8), which for **NG1** accounts well for the lowest-energy negative band observed in the experimental data. In contrast, for the B(III) system, the *P* enantiomer shows a reversed trend in the sign of *R* for these excitations (Table S5). However, since they are nearly isoenergetic, excitation no. 2 – with its negative *R* value – dominates in the broadened spectrum, correctly reproducing the negative sign of the lowest-energy experimental band. In the case of **NG1**, the main positive ECD band centered at ca. 400 nm stems from the excitations nos. 6 and 9, with the former corresponding to acac→quinoline ligand-to-ligand CT (LLCT) admixed with quinoline-nanographene-localized ππ* and MLCT, and the latter dominated by nanographene-centered ππ* with some nanographene→quinoline ILCT and MLCT contributions. A similar mixed nature, although obviously without the acac→quinoline LLCT component, was observed for the excitation no. 8 predominantly underlying the main positive ECD band in the Pt(II) precursor **8**. As far as the **NG2** derivative is concerned, such a band, blue-shifted relative to **NG1** and centered at ca. 370 nm, originates predominantly from excitations nos. 5, 6, and 7 that correspond mainly to ππ* transitions within nanographene skeleton with some nanographene→quinoline ILCT signature.

Finally, based on the computations performed for two diastereoisomers of helically/axially chiral ligand **7**, non-negligible ECD signal could be observed for this compound provided that racemization process is blocked (Figure S21).

Analysis of emission properties

The calculations reproduce experimental fluorescence and phosphorescence energies for helicenic complexes **NG1** (and its corresponding precursor **8**) and **NG2** and their parent ligand **7** reasonably well (Table S9). In line with the experiments, the red-shift of $S_1 \rightarrow S_0$ transition for **NG2** vs. **7** and the red-shift of $T_1 \rightarrow S_0$ transition for **NG1** vs. **7** is observed, which can be traced back, as for the UV-Vis absorption, to more ILCT (and MLCT in the case of **NG1**) character of the corresponding excited states for the complexes resulting from the formation of an helicenic structure due to the nanographene–quinoline ring closure (Table S9, Figures S27-S28). The S_1 geometry optimization for **NG2** suggested that the CPL sign should invert relative to the lowest-energy ECD band, which contradicts the experimental observation indicating negative CPL responses for *P*-**NG2**. This discrepancy may imply that the CPL sign in this system is dictated by vibronic coupling or state-specific solvation effects, both neglected in the presented studies, or that emission preferentially occurs from S_2 excited state (notably, absorption data indicate that S_1 and S_2 are nearly isoenergetic). Luminescence dissymmetry factor g_{lum} for triplet excited state of *P*-**NG1** computed using TDDFT-TDA including spin-orbit coupling (SOC) was determined to be negative, thus correctly reproducing the experimental finding.

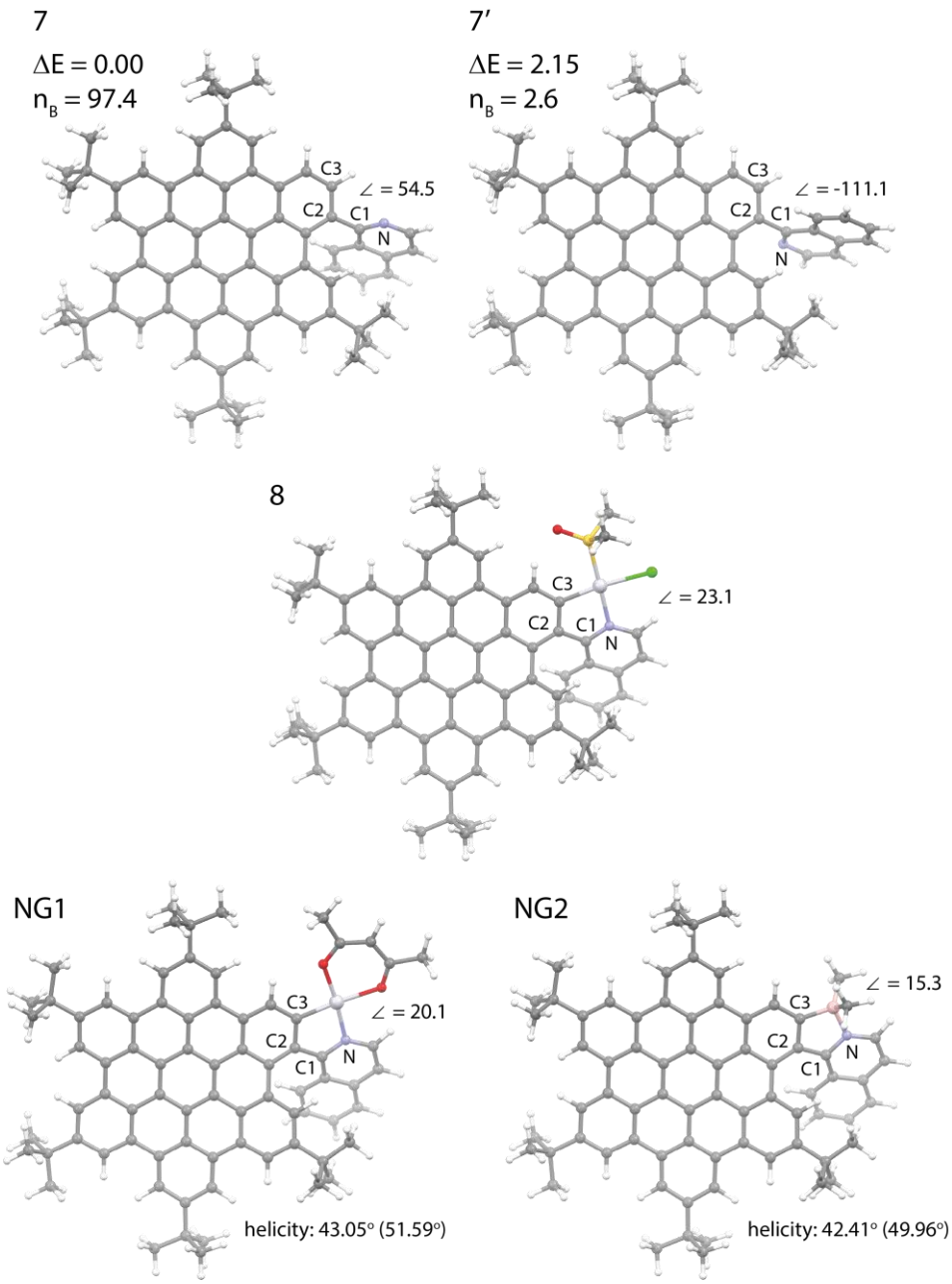

Figure S17. DFT-optimized (B3LYP+D4/SV(P)(-ECP)/CPCM(toluene)) structures of the examined helicenic Pt(II)- and B(III)-based nanographene complexes along with their parent ligand. Values listed correspond to NC1C2C3 dihedral angles (defined on each structure, ∠ in degree) and, for the ligand, relative energies (ΔE in kcal/mol) along with Boltzmann populations at 298 K (n_B, in %). For **NG1** and **NG2**, the corresponding helicity values (defined as the angle between the planes of the two terminal aryl groups forming the helix) are also reported and compared with those obtained for structures optimized without dispersion corrections (given in parentheses); note that at the DFT+D4 level of theory, a significant reduction in helicity is observed (consistent with experimental findings) indicating that this structural feature arises from stabilizing attractive van der Waals / CH-π interactions between the bulky *tert*-butyl group and the quinoline moiety.

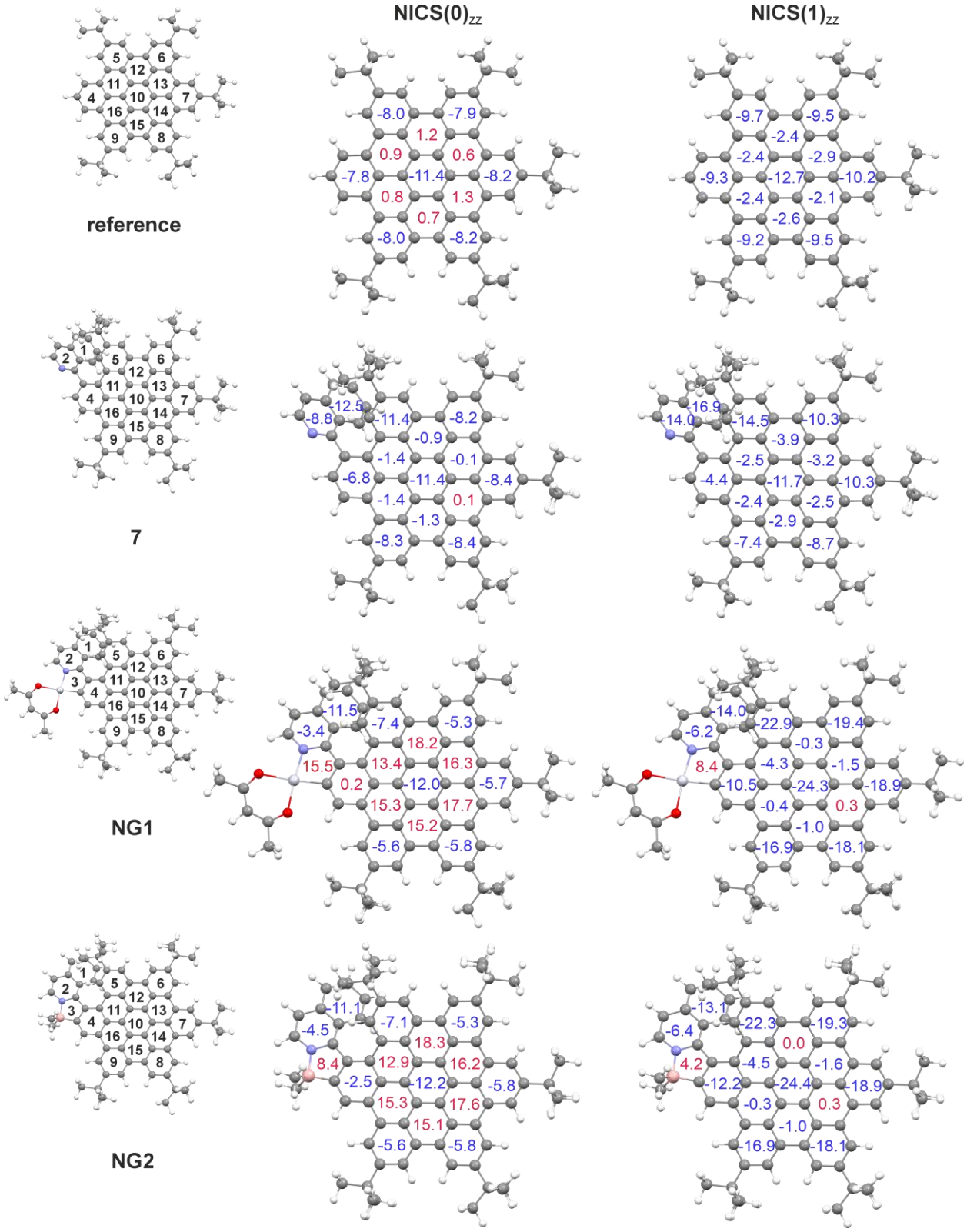

Figure S18. NICS(0)$_{zz}$ and averaged NICS(1)$_{zz}$ values (in ppm) computed for the considered nanographene systems. Negative values (in blue) signify aromaticity and positive (in red) – antiaromaticity/non-aromaticity. On the left, ring numbering is shown.

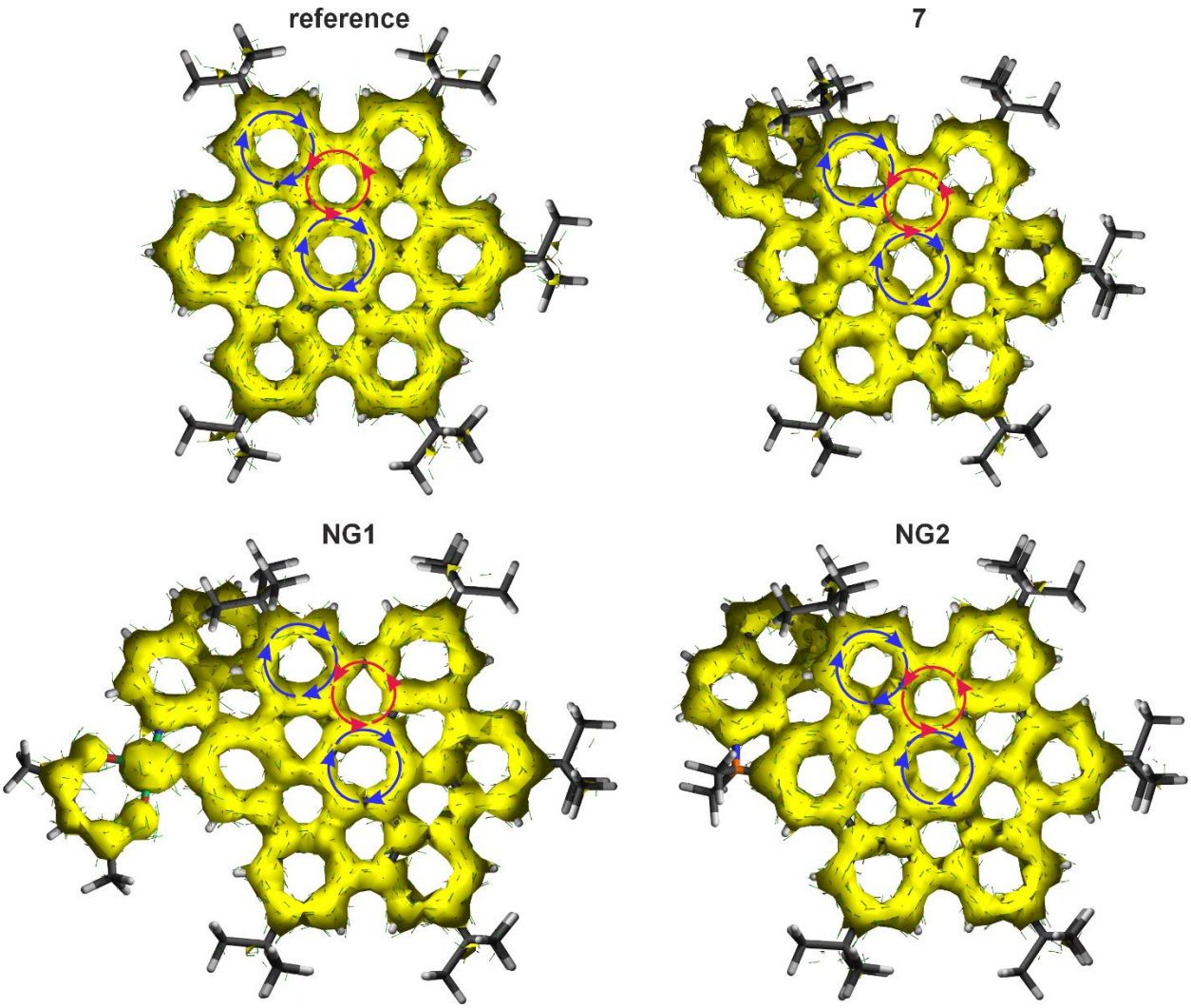

Figure S19. Anisotropy of the induced current density (AICD) isosurfaces (0.05 au). Blue arrows indicate diatropic currents (aromaticity) and red – paratropic currents (antiaromaticity).

Table S3. Calculated (B3LYP/SV(P)(-ECP)/PCM(toluene)) NICS(r)$_{iso}$ and NICS(r)$_{zz}$ values (in ppm) with r = 0, 1 denoting the distance between the NICS probe and the ring plane (in Å). Because the studied molecules are non-planar, the probes were positioned 1 Å above and below the plane; the reported NICS(1) values represent the average of these two positions. For ring numbering, see Figure S18.

ring no.	NICS(0)$_{iso}$	NICS(0)$_{zz}$	NICS(1)$_{iso}$	NICS(1)$_{zz}$
		reference		
1	-	-	-	-
2	-	-	-	-
3	-	-	-	-
4	-8.3	-7.8	-10.7	-9.3
5	-8	-8	-10.5	-9.7
6	-7.9	-7.9	-10.5	-9.5
7	-8	-8.2	-10.6	-10.2
8	-7.9	-8.2	-10.4	-9.5
9	-8.1	-8	-10.6	-9.2
10	-11.7	-11.4	-14	-12.7
11	1.9	0.9	-2.7	-2.4
12	2.7	1.2	-2.1	-2.4
13	1.8	0.6	-2.8	-2.9
14	2.6	1.3	-2.1	-2.1
15	2.2	0.7	-2.5	-2.6
16	2	0.8	-2.6	-2.4
		7		
1	-8.8	-12.5	-11	-16.9
2	-5.7	-8.8	-8.7	-14
3	-	-	-	-
4	-7.3	-6.8	-9.8	-4.4
5	-8.6	-11.4	-11.1	-14.5
6	-8.1	-8.2	-10.6	-10.3
7	-8	-8.4	-10.5	-10.3
8	-7.8	-8.4	-10.4	-8.7
9	-8	-8.3	-10.6	-7.4
10	-11.4	-11.4	-13.7	-11.7
11	2.7	-1.4	-2.2	-2.5
12	2.4	-0.9	-2.3	-3.9
13	1.9	-0.1	-2.7	-3.2
14	2.7	0.1	-2	-2.5

15	2.3	-1.3	-2.4	-2.9
16	2	-1.4	-2.6	-2.4
		NG1		
1	-7.9	-11.5	-10.1	-14
2	-4.2	-3.4	-7.1	-6.2
3	4.1	15.5	0.9	8.4
4	-3.8	0.2	-7.7	-10.5
5	-8	-7.4	-10.5	-22.9
6	-7.9	-5.3	-10.5	-19.4
7	-7.9	-5.7	-10.5	-18.9
8	-7.8	-5.8	-10.4	-18.1
9	-7.7	-5.6	-10.3	-16.9
10	-11	-12	-13.3	-24.3
11	2.1	13.4	-2.9	-4.3
12	2.7	18.2	-2	-0.3
13	1.8	16.3	-2.8	-1.5
14	2.7	17.7	-2	0.3
15	2.1	15.2	-2.5	-1
16	2.3	15.3	-2.3	-0.4
		NG2		
1	-7.7	-11.1	-10	-13.1
2	-4.6	-4.5	-7.4	-6.4
3	3.8	8.4	-0.4	4.2
4	-5.5	-2.5	-9.1	-12.2
5	-7.8	-7.1	-10.2	-22.3
6	-7.9	-5.3	-10.5	-19.3
7	-7.9	-5.8	-10.5	-18.9
8	-7.9	-5.8	-10.4	-18.1
9	-7.7	-5.6	-10.4	-16.9
10	-11.1	-12.2	-13.4	-24.4
11	2	12.9	-3	-4.5
12	2.8	18.3	-1.9	0
13	1.9	16.2	-2.7	-1.6
14	2.7	17.6	-2	0.3
15	2.1	15.1	-2.5	-1
16	2.4	15.3	-2.3	-0.3

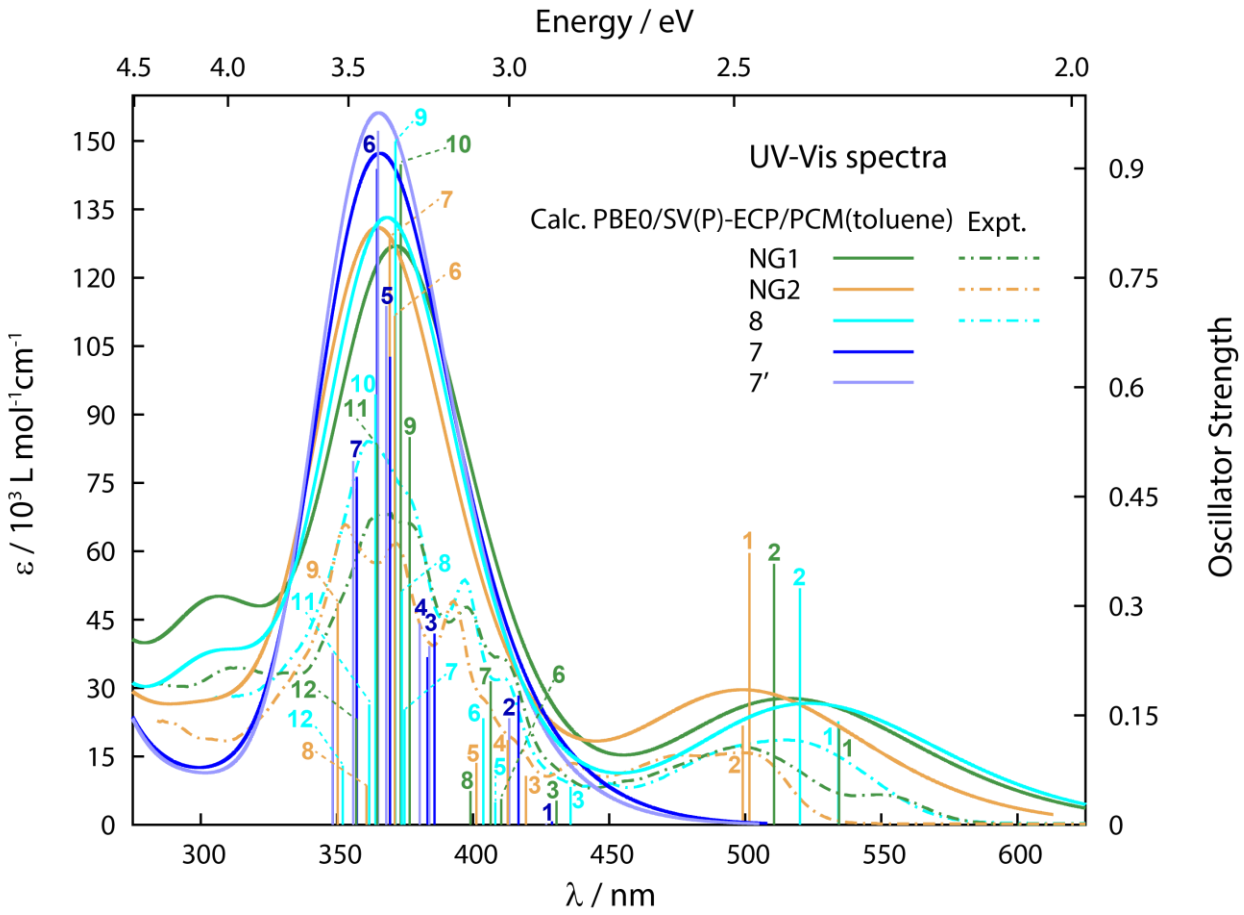

Figure S20. Experimental (dash line) and TDDFT-simulated (PBE0/SV(P)(-ECP)/PCM(toluene)) UV-Vis spectra of helicenic Pt(II)- and B(III)-based nanographene complexes along with their parent ligand. No spectral shift has been applied. Excitation energies and corresponding rotatory strengths indicated as 'stick' spectra with numbered excitations correspond to those analyzed in detail in Tables S4-S8.

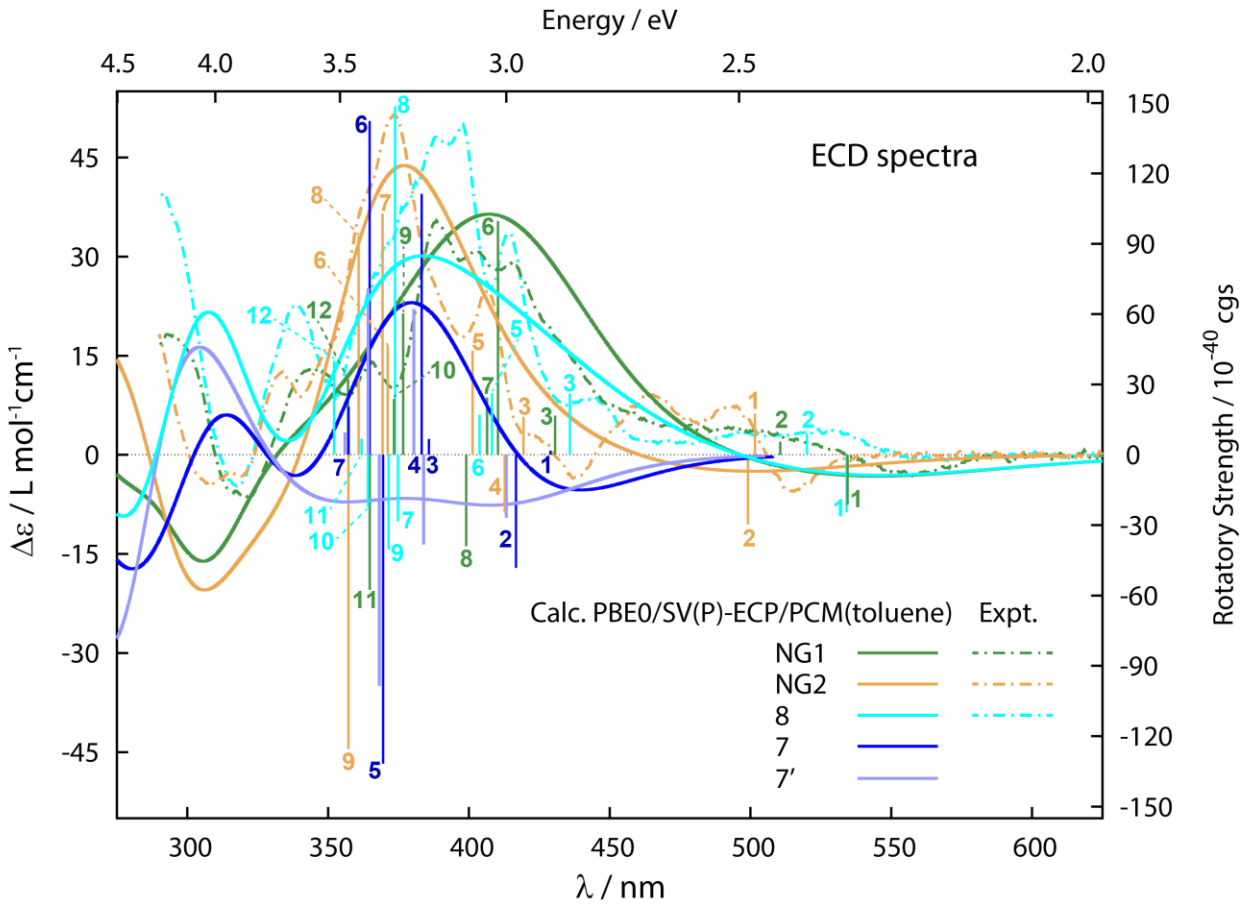

Figure S21. Experimental (dash line) and TDDFT-simulated (PBE0/SV(P)(-ECP)/PCM(toluene)) ECD spectra of helicenic Pt(II)- and B(III)-based nanographene complexes along with their parent ligand (in their *P* stereochemistry). No spectral shift has been applied. Excitation energies and corresponding rotatory strengths indicated as 'stick' spectra with numbered excitations correspond to those analyzed in detail in Tables S4-S8.

Table S4. Selected dominant excitations and occupied (occ) – unoccupied (unocc) MO-pair contributions (≥ 9%) for (*P*)-**NG1**. Based on TDDFT-PBE0/SV(P)-ECP/PCM(toluene) calculations. See Figures S20-S21 for the corresponding simulated UV-Vis and ECD spectra. See Figure S22 for MOs isosurfaces.

Excitation	*E* / eV	λ / nm	*f*	*R* / 10^{-40} esu^2 cm^2	occ no.	unocc no.	%
1	2.320	534	0.136	-21.29	283	284	91.8
2	2.428	511	0.358	5.64	282	284	93.5
3	2.879	431	0.033	16.74	281	284	63.0
					280	284	13.1
					279	284	10.9
6	3.021	410	0.035	99.72	280	284	50.0
					278	284	22.9
					282	285	8.2
7	3.050	406	0.197	24.41	283	285	65.7
					282	286	20.2
8	3.107	399	0.046	-39.03	279	284	70.4
					278	284	8.4
9	3.291	377	0.531	60.22	283	286	32.7
					283	287	24.0
					282	285	21.8
					282	286	9.4
10	3.320	373	0.906	23.77	282	286	49.1
					282	285	15.4
					283	285	14.1
					283	286	10.9
11	3.399	365	0.521	-57.53	283	287	61.8
					282	286	12.6
					282	285	10.4
12	3.472	357	0.144	32.06	282	287	84.5

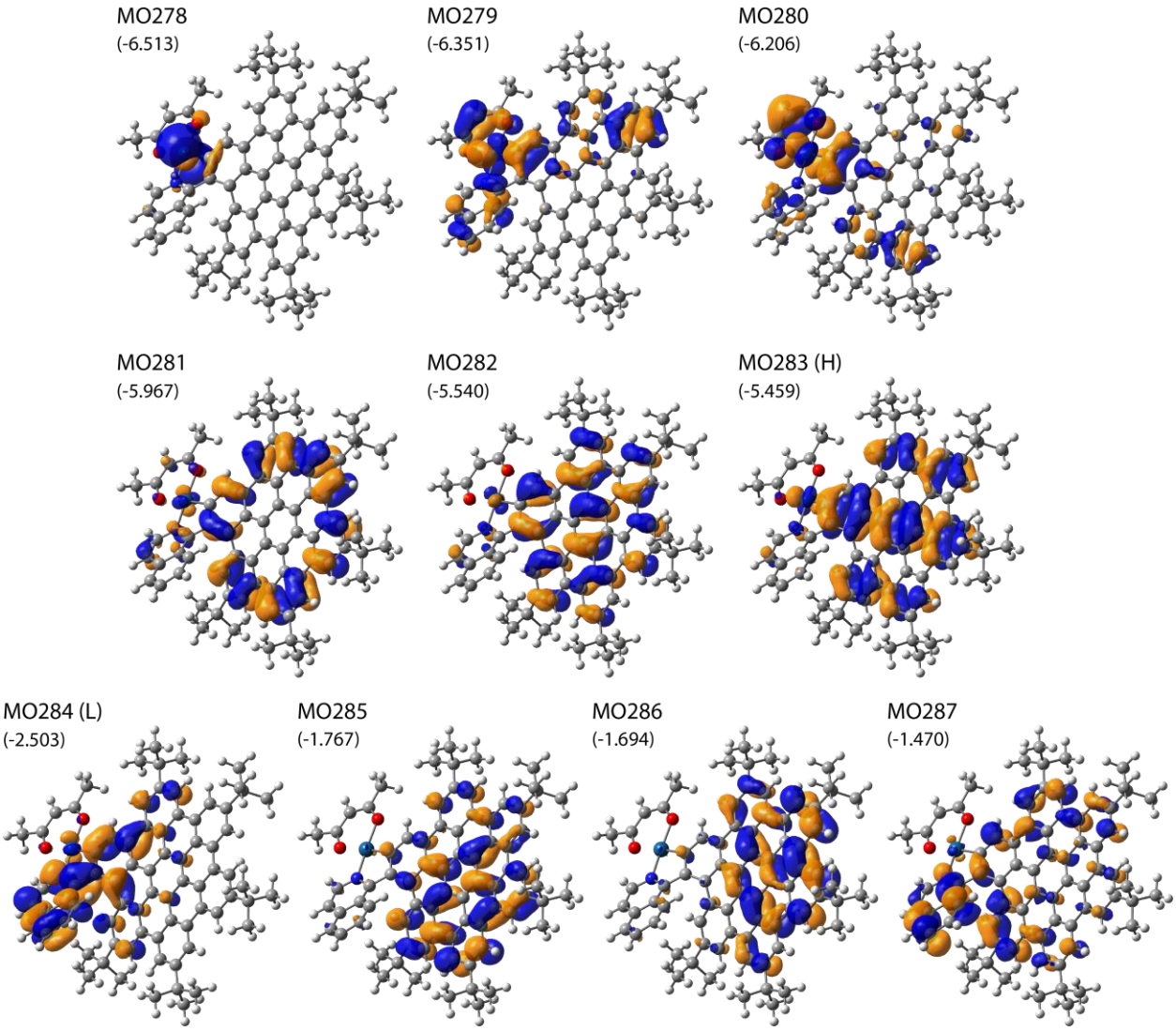

Figure S22. Isosurfaces (±0.025 au) of MOs involved in selected electronic transitions of **NG1**. Based on TDDFT-PBE0/SV(P)-ECP/PCM(toluene) calculations. H = HOMO, L = LUMO. In parentheses, orbital energies in eV are listed.

Table S5. Selected dominant excitations and occupied (occ) – unoccupied (unocc) MO-pair contributions (≥ 8%) for (*P*)-**NG2**. Based on TDDFT-PBE0/SV(P)/PCM(toluene) calculations. See Figures S20-S21 for the corresponding simulated UV-Vis and ECD spectra. See Figure S23 for MOs isosurfaces.

Excitation	*E* / eV	λ / nm	*f*	*R* / 10^{-40} esu^2 cm^2	occ no.	unocc no.	%
1	2.472	502	0.373	17.55	259	260	53.7
					258	260	42.2
2	2.484	499	0.136	-29.67	258	260	51.7
					259	260	42.1
3	2.956	419	0.067	16.16	257	260	91.2
4	3.004	413	0.116	-24.59	258	261	54.2
					259	262	34.6
5	3.090	401	0.085	44.48	259	261	65.1
					258	262	27.8
6	3.340	371	0.698	46.75	258	262	30.7
					259	262	18.8
					259	261	13.8
					259	263	12.8
					258	261	12.0
7	3.357	369	0.807	102.87	259	262	33.2
					258	262	25.8
					258	261	18.2
					259	261	8.2
8	3.436	361	0.054	93.24	256	260	52.3
					258	263	33.6
9	3.471	357	0.461	-125.40	259	263	72.0

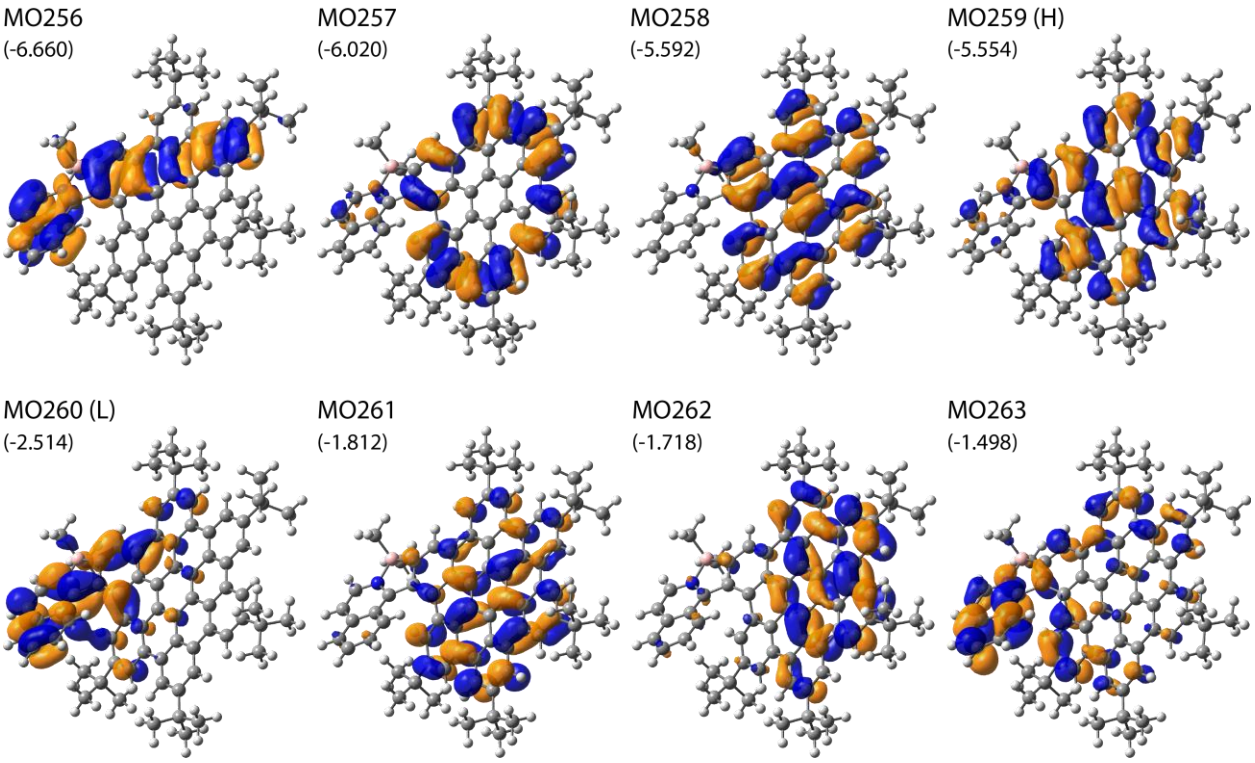

Figure S23. Isosurfaces (±0.025 au) of MOs involved in selected electronic transitions of **NG2**. Based on TDDFT-PBE0/SV(P)/PCM(toluene) calculations. H = HOMO, L = LUMO. In parentheses, orbital energies in eV are listed.

Table S6. Selected excitations and occupied (occ) – unoccupied (unocc) MO-pair contributions (≥ 8%) for (*P*)-**7**. Based on TDDFT-PBE0/SV(P)/PCM(toluene) calculations. See Figures S20-S21 for the corresponding simulated UV-Vis and ECD spectra. See Figure S24 for MOs isosurfaces.

Excitation	*E* / eV	λ / nm	*f*	*R* / 10^{-40} esu^2 cm^2	occ no.	unocc no.	%
1	2.890	429	0.005	1.80	247	249	50.2
					248	250	39.2
2	2.975	417	0.177	-48.20	248	249	76.6
					247	250	17.3
3	3.214	386	0.262	6.81	248	251	44.0
					247	250	21.9
					248	250	14.0
4	3.235	383	0.230	111.26	247	251	28.0
					247	249	28.0
					248	250	14.5
					248	251	11.4
5	3.356	369	0.642	-131.73	247	250	26.5
					246	249	21.3
					248	251	19.0
					248	252	12.9
					247	251	8.9
6	3.399	365	0.899	142.36	247	251	43.5
					248	250	21.1
					247	250	11.0
7	3.470	357	0.477	20.49	246	249	44.9
					248	251	18.2
					247	250	11.6
					248	252	8.7

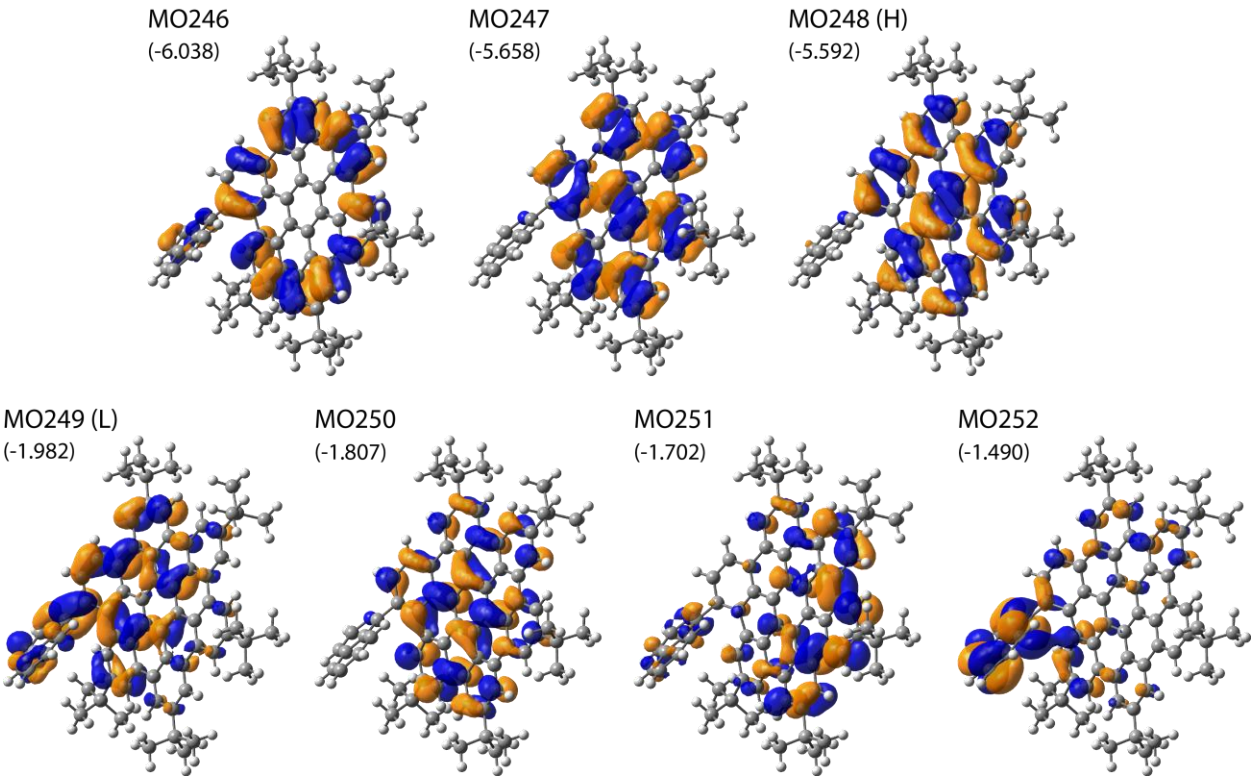

Figure S24. Isosurfaces (±0.025 au) of MOs involved in selected electronic transitions of **7**. Based on TDDFT-PBE0/SV(P)/PCM(toluene) calculations. H = HOMO, L = LUMO. In parentheses, orbital energies in eV are listed.

Table S7. Selected excitations and occupied (occ) – unoccupied (unocc) MO-pair contributions (≥ 8%) for (*P*)-**7'**. Based on TDDFT-PBE0/SV(P)/PCM(toluene) calculations. See Figures S20-S21 for the corresponding simulated UV-Vis and ECD spectra. See Figure S25 for MOs isosurfaces.

Excitation	*E* / eV	λ / nm	*f*	*R* / 10^{-40} esu^2 cm^2	occ no.	unocc no.	%
1	2.904	427	0.002	0.49	247	249	46.3
					248	250	41.9
2	3.000	413	0.146	-26.88	248	249	73.2
					247	250	20.3
3	3.229	384	0.245	-38.25	248	251	52.8
					247	250	24.1
					248	249	12.3
4	3.259	380	0.276	62.22	247	249	36.6
					247	251	32.7
					248	250	18.6
5	3.368	368	0.711	-98.50	247	250	24.3
					248	252	18.1
					248	251	16.9
					246	249	15.0
					247	251	10.7
6	3.404	364	0.952	70.97	247	251	35.2
					248	250	20.9
					247	250	14.2
					247	249	8.2
7	3.483	356	0.499	9.42	246	249	34.0
					248	252	18.8
					248	251	15.1
					247	250	10.4

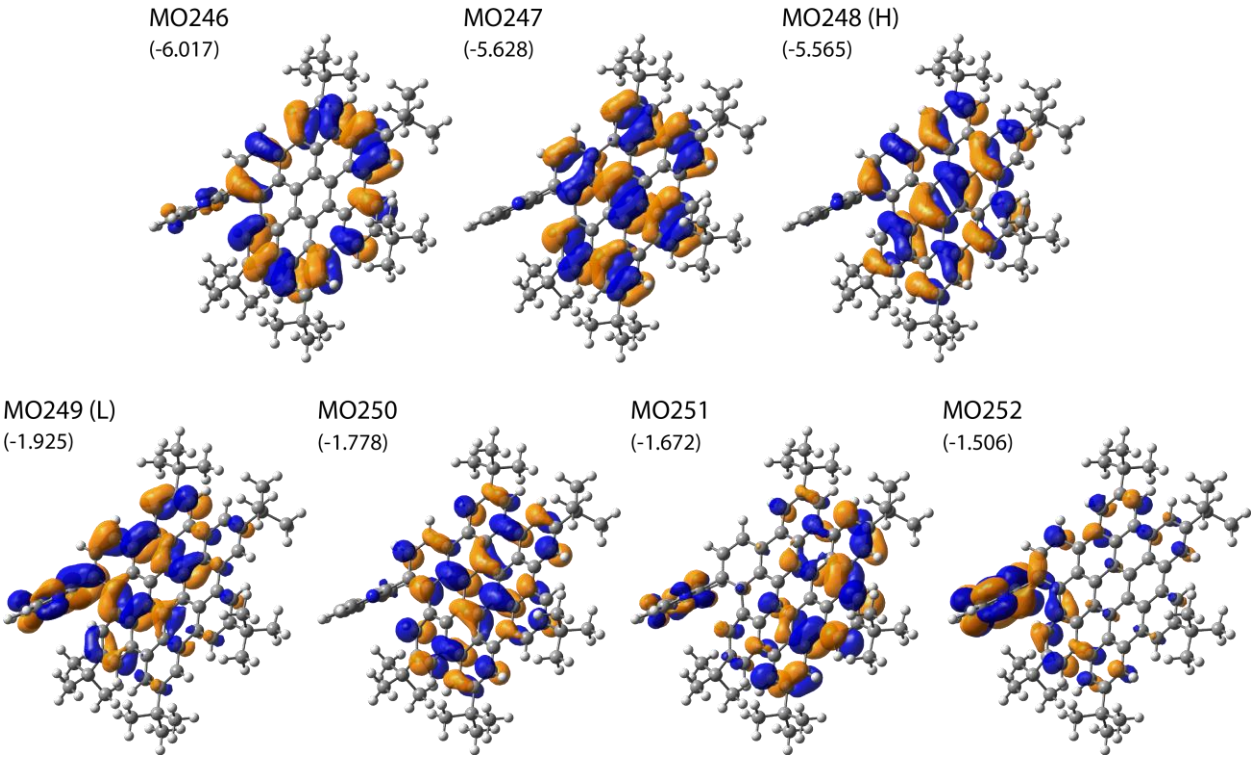

Figure S25. Isosurfaces (±0.025 au) of MOs involved in selected electronic transitions of **7'**. Based on PBE0/SV(P)/PCM(toluene) calculations. H = HOMO, L = LUMO. In parentheses, orbital energies in eV are listed.

Table S8. Selected excitations and occupied (occ) – unoccupied (unocc) MO-pair contributions (≥ 8%) for (*P*)-**8**. Based on TDDFT-PBE0/SV(P)-ECP/PCM(toluene) calculations. See Figures S20-S21 for the corresponding simulated UV-Vis and ECD spectra. See Figure S26 for MOs isosurfaces.

Excitation	*E* / eV	λ / nm	*f*	*R* / 10^{-40} esu^2 cm^2	occ no.	unocc no.	%
1	2.321	534	0.142	-24.54	286	287	88.3
2	2.384	520	0.324	9.06	285	287	88.4
3	2.845	436	0.052	26.05	284	287	85.1
5	3.038	408	0.031	26.25	283	287	52.7
					285	288	14.7
					286	289	11.2
6	3.071	404	0.146	17.05	286	288	64.3
					285	289	23.6
7	3.308	375	0.158	-28.30	281	287	47.0
					286	290	17.6
					285	289	14.5
8	3.317	374	0.320	148.66	281	287	29.9
					286	290	19.0
					286	289	15.6
					285	288	10.6
					285	289	9.9
9	3.338	371	0.937	-40.38	286	289	27.8
					285	288	27.8
					285	289	19.0
					281	287	8.5
10	3.405	364	0.590	-22.35	286	290	51.6
					285	289	23.9
11	3.426	362	0.165	6.85	285	290	52.7
					282	287	32.3
12	3.521	352	0.081	40.06	282	287	46.6
					285	290	33.6

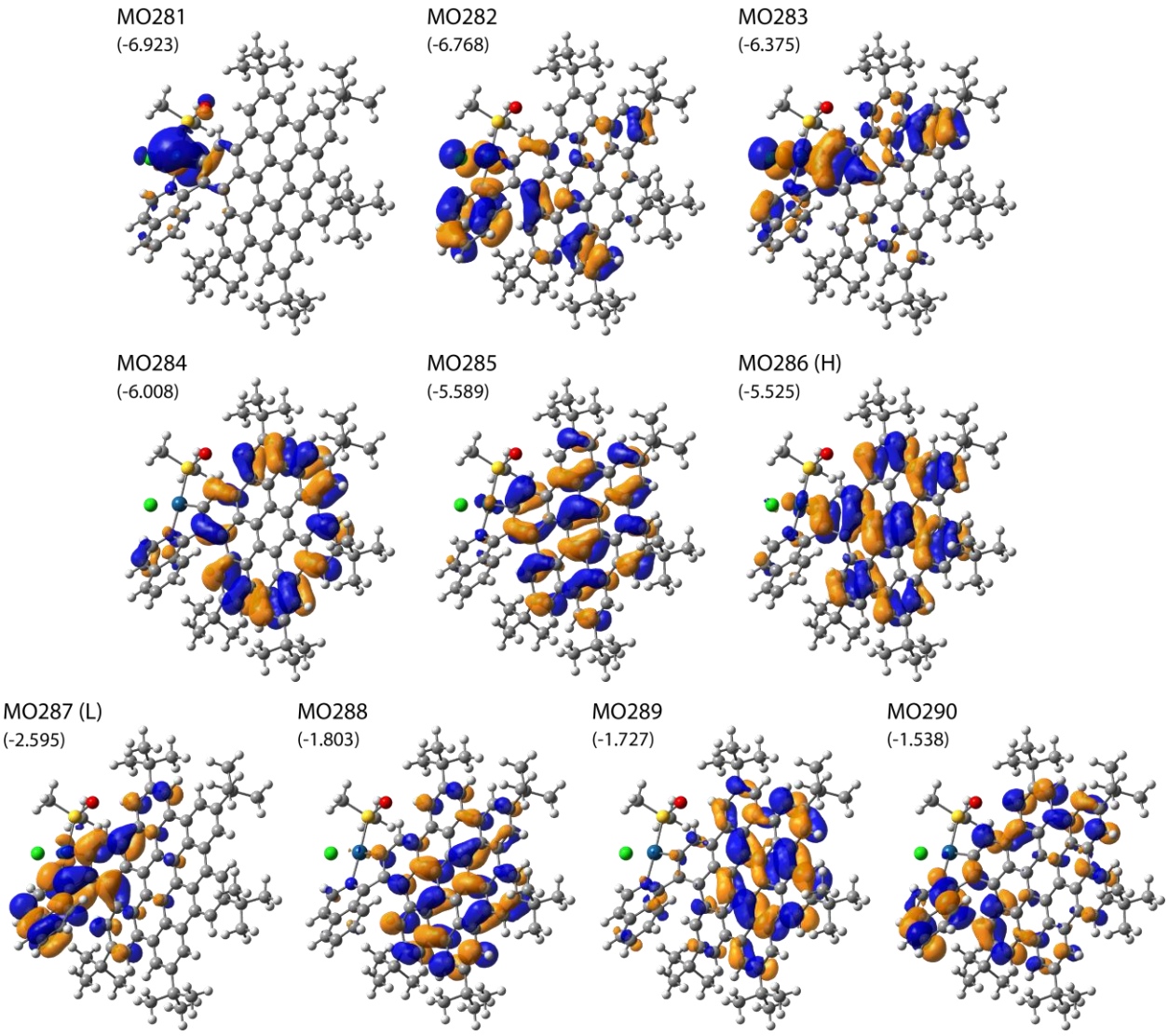

Figure S26. Isosurfaces (±0.025 au) of MOs involved in selected electronic transitions of **8**. Based on PBE0/SV(P)-ECP/PCM(toluene) calculations. H = HOMO, L = LUMO. In parentheses, orbital energies in eV are listed.

Table S9. Experimental and calculated (TDDFT(/TDA)-PBE0/SV(P)(-ECP)/PCM(toluene)) emission data of helicenic Pt(II)- and B(III)-based nanographene complexes along with their parent ligand (in their *P* stereochemistry): relative energy values, Δ*E*, in kcal/mol, with respect to the lowest-energy structure, for different conformational isomers in the case of **7**, vertical S_1-S_0 and T_1-S_0 energy difference representing respectively fluorescence and phosphorescence energy, E_{em}, in eV, and λ, in nm, the corresponding oscillator strength *f*, rotatory strength, *R*, in 10^{-40} esu² cm², luminescence dissymmetry factor, $g_{lum} = 4R/D$ (*D* – dipole strength), and occupied (occ) – unoccupied (unocc) MO-pair contributions (≥ 8%). For MOs isosurfaces, see Figures S27-S28.

System	Δ*E*	E_{em}	λ_{em}	*f*	*R*	g_{lum}	occ no.	unocc no.	%
				S_1 [a]					
7	0.00	2.754	450	0.011	2.16	$+8.18\times10^{-4}$	247	249	51.9
							248	250	35.0
7'	1.30	2.752	451	0.012	1.96	$+7.04\times10^{-4}$	247	249	50.8
							248	250	34.3
NG2	–	2.205 (2.352)	562 (527)	0.341 (0.278)	90.28 (-82.19)	$+8.87\times10^{-4}$ (-1.06×10^{-3})	259 (258)	260 (260)	94.5 (92.1)
				T_1 [b]					
7	0.00	1.711	725	–	–	–	248	249	81.3
							246	249	8.4
7'	1.54	1.809	686	–	–	–	248	249	79.7
							246	249	8.4
8	–	1.444	858	–	–	–	286	287	81.9
							284	287	9.8
NG1	–	1.466	845	(1.88×10^{-4})	(-2.42×10^{-2})	(-3.16×10^{-4})	283	284	82.5
							281	284	8.8

[a] Values in parentheses correspond to the S_2 excited state, calculated at the optimized S_1 geometry.

[b] Values in parentheses correspond to results obtained based on TDDFT/TDA-PBE0/TZ2P&DZ(P)/COSMO(toluene) ZORA-SOC calculations: *f* (*R*) – sum of oscillatory (rotatory) strengths of three triplet components; g_{lum} – computed using *R* and *D* averaged over three triplet components. Note that the computed g_{lum} sign proved highly sensitive to the basis set used for Pt (negative for TZ2P and QZ4P, positive for TZP).

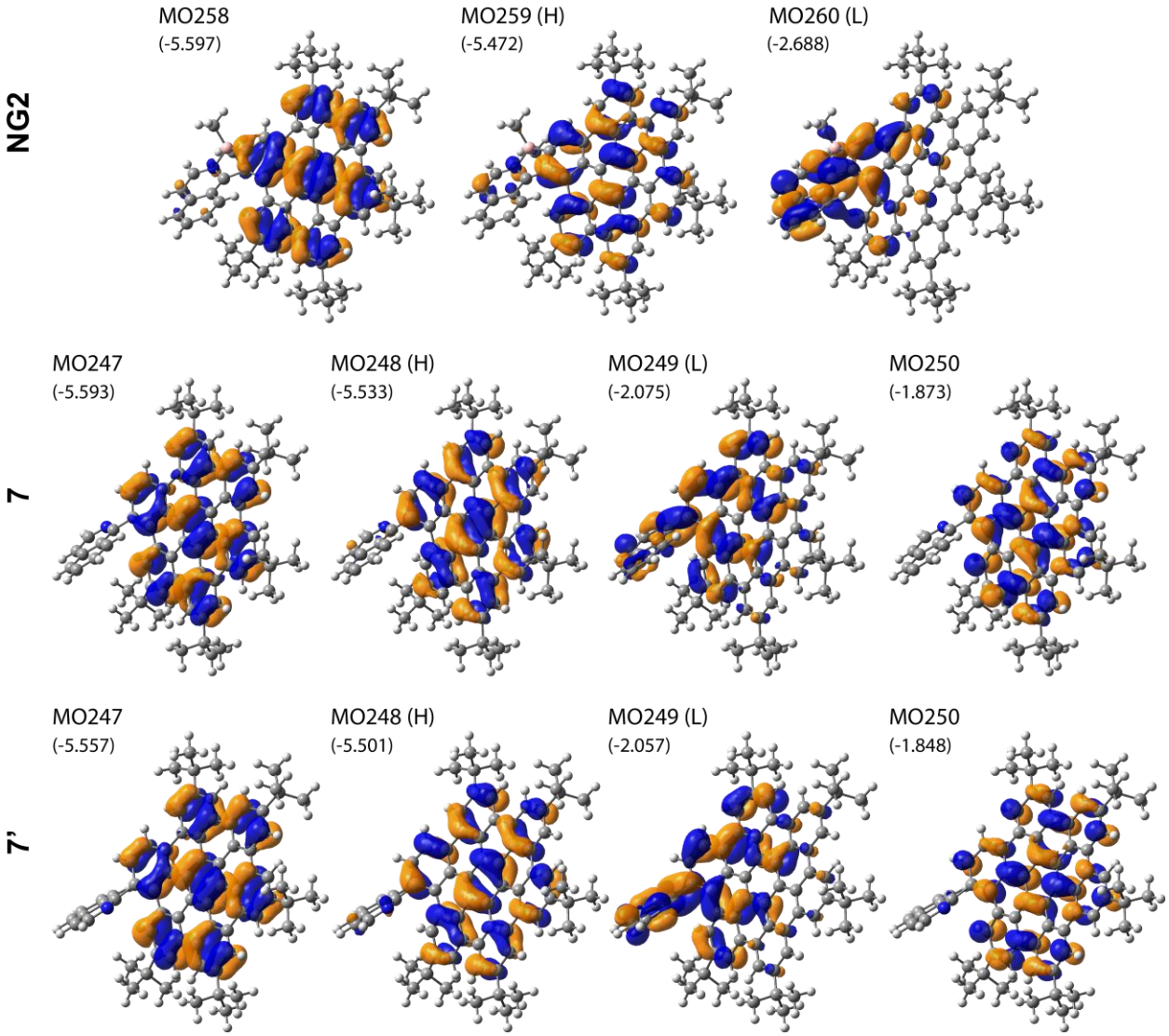

Figure S27. Isosurfaces (±0.025 au) of MOs involved in singlet-singlet emission transitions for helicenic B(III)-based nanographene complex and its parent ligand. Based on PBE0/SV(P)/PCM(toluene) calculations. H = HOMO, L = LUMO. In parentheses, orbital energies in eV are listed.

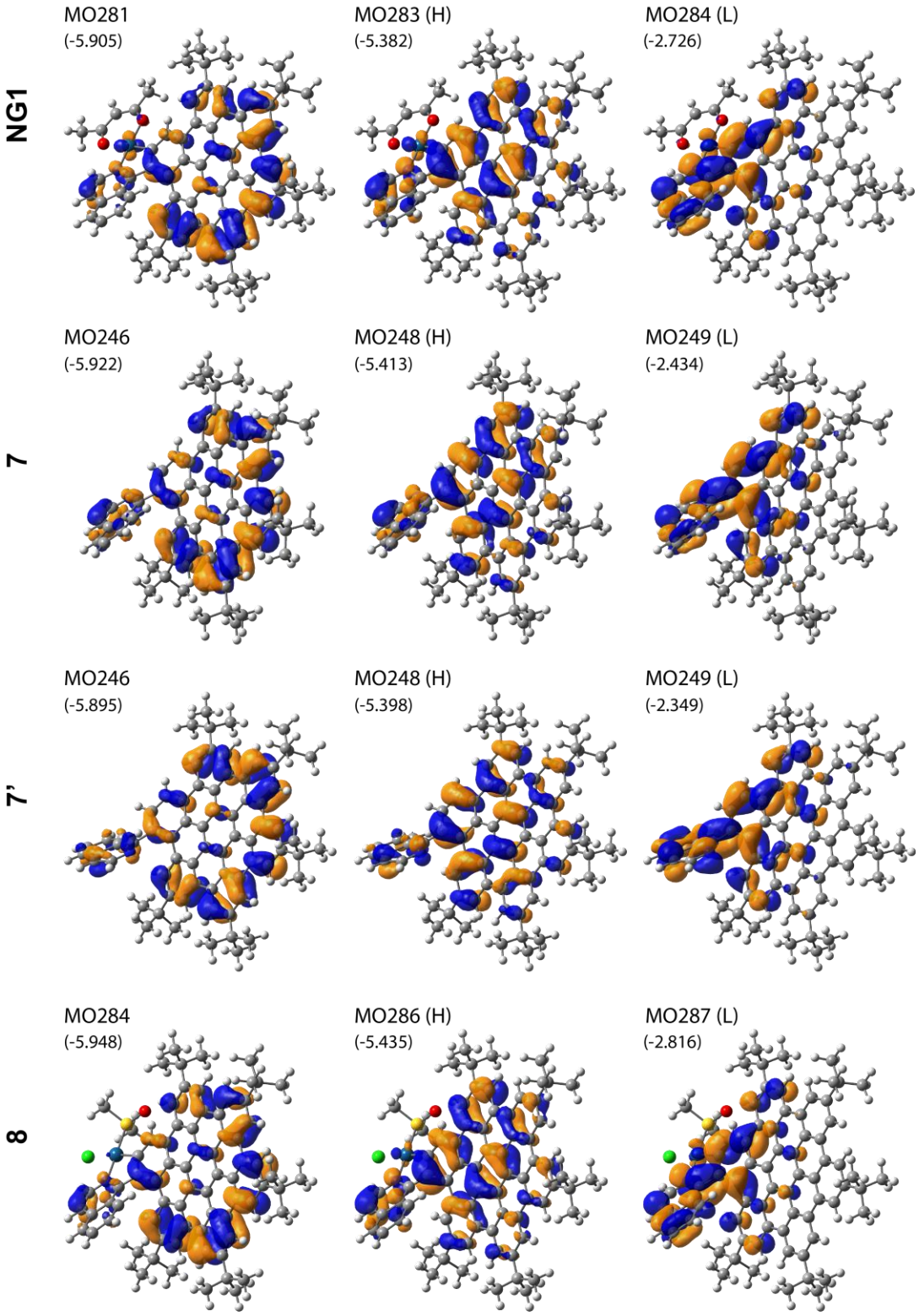

Figure S28. Isosurfaces (±0.025 au) of MOs involved in triplet-singlet emission transitions for helicenic Pt(II)-based nanographene complexes and their parent ligand. Based on PBE0/SV(P)(-ECP)/PCM(toluene) calculations. H = HOMO, L = LUMO. In parentheses, orbital energies in eV are listed.

Cartesian coordinates for optimized structures

Optimized (DFT-B3LYP+D4/SV(P)(-ECP) with continuum solvent (toluene) model) geometries of the examined systems in their ground state along with the corresponding absolute energies:

The atomic symbol followed by three Cartesian coordinates, in Å.

NG1

Total energy = -3260.589213 au

Pt	-0.14284727619624	-0.03331579131578	0.06921542248312
O	-0.96767992129507	-1.79325059707758	-0.84234081037401
C	-0.58271087168016	-2.97733097592640	-0.59411183737123
C	-1.30568879148001	-4.06268610328729	-1.36031578978842
H	-2.38996316686026	-3.98890969095959	-1.16002879103671
H	-0.95662812962951	-5.07410887602318	-1.10144690589327
H	-1.16561892557847	-3.89727605219346	-2.44424161554784
C	0.43852692177337	-3.34301737109625	0.31216786884195
H	0.64892232088261	-4.40933726624632	0.40629064373806
C	1.21422341191609	-2.48217098504478	1.10555265834254
C	2.27172665287570	-3.05956049128639	2.01754031207625
H	3.25600850598618	-2.63313525771947	1.75111822819568
H	2.32522215877647	-4.15753470750460	1.96260263912073
H	2.06071929050169	-2.75638447937259	3.05912084864181
O	1.13535514131687	-1.20566783756419	1.15825556136538
N	-1.26585921500717	1.28601648794828	-0.98578067444137
C	-2.06860328749008	0.88373291050907	-2.00784917532886
H	-2.20621236236629	-0.19607696576851	-2.09209519629878
C	-2.65420514181792	1.78262808535638	-2.85999917764156
H	-3.32718531752119	1.43729949364116	-3.64804803401501
C	-2.31170932867972	3.15760831079561	-2.75784568775008
C	-2.77990710810538	4.11811476154380	-3.69356341413319
H	-3.47755476401561	3.79592794552841	-4.47186666492525
C	-2.33816063016246	5.42326330777049	-3.63720891950088
H	-2.69755016928117	6.15695762953367	-4.36468573898433
C	-1.38778653179236	5.80886444369698	-2.66039771923079
H	-0.99894306367599	6.83081654032159	-2.65327873047578
C	-0.94378702374096	4.90359512131975	-1.71970358969577
H	-0.19675546421155	5.21075668291806	-0.99067345720630
C	-1.42506710460577	3.56726635965662	-1.71228440691128
C	-1.02624263944309	2.59331279266551	-0.73309836459194
C	-0.23432121685307	2.81532353289854	0.48058110616268
C	-0.12246729104093	3.99594401291126	1.26319094430125
C	-1.14671647572734	5.03055390712437	1.30960594308269
C	-2.46168315902653	4.77308047318350	0.89186426588101
H	-2.72217959765839	3.75455622194493	0.62009677083292
C	-3.42895519123938	5.77374484869749	0.82773011251348
C	-4.85829749775397	5.50888632424776	0.33393478871346
C	-5.86604254523727	5.90680367330592	1.43417481470735
H	-5.69603952686365	5.31752252894196	2.35300601800726
H	-6.90078668918093	5.72060640332526	1.09277484382340
H	-5.78707997110005	6.97566514883745	1.69769312064664
C	-5.11330039713850	6.35291814274569	-0.93479391824030
H	-4.99968261684740	7.43320505475891	-0.73822300410470
H	-6.14078894813182	6.18459060479363	-1.30646851774273

H	-4.40629022979841	6.07608371587021	-1.73623287892818
C	-5.08448096586305	4.02901452860627	-0.01916894807367
H	-4.41873309021892	3.69408257993926	-0.83275873970695
H	-6.12531381252845	3.88380125021116	-0.35854859511901
H	-4.92305140910878	3.37097898831494	0.85232194073064
C	-3.04903170598604	7.06669008445538	1.21222546196607
H	-3.78780263700998	7.86442865797161	1.14852640478075
C	-1.77854879538347	7.35754926000034	1.72567500670246
C	-1.40645433159566	8.70250379699179	2.17152624651261
C	-2.25415374255353	9.79806805599648	1.97488953703652
H	-3.20049214961735	9.64603045005525	1.45818040480147
C	-1.92810112914177	11.08920712003662	2.40651719514922
C	-2.90710480996013	12.24577575712971	2.15440879425898
C	-4.25412650704186	11.93097234158246	2.84239996302367
H	-4.97450525909250	12.75178869996493	2.67103791533607
H	-4.12025373736290	11.81324325113266	3.93268458089083
H	-4.70578604240068	11.00140316405845	2.45500044575358
C	-2.38412397927084	13.58295054649354	2.70566866203749
H	-3.11915892499202	14.38146557831569	2.50212007957097
H	-1.43169716344588	13.87686886677920	2.23124825457999
H	-2.22803951836274	13.54302157312481	3.79773392687990
C	-3.12858216755149	12.40234815598005	0.63363640128840
H	-3.54739321153831	11.48600574248129	0.18304567174480
H	-2.17717457106198	12.62889315757000	0.11979590288243
H	-3.83392675351942	13.22923473975721	0.43178928814742
C	-0.70908118641674	11.26237705176564	3.06137321825370
H	-0.44370904381013	12.25394187564778	3.41583640979280
C	0.18606719680981	10.20170446482016	3.28332393950781
C	1.45217152456349	10.40545829773239	3.98962739084943
C	1.83912709256654	11.67823562463630	4.44215448608302
H	1.18942143757415	12.52510147065687	4.24237131043516
C	3.02841189994631	11.89507345134734	5.13675663342123
C	3.46390882754267	13.28477474404835	5.62581391519903
C	4.80461685851758	13.65905605804945	4.95605565944106
H	4.70017326756540	13.68487771871776	3.85658505364222
H	5.13853202268006	14.65747241726415	5.29341714991453
H	5.60208520391036	12.93713485572959	5.20277791360762
C	3.64332417296667	13.25380640581165	7.15994006678555
H	2.69782011583193	12.97733090692530	7.65997583707586
H	4.41453509144747	12.52754569421714	7.46927293676019
H	3.95079425217155	14.24868893010931	7.53086226224212
C	2.43191957713318	14.37264304549832	5.28394988467427
H	2.28189865622782	14.46895142732524	4.19449905012771
H	1.45223031670443	14.16831715004318	5.75001323383189
H	2.78382229370770	15.34949739827974	5.65979819245565
C	3.84298298372522	10.78523723136561	5.38827445090852
C	3.51076804443114	9.49329890210018	4.96475839084092
C	4.37440339722225	8.34496508649442	5.25585818181708
C	5.54391861846276	8.48427127635173	6.01259212059466
H	5.81205507568730	9.46716884948454	6.39567154289261
C	6.38601229720412	7.40627138309521	6.30667849132223
C	7.65089562422348	7.63400744630345	7.14791178506220
C	8.56156577855805	8.65729976633319	6.43388257097410
H	9.47917602202540	8.83280952180309	7.02484396165354

H	8.86059552994209	8.28868247967806	5.43628129883390
H	8.05886940432232	9.63044815997196	6.29844790101894
C	7.24706091552857	8.18217455453390	8.53469950727796
H	6.58841156577032	7.46906079357003	9.06199351437521
H	8.14486412992549	8.34721894505321	9.15810991882707
H	6.71132844531828	9.14395269696315	8.45655082856547
C	8.45255579043755	6.33804936053628	7.35686640281161
H	7.86293869647936	5.57264749193046	7.89100501894193
H	8.79093699275941	5.90605403614484	6.39892542210546
H	9.35064632519187	6.55052421548427	7.96313420078030
C	6.02524962620407	6.15338885218680	5.81246142941027
H	6.66711961459049	5.30358473543599	6.02464761107868
C	4.86369072643792	5.95030177808608	5.04932252261962
C	4.51340185323805	4.62372870703319	4.53704643720427
C	5.30786619797901	3.49999172328547	4.80030464182623
H	6.19900750611235	3.61589598610727	5.41457278839525
C	5.00620573819557	2.22643400362909	4.30377576891355
C	5.92282999133720	1.03939835855904	4.63558144217413
C	7.34176487536293	1.32494304697990	4.09617317592669
H	8.01724789890805	0.48105903119618	4.32761186779527
H	7.77629896370749	2.23573330551408	4.54352604756363
H	7.32453476969494	1.46101744297272	2.99999619031534
C	5.42360120694317	-0.27455460061008	4.00948773072340
H	5.39073686099263	-0.21821664472589	2.90746861529000
H	4.41529095368131	-0.54415491200916	4.36915394392611
H	6.10733687524766	-1.09783108967327	4.28172968645671
C	5.98010975020650	0.85512895404362	6.16822525740384
H	6.64128275075935	0.00849206446775	6.42892996847696
H	4.97513539388167	0.64501167749268	6.57604103106402
H	6.37011519631841	1.75437684682600	6.67548921380450
C	3.86786463345183	2.09795891035224	3.50961826107014
H	3.62068690995959	1.12545824048622	3.09495370851423
C	3.02788034221897	3.18592474937836	3.21963444167783
C	1.85248051662442	3.01995284114690	2.37109130418892
C	1.50418726030419	1.77432399406036	1.82122901305109
H	2.04322619327648	0.86975101629185	2.10000920494502
C	0.48928767623977	1.65800799319742	0.88019184915382
C	1.00880878639441	4.13908909427047	2.11660390327644
C	1.30209761700100	5.42002038717307	2.71114175091668
C	0.43045531052296	6.51882740516349	2.50095526190670
C	-0.82326065138796	6.30989865940761	1.82800953450919
C	0.75001673132094	7.79751029212839	3.02388119462701
C	-0.15454687599419	8.90204704493613	2.82245975215560
C	1.95394517872116	7.98331995665129	3.75042797124239
C	2.30280904350168	9.29393320199494	4.23819329074813
C	2.81156240430695	6.87719498451527	3.99452849638292
C	4.01778971091412	7.05653153041195	4.76510864275585
C	2.48079919342825	5.59446695209005	3.48408231450139
C	3.34093910223107	4.46865427376913	3.74554522832395
H	4.77306541112290	10.94181625459747	5.93124173948524

NG2

Total energy = -2900.817250 au

B	0.25346929333763	0.01358531347191	0.00602797391364
C	-0.62248235033775	-0.96393223498767	0.97564788420383

H	0.03807987282984	-1.45007220360212	1.71975896398322
H	-1.40712028007223	-0.42207596562948	1.53890920484577
H	-1.11719986789911	-1.77587385721676	0.40489409981397
C	1.34841253634044	-0.78610495416894	-0.90031318597467
H	1.88506466041341	-0.12937061289074	-1.61255472111013
H	2.11046539179760	-1.24054421132704	-0.23687781791340
H	0.89510098826051	-1.61440230427034	-1.48117873590420
N	-0.72517071386238	0.82849507406769	-0.99026343852075
C	-1.46031355984151	0.27045161382618	-1.98231134932784
H	-1.47118527878030	-0.82115687177254	-2.00594676949582
C	-2.14244356976418	1.04031464654106	-2.88710113348565
H	-2.75745420683523	0.57383254750566	-3.65974533924145
C	-1.97708360502850	2.45359402889673	-2.85677202147366
C	-2.55216171226292	3.29702409526877	-3.84378455975263
H	-3.19568143237720	2.85083084964644	-4.60738128147138
C	-2.27692688066551	4.64917840786744	-3.85579653474998
H	-2.71795521764050	5.29135871283170	-4.62380132805901
C	-1.39523254546520	5.20472674701487	-2.89769968465515
H	-1.14135953587198	6.26720924091895	-2.94325119574363
C	-0.85245297176838	4.41411156151311	-1.90547176905540
H	-0.15981467816612	4.84980877957414	-1.18813943414113
C	-1.16134902624937	3.03142226079663	-1.83227377840281
C	-0.64734227219197	2.16191467019300	-0.81153335567130
C	0.11991857879672	2.46387050645890	0.40089059388271
C	0.22861578029315	3.65029105193674	1.17118730817118
C	-0.78501769984130	4.69296429571593	1.21077080836133
C	-2.09779124642722	4.44794261107324	0.77798731236810
H	-2.36044840218441	3.43476382806476	0.48917888144092
C	-3.06106398200023	5.45330648971723	0.72519436484116
C	-4.49132686904191	5.20025712193430	0.22703214290812
C	-5.49117095474238	5.52601016317272	1.35793800844914
H	-5.30687488634912	4.88672194331617	2.23983054526299
H	-6.52818360004912	5.35131579258703	1.01707635967050
H	-5.41575959977968	6.57875643123669	1.68108730639396
C	-4.77144233049147	6.10857829607959	-0.99076452601102
H	-4.67786577966142	7.17840107240435	-0.73627398688125
H	-5.79849953446233	5.94125334173228	-1.36360394975553
H	-4.06696366599034	5.88979931655612	-1.81237792840703
C	-4.70387530875448	3.73944949811375	-0.20526857766151
H	-4.03042986333857	3.45383448362053	-1.03119959818725
H	-5.74179386150921	3.60428899758163	-0.55745221648403
H	-4.54258032657825	3.03684207159450	0.63069785051044
C	-2.67862953338976	6.73813047368531	1.13360703935843
H	-3.41463830036020	7.53919915708935	1.08133149411530
C	-1.40852485280567	7.01685758264926	1.65484716331913
C	-1.03154467327485	8.35454639423885	2.11727994370287
C	-1.87375649658078	9.45619442475258	1.93114660439731
H	-2.81998865868873	9.31416431978179	1.41142436927018
C	-1.54208716254080	10.74104411689464	2.37692575910915
C	-2.51546070381879	11.90505432126523	2.13782798883367
C	-3.86332267313118	11.58959992075249	2.82377941812945
H	-4.57983711785436	12.41568858305603	2.66195289761116
H	-3.72893808306104	11.45955982834183	3.91260054621451
H	-4.31985000348325	10.66639509965585	2.42690701447676

C	-1.98519549719139	13.23377622628276	2.70245093703598
H	-2.71644003538959	14.03800734818195	2.50799778383729
H	-1.03180820177603	13.52768740190293	2.22995062589734
H	-1.82801685165927	13.18202477180872	3.79389681036908
C	-2.73756865280634	12.07871162982247	0.61903530660265
H	-3.16206921517617	11.16961454219630	0.15924378664621
H	-1.78546935169019	12.30532796666594	0.10653280111164
H	-3.43846444478574	12.91160714716159	0.42662907435834
C	-0.32253091196577	10.90114910019914	3.03388829794987
H	-0.05276703631014	11.88752176867519	3.39930185349124
C	0.56722610119026	9.83385470345447	3.24529166270932
C	1.83378874988255	10.02466208257582	3.95383385233459
C	2.22889893061292	11.29210744703990	4.41416680660326
H	1.58612042720489	12.14483646036848	4.21717226818746
C	3.41777767452838	11.49630465225439	5.11321535933186
C	3.86081190395807	12.87947375610646	5.61374984330594
C	5.21245749001949	13.24533520845143	4.96149528638620
H	5.12127875387403	13.27632725844438	3.86097412427108
H	5.55037522477074	14.23969110430494	5.30683682287300
H	6.00112803187850	12.51609071218944	5.21502997397384
C	4.02240388128872	12.83822046715768	7.14961183609536
H	3.06872583023581	12.56800921961786	7.63739122171363
H	4.78289660128651	12.10249261939100	7.46316557202525
H	4.33529178657037	13.82784552649883	7.52996702421599
C	2.84291091719930	13.97863519111674	5.26568347204435
H	2.70462150337357	14.07988271409238	4.17510758708843
H	1.85659797839052	13.78270989489901	5.72126638374061
H	3.20066860691456	14.95067275550304	5.64837144521605
C	4.22363250540065	10.37916156826146	5.36000015458236
C	3.88362399059094	9.09237621937293	4.92704067319011
C	4.73848498328747	7.93645494334940	5.21266395344785
C	5.90869800412554	8.06374802617761	5.97018947771621
H	6.18440941441380	9.04300984900552	6.35708118432280
C	6.74267474149084	6.97829213541367	6.25967921795107
C	8.00966574843574	7.19322136019126	7.10098441347469
C	8.92749697290607	8.21270990508655	6.39063329210147
H	9.84689802447032	8.37830115453725	6.98163921924595
H	9.22288176296380	7.84618152361062	5.39118002968928
H	8.43229281340840	9.19036942616088	6.25993044019735
C	7.61073469055436	7.73853780160599	8.49031374688838
H	6.94738421681275	7.02801072693445	9.01519798556698
H	8.51016752956920	7.89444232644676	9.11370987170879
H	7.08193294185384	8.70450894975020	8.41665958868339
C	8.80191704961771	5.89056031740767	7.30400758010882
H	8.20734447959274	5.12744918355118	7.83589950701998
H	9.13611064958302	5.45982068342012	6.34402628824771
H	9.70209205442606	6.09419209847677	7.91016940833314
C	6.37185968939395	5.73027475057490	5.76090562389686
H	7.00734876707462	4.87491853412673	5.96956609642581
C	5.20863744068876	5.53935023100554	4.99692401661543
C	4.84717377492431	4.21750280329420	4.48075661072965
C	5.63149291291101	3.08762075227221	4.74584643067752
H	6.52076418749764	3.19567011378226	5.36396886614820
C	5.32263488555367	1.81791578817860	4.24587849203936

C	6.23316495359269	0.62667719890045	4.57959445444056
C	7.65634131461694	0.90848383570711	4.04931487426486
H	8.32664486862082	0.06073866810839	4.28151355279553
H	8.09265689619748	1.81560576314585	4.50227056183859
H	7.64610189458237	1.04835544722058	2.95351135759805
C	5.73351714915466	-0.68322843474712	3.94715905740837
H	5.70715503479512	-0.62268699907800	2.84524742440768
H	4.72287152172899	-0.95046485485336	4.30173655433849
H	6.41299713474837	-1.50981377662986	4.21984941657687
C	6.28085820718718	0.43838528810081	6.11210973800033
H	6.93665942566611	-0.41195531797871	6.37420448591809
H	5.27270379068406	0.23164855595107	6.51376093148218
H	6.67204328003491	1.33448941219651	6.62398662043654
C	4.18536817837702	1.69914619918384	3.44775804723862
H	3.93556232033389	0.72875857526961	3.02941967954300
C	3.35286521034894	2.79315528208584	3.15663336131059
C	2.17829390343975	2.63725105134090	2.30223640465227
C	1.81453442517663	1.39533293166177	1.75004155273129
H	2.34588866398259	0.48785983088104	2.04123194495013
C	0.81915497984642	1.29649328028912	0.78762502326540
C	1.35335105530195	3.77172375610479	2.03634084293642
C	1.65431800473878	5.04817098718759	2.63960031429341
C	0.79257163517734	6.15580554804918	2.43105294220328
C	-0.45819509570095	5.96362606356433	1.74789627851977
C	1.11755054404445	7.42842668781701	2.96663188358291
C	0.22024788224175	8.54031755332996	2.77222191913213
C	2.31937580995391	7.60049672268679	3.69931753438629
C	2.67613876456343	8.90567902733012	4.19668357036583
C	3.16736502881914	6.48608867603552	3.94047923810452
C	4.37240394701071	6.65311219485324	4.71565220393849
C	2.82846871237129	5.20835808784653	3.42219471970535
C	3.67629425780928	4.07306693015981	3.68476556642280
H	5.15256064777984	10.52573411079232	5.90770232476468

7

Total energy = -2796.755601 au

C	0.21228814213707	0.04973166899541	-0.24551469559615
C	1.26132814188734	0.89811212988117	0.48659458219083
C	2.60066349742276	0.92600857064441	0.09904140642981
C	3.54194907681466	1.76191442541831	0.71848934369393
C	4.89971377782235	1.90454225789788	0.19924256864851
C	5.24482158815320	1.57648791887421	-1.13454471117141
C	4.27278753492051	1.33019238712853	-2.24139461574035
N	4.44347214494971	0.21612176395921	-2.93159788619552
C	3.61247838466656	-0.06193092699030	-3.96459054451868
H	3.80901628922217	-1.00095668777514	-4.49547545255048
C	2.56583018936792	0.74985052652515	-4.33677536504230
H	1.90029243884799	0.46859845440716	-5.15770160880109
C	2.36308174674634	1.97130317738924	-3.64185489456951
C	1.31197311952704	2.87107185488305	-3.96826410311553
H	0.62412955206925	2.60683000375200	-4.77696733953446
C	1.16703078398761	4.05586601379154	-3.27789795526490
H	0.35349462068614	4.74257842619324	-3.53047742888664
C	2.07887159969418	4.39791567638421	-2.24750931606911
H	1.96813043648491	5.34968041500196	-1.71995304153181

C	3.10588335222151	3.54139737507717	-1.90962375502813
H	3.80684373302058	3.81891605616248	-1.12200913444617
C	3.26177036562446	2.29822533876657	-2.57909069968826
C	6.59720213085250	1.54684358647042	-1.49795248644642
C	7.59344901693531	1.90099051280204	-0.60225215477942
C	7.27631205794684	2.37122607120069	0.68267439315793
C	8.30836140774020	2.82798272497255	1.61043522189649
C	9.67273720407399	2.67604383332660	1.31258820276931
C	10.67684208959381	3.12105834040546	2.17203818306254
C	10.28137932116695	3.75125027908755	3.35710846935257
C	8.93737029953399	3.92749469738437	3.70861631151474
C	8.55048138242356	4.60795408746469	4.94581270698368
C	9.51573149108585	5.10958491230830	5.83436928292598
C	9.17492491859211	5.77401561627097	7.01181908359907
C	7.81371980751853	5.94143397971470	7.28811824678824
C	6.80679399979327	5.46763668162973	6.43892566487909
C	5.38881713055615	5.66779832792000	6.74986184768776
C	4.98251671239129	6.40428958868598	7.86870056821614
C	3.63582932795137	6.60006222235297	8.19449743056822
C	2.68051935050252	6.02066497187838	7.36057199009488
C	3.02662333649294	5.27381962670201	6.22196372699525
C	2.00266309690626	4.66060182546088	5.37500168883972
C	0.63535942044279	4.77611696147462	5.67878031248594
C	-0.35724661341345	4.18537616128108	4.89754206798852
C	0.05159163415094	3.44281859062211	3.78414140308738
C	1.39777685455220	3.28860502114703	3.43479174715823
C	1.80037909315767	2.48703291868229	2.27770347252850
C	0.87915620776324	1.72178815845157	1.55108045840929
H	-0.16774969657102	1.73102498068851	1.84911173453590
C	3.16663840266322	2.47414871538095	1.88624172712107
C	4.16840476140832	3.12347201083731	2.69118874127190
C	5.53631596465290	3.02043952176856	2.32932557487286
C	5.90873665845445	2.41252499916616	1.07200301421595
C	6.53322062907069	3.56813200273355	3.18036589446934
C	6.15845706113212	4.23965833268107	4.37443583381098
C	4.78572918941188	4.37849309179860	4.71086101416087
C	3.79090476345635	3.80853026120310	3.87498549774722
C	2.39713495448032	3.92160976990399	4.22783139048517
C	4.39953004075811	5.10251310638974	5.89667666218348
C	7.17272585028522	4.77510106659009	5.24984759535726
C	7.92597606404652	3.44089226158435	2.83322420625258
H	-0.71152429107183	2.97595763722309	3.16360332705071
C	-1.85420920492101	4.31843804755632	5.21532548667410
C	-2.45767951691562	2.91240557518687	5.42952291439467
H	-3.53617317585760	2.98888903457871	5.65964712945974
H	-1.96222221734982	2.39651135463157	6.27150023788749
H	-2.35014814095743	2.27729954723431	4.53334051590443
C	-2.10967514637630	5.15038309618246	6.48332689445642
H	-3.19582241211448	5.21679210753624	6.67071208772440
H	-1.72495870323941	6.18035589430893	6.38385416505899
H	-1.64454532171149	4.69353853879458	7.37428222003116
C	-2.56427465489528	5.00918843613670	4.02983906592942
H	-2.45561897062115	4.43264169624205	3.09503700929990
H	-2.14791316612073	6.01761364600531	3.85609512111479

H	-3.64499354824149	5.11396477188828	4.23728731970250
H	0.33930842284683	5.34522310887540	6.55493888489936
H	1.62964954812829	6.15432218006702	7.59916820509950
C	3.26403419750660	7.42985159102482	9.43260079126694
C	3.81847229683842	8.86222012347540	9.26749168609865
H	3.39075502094543	9.34758606024331	8.37198004026505
H	3.56140683782061	9.47796755610090	10.14885311490307
H	4.91720314644249	8.86770721457260	9.16299261684517
C	3.88276991949023	6.77812659498648	10.68899567914963
H	3.50252916499552	5.74995340447870	10.82583891574657
H	4.98328134885770	6.72637185972653	10.62568560686438
H	3.62521624951725	7.36315024845259	11.59078428365626
C	1.74236272868545	7.52140131117569	9.63732334783202
H	1.24122628273575	8.00887941704525	8.78296006768261
H	1.28773907206003	6.52578084707403	9.78137337765232
H	1.52435297904437	8.12137749956817	10.53827287902336
H	5.73932038239514	6.85193778458333	8.51017227241583
H	7.53266578467764	6.45466883725579	8.20590776074178
C	10.22415055523350	6.31499327553415	7.99459463830692
C	10.03480582509301	7.83975743931538	8.15460428007390
H	10.78599666708422	8.24834984443556	8.85504490908635
H	10.15310338202320	8.35460364535717	7.18434622130053
H	9.03565075449877	8.08998006450815	8.55086670953588
C	10.03803369024631	5.62510279515362	9.36437230746775
H	10.16888167665063	4.53198616727402	9.27358616935079
H	10.78265235540135	6.00208270246416	10.08927863377061
H	9.03484221322754	5.81245279081970	9.78448534838492
C	11.66194601418073	6.05507174121529	7.51450232607072
H	11.87044732239210	4.97619931347025	7.40814445554004
H	11.86593013018761	6.54278050571261	6.54519662730077
H	12.37791355229764	6.46182756632257	8.25013712446099
H	10.56682743084969	4.97422208928030	5.59726886139752
H	11.05551218875869	4.11484731685760	4.03000115734120
C	12.17194916826939	2.94866462710023	1.86451631697223
C	12.84248791844208	4.33924141989190	1.80208375369202
H	13.91976109075002	4.23613863274828	1.57678228727354
H	12.74999705355028	4.88258879149003	2.75818638373729
H	12.38360698461125	4.96113874382601	1.01275742584649
C	12.41271613933034	2.23527874759851	0.52345584223229
H	11.98914032971146	2.80078404576785	-0.32486451313997
H	11.97620503000970	1.22137718225323	0.51480544962538
H	13.49796977474685	2.13307757614135	0.34742464629839
C	12.82732249975641	2.10906568237791	2.98355398195824
H	13.90620927196195	1.97688822805028	2.78245505421998
H	12.36416110176791	1.10801149521201	3.04495343562941
H	12.72603884038678	2.59023658959209	3.97162038840750
H	9.95435128766277	2.18402372242820	0.38610796380561
H	8.62922836908408	1.86000099098608	-0.93824659615919
H	6.85666637108492	1.25717199099816	-2.51868039338692
H	2.93417451093693	0.27469514979121	-0.70117632070777
C	-0.60860857746090	-0.77577624056247	0.76861035751351
H	0.04606282204578	-1.45196790676006	1.34726114809741
H	-1.35759106631334	-1.39269575062235	0.23972914281755
H	-1.15227822070157	-0.13570782293155	1.48436479926370

C	-0.72566116215823	1.00607833045869	-1.01716196500580
H	-1.23694461771020	1.70758568857841	-0.33444822454720
H	-1.50098602755976	0.43316096548427	-1.55900696911819
H	-0.15845911480708	1.60245277362437	-1.75341800610712
C	0.85216873223028	-0.92395980819659	-1.24972366256143
H	1.39212322431683	-0.39769241953687	-2.05326040400579
H	0.06524610508903	-1.53541308103025	-1.72569534371939
H	1.55891064201213	-1.61193494948178	-0.75314799261316

7'

Total energy = -2796.752175 au

C	-0.01379283064418	-0.00795070730411	0.01736045683367
C	0.23223012775256	0.11648583984801	1.52796648865592
C	-0.05578330819164	1.27877246816043	2.24094565827887
C	0.16713475329317	1.39397892789469	3.62263008616991
C	-0.20550208018558	2.59805094594985	4.36437395537160
C	-1.13524680109422	3.54356776336546	3.86823160936809
C	-2.08716861053834	3.27591750721779	2.74668478307395
N	-2.95344260184841	2.30013109380107	2.94469861783554
C	-3.88953346671277	2.04736047129353	2.00014800354187
H	-4.57794627373564	1.22243967858921	2.21929568104063
C	-4.00546541138319	2.76503027902339	0.82981520565355
H	-4.78370311439714	2.52643853572301	0.09934007988372
C	-3.08706463585504	3.81580577301303	0.57388206599658
C	-3.10392928877587	4.58148858119750	-0.62354586606406
H	-3.87616458659620	4.37554971900947	-1.37075057341049
C	-2.15413714653274	5.55731597553855	-0.84214320265468
H	-2.16970325390362	6.13906879303955	-1.76875404338988
C	-1.14560655751593	5.80621067838926	0.12363822817153
H	-0.38901519705459	6.57224206955987	-0.06989096447186
C	-1.11199844684241	5.08554800229913	1.30006275550953
H	-0.32796940072026	5.27315069250962	2.03658472336119
C	-2.08561024104874	4.08305458556387	1.55977119309039
C	-1.31388575373025	4.75257908855471	4.54895825959987
C	-0.62849745382914	5.02792904259923	5.72224265275249
C	0.21570846969864	4.07060018458076	6.30449750258883
C	0.88805610420260	4.32086265683745	7.57750293627932
C	0.83692664714183	5.58391677095842	8.19019884366680
C	1.44632427178191	5.84177929376494	9.41764925072010
C	2.11233646443644	4.78239369125051	10.04312109998398
C	2.20229357115609	3.50487355316649	9.47694294106813
C	2.89233220877082	2.41047496473196	10.16078562588790
C	3.48691382194508	2.59748883903851	11.41961498092108
C	4.13944708141246	1.56932484579249	12.09821649634237
C	4.18209551596641	0.31436381385896	11.48173581433580
C	3.60686739528442	0.06760871539876	10.22971889969048
C	3.66688219277641	-1.25900059840807	9.61083220420578
C	4.24525080881958	-2.34838278028592	10.27259036898369
C	4.32955947096376	-3.62173673169523	9.69893052382441
C	3.81542859469359	-3.78372053114253	8.41342661611095
C	3.22084494414304	-2.72894906307119	7.70049758206083
C	2.70827260529582	-2.92292256353384	6.34398759801078
C	2.81152729938114	-4.16427859941412	5.69326458539686
C	2.34390126185496	-4.36967385651897	4.39603557332320
C	1.77023732400986	-3.27792553671306	3.73461980120741

C	1.64859311648414	-2.01673219713080	4.32838412522142
C	1.06519669584822	-0.88536827084038	3.60545303466304
C	0.75469491679767	-0.96656341280992	2.24295252287980
H	0.96570928956038	-1.89025606796042	1.70637410315292
C	0.82328820023830	0.33277984853798	4.29944545947078
C	1.29584452577468	0.51109402498647	5.64835828835455
C	1.14968172862803	1.77143393225018	6.28342798557777
C	0.39641978226953	2.82434304913465	5.63954745277107
C	1.70774748527717	1.97815908443447	7.57459812890482
C	2.37835141065292	0.91727043925376	8.23904402780273
C	2.48804424108072	-0.35436080322980	7.61621303819525
C	1.96192527359030	-0.55187192111281	6.31343575443284
C	2.10442599436913	-1.83181810370699	5.66403519375221
C	3.12902650485447	-1.44680158554252	8.30643651132949
C	2.95524790000705	1.13208670068822	9.54460861206019
C	1.59867174475348	3.26727302929135	8.20975221046314
H	1.39591190555315	-3.42366373250802	2.72257262782056
C	2.44039187263915	-5.72709916215897	3.68335526706845
C	3.27764705466113	-5.56717089390006	2.39494462683592
H	3.36076288092164	-6.53526991533353	1.86780119911467
H	4.29796795533554	-5.21595213498794	2.63166515355406
H	2.82370928257720	-4.84283693387827	1.69707196142891
C	3.10698060445572	-6.80057020616454	4.56016951948035
H	3.15445223138560	-7.75466189250201	4.00625616878540
H	2.53994586404789	-6.98252605171378	5.48977910998721
H	4.13958529894836	-6.52303742614944	4.83516521339481
C	1.01927678581898	-6.21170414789228	3.32005290561567
H	0.50296604823312	-5.50389376393437	2.64884965889569
H	0.40120793919625	-6.32935712027039	4.22810224003240
H	1.06600575535999	-7.18959222013841	2.80659511132254
H	3.27267928106341	-4.99476868641672	6.21930999585661
H	3.87509878503279	-4.76223409278748	7.94657904894151
C	4.97379846583660	-4.77170471348105	10.48728263632136
C	4.17956549395576	-5.00168083149878	11.79208427868004
H	3.13096629489540	-5.26984371918382	11.57092342186332
H	4.63021299918578	-5.82570772861418	12.37500421886966
H	4.17084959118714	-4.10276841769159	12.43255588047101
C	6.43350466124902	-4.40009103924875	10.82961807117645
H	7.02158351848108	-4.23110578355789	9.90980058729963
H	6.49226374418964	-3.48379218035597	11.44193803973649
H	6.91351474656087	-5.21671142280279	11.39938279617459
C	4.98597048849305	-6.08841688463030	9.69227042878306
H	3.96515610279520	-6.42555074480221	9.44111823797540
H	5.55912145030102	-5.99586317623595	8.75329196943603
H	5.46038867323366	-6.88195385943016	10.29600979162403
H	4.64141278368506	-2.20718336396928	11.27653730213583
H	4.69138131752344	-0.49647502921064	11.99912898688333
C	4.79874598573365	1.76654304623456	13.47162265147958
C	4.13430041585918	0.81981539458817	14.49560219134824
H	4.59937537412886	0.94295987102452	15.49085074936528
H	3.05569096793274	1.03897741719518	14.59060890265796
H	4.23997490397012	-0.23936617775927	14.20408864511617
C	6.30403825275280	1.43623917007410	13.36481325127845
H	6.80130101091207	2.10114370223862	12.63604651850545

H	6.79727113960159	1.56965800114868	14.34508516531561
H	6.47380945522564	0.39434135401747	13.04305930288393
C	4.65696164550198	3.20934238778821	13.98504106108709
H	5.13589940654704	3.93552950664848	13.30518758620879
H	3.59891786972433	3.49902809799147	14.10925529420735
H	5.14585923359088	3.30247767598829	14.97069692449763
H	3.43751700375129	3.57832988045003	11.88315821724600
H	2.58078021032258	4.96714633796690	11.00791554742121
C	1.40744933335783	7.22086907692234	10.09310591468894
C	0.72119008017908	7.09454462549440	11.47152571181751
H	0.68636851629733	8.07869442738070	11.97368212297836
H	1.25955061494141	6.39743461759634	12.13639008592714
H	-0.31499787219571	6.72708281249730	11.36286298367852
C	0.63177253342598	8.25656476756626	9.26207243133239
H	-0.42054917951651	7.95815338254540	9.11207066539590
H	1.09035875254592	8.41472651267295	8.27026718503387
H	0.63079636573204	9.22785842371478	9.78739344372986
C	2.85199497328764	7.73470985807648	10.28210147353573
H	2.84566418822967	8.72591209915059	10.77141534355380
H	3.36402862713942	7.83494827995089	9.30831724420666
H	3.45052142496261	7.05323520359937	10.91084404270526
H	0.31363720292049	6.39025428706662	7.68477324470668
H	-0.80633503804024	5.98451592962422	6.21247391825030
H	-2.03391447963409	5.47919227900813	4.16303530769938
H	-0.43723089063897	2.13740489287695	1.70317587365485
C	1.31046638116540	-0.36542445198908	-0.69209791417000
H	2.06880280750017	0.42096972147183	-0.52728460048463
H	1.14817156649298	-0.46271895530542	-1.78122578336042
H	1.72902545266485	-1.32008076136467	-0.32887295611784
C	-1.05342117448552	-1.12351515293981	-0.23030963486278
H	-0.70845666968815	-2.09936393824066	0.15328113988846
H	-1.24639959882028	-1.23567552559675	-1.31316711392033
H	-2.01000174331720	-0.88153904319702	0.26660639617018
C	-0.55567341655408	1.29576741527838	-0.59250270960394
H	-1.52868315792163	1.57550926821850	-0.15756457347047
H	-0.70078025012294	1.16464745833381	-1.67939249474832
H	0.14051301390410	2.14020311976536	-0.44776332023788

8

Total energy = -3928.712240 au

Pt	-0.15953071018542	-0.02645324220410	0.14915263549667
Cl	-1.29638004863740	-2.02598078399734	-0.79297650358649
S	1.23751743850405	-1.51975965691259	1.24068176675183
C	0.22465044700745	-2.63996273570287	2.23444727341351
H	0.90206120141890	-3.40271627513691	2.65120416985691
H	-0.20637648553833	-2.02005472239284	3.03560094027639
H	-0.56161872224333	-3.06279929436389	1.59122161886601
O	2.37390155576142	-1.06080095187117	2.10969924313765
C	1.94270171557960	-2.63869607697419	0.00680516102381
H	2.60342278710297	-2.01727262607576	-0.61700541394851
H	2.52086054533170	-3.39703909280816	0.55888237552539
H	1.12058568695012	-3.06542398766642	-0.58668568063144
N	-1.29451159980907	1.35054036793306	-0.91976890511366
C	-2.12605613831334	0.98087500931912	-1.93101631710797
H	-2.33257970794452	-0.08893384852131	-1.99531340900833

C	-2.66055506565781	1.90023579565520	-2.79581329629723
H	-3.36034445561230	1.58174943346339	-3.57179039903221
C	-2.23418468690936	3.25233208379473	-2.72280206941095
C	-2.65095801313154	4.22513723356943	-3.67042919796168
H	-3.37065524800580	3.93349994162944	-4.44050674465374
C	-2.13513831411459	5.50314927079381	-3.63252677546847
H	-2.45608157086253	6.24699088392912	-4.36765153024909
C	-1.15973944525589	5.84781267931506	-2.66433083033689
H	-0.71408055497342	6.84627529583619	-2.67261676450053
C	-0.76174830287299	4.93102494440019	-1.71492456509569
H	0.00520236472535	5.20421310042955	-0.99295853318852
C	-1.31912272491085	3.62450811892209	-1.68882759881399
C	-0.97602318874155	2.64184894562037	-0.69725534677212
C	-0.17135857009105	2.85192699181154	0.50723408095483
C	-0.04566619918996	4.04803210351599	1.26362826221356
C	-1.05955952373643	5.09432189400458	1.28823635901839
C	-2.37825658900654	4.84236272936908	0.88001548682599
H	-2.65440295896599	3.82024092139987	0.63844947009172
C	-3.33156391941286	5.85400130345786	0.78589457556400
C	-4.76275042390952	5.59531508162800	0.29432958390146
C	-5.77051673682433	6.05132749379453	1.37162796355940
H	-5.61659974186828	5.49449318769946	2.31324672106280
H	-6.80587630583158	5.86933703179878	1.03008284307300
H	-5.67589417089575	7.12797885185634	1.59515483900373
C	-4.99371608946004	6.39573081275164	-1.00690518255082
H	-4.86347593136885	7.48060354044969	-0.84921988500598
H	-6.02082066150364	6.23061170689245	-1.38103860740766
H	-4.28455349368100	6.07836180118320	-1.79123206975055
C	-5.01288710571718	4.10731677925910	-0.00468371931303
H	-4.35208316657631	3.73094159874147	-0.80398274511477
H	-6.05529718205620	3.96691323410873	-0.34106684473212
H	-4.86400872791640	3.47884213231893	0.89057245344038
C	-2.93509212487654	7.15147089108254	1.13689143941487
H	-3.66340312193995	7.95669262666935	1.05109787397007
C	-1.66226608775416	7.43898478332278	1.64689257809055
C	-1.27637165950673	8.78879576068065	2.06652772151435
C	-2.11244100902072	9.88907621907431	1.84748324910082
H	-3.05894162782926	9.73738366583510	1.33096223476197
C	-1.77483055735250	11.18443436738580	2.25707888595500
C	-2.74045301328887	12.34640018979921	1.97979940044112
C	-4.09595162389192	12.05590372399490	2.66201035758098
H	-4.80648972991901	12.88100905732553	2.47162828374727
H	-3.97157768851469	11.95442797370132	3.75503124942276
H	-4.55369150197055	11.12488728999332	2.28554895517976
C	-2.20824887098918	13.68695030366530	2.51360265752924
H	-2.93415349875811	14.48919141451295	2.29281414497841
H	-1.25006140462543	13.96423923067950	2.04074935154139
H	-2.05912415828374	13.66285793868160	3.60714310216749
C	-2.94867705430637	12.48079431021821	0.45488734065318
H	-3.37215754347384	11.56121483594348	0.01541399972732
H	-1.99133773053990	12.69090596074784	-0.05489088021297
H	-3.64494395688222	13.31064956022785	0.23457236666257
C	-0.55655919177309	11.35731297083071	2.91344604713730
H	-0.28250364907697	12.35245366904357	3.25080840437334

C	0.32758321992272	10.29222964387899	3.15701020621110
C	1.59317462359293	10.49601041264861	3.86460464415545
C	1.98600421364035	11.77117866553218	4.30511610379895
H	1.34072166454429	12.61929391942546	4.09659185692647
C	3.17482072166314	11.98828774518363	5.00056317655787
C	3.61395362980638	13.37971151916818	5.48166043530293
C	4.96182369436691	13.74238162829364	4.81999154988464
H	4.86675964278878	13.75925272638330	3.71949589037502
H	5.29751359049361	14.74211087660759	5.15175292805076
H	5.75402771267767	13.01915930679763	5.07975972832185
C	3.78081182204158	13.35930458308222	7.01728739751541
H	2.83004533396389	13.09116032641534	7.51186351629071
H	4.54585136168255	12.63147847859459	7.33813500832794
H	4.09012057616868	14.35538952892105	7.38344714154958
C	2.59027628959960	14.47007958983804	5.12290786674478
H	2.44833360325994	14.55776265093336	4.03162288455768
H	1.60612358506008	14.27541786353359	5.58368403842350
H	2.94496569532172	15.44826754942381	5.49257645381469
C	3.98458107903133	10.87736911936432	5.26216375337347
C	3.64720577145814	9.58309059661137	4.84981498731945
C	4.50794751889893	8.43435178339405	5.14870526187054
C	5.68517658707374	8.57775957574579	5.89265384476886
H	5.96315749232790	9.56442794989297	6.25857382870458
C	6.52453938018193	7.49941637323551	6.19337602949007
C	7.79973653807036	7.73342418619346	7.01725855915086
C	8.70779511817388	8.73979287769487	6.27638104923042
H	9.63336826327804	8.91910818031329	6.85361225457638
H	8.99269875084263	8.35342915512545	5.28138813502803
H	8.20906556240437	9.71361383631915	6.13118917274647
C	7.41436325581324	8.30595469102872	8.39939667834523
H	6.75888171424922	7.60436901304501	8.94572022915115
H	8.32005542594685	8.47695705775475	9.00962879011685
H	6.88196428905146	9.26876146266490	8.31179819859209
C	8.59666762636262	6.43645711723700	7.23802981448744
H	8.00905512615786	5.68277032080341	7.79067256062917
H	8.92230421662197	5.98768455155679	6.28341070102205
H	9.50247437609523	6.65366920965899	7.83099937495074
C	6.15255593138917	6.24142910203018	5.72050316125621
H	6.79170634857326	5.39092521136131	5.93841143625626
C	4.98329120110808	6.03390778493898	4.97055434315455
C	4.62168226483784	4.70217204620944	4.47943895052022
C	5.41102156125034	3.57589335190490	4.74900641400196
H	6.30790913730691	3.69304173309358	5.35487801445827
C	5.09721706151159	2.29794204184284	4.26967605008026
C	6.00618557540847	1.10687847615048	4.60758610726464
C	7.42769049234295	1.38052564391895	4.06903580004618
H	8.09623140500574	0.53219623079299	4.30429278565775
H	7.86942922277705	2.28945295543356	4.51324529497353
H	7.41239703886675	1.51196803860873	2.97224789902145
C	5.49822025179291	-0.20616893935537	3.98641007915344
H	5.46487233122752	-0.15522308192091	2.88459716134903
H	4.48690187129410	-0.46896180753140	4.34043898744621
H	6.17691099657886	-1.03217621887891	4.26355747676528
C	6.05966903672067	0.93102354369973	6.14131843389683

H	6.71637898123706	0.08274810687925	6.40806718394505
H	5.05279257716365	0.72711330630253	6.54753350498849
H	6.45237324038649	1.83146647361599	6.64469788385685
C	3.95097264080880	2.16519689032310	3.48792507404571
H	3.69382373922644	1.18893697703042	3.08767570084267
C	3.11599136368529	3.25636362725495	3.19490701832304
C	1.93038027360650	3.08842925305168	2.36407823814054
C	1.57217757370064	1.83289632018212	1.84129812998335
H	2.11874999379904	0.94224457496267	2.14248441843908
C	0.54804023604473	1.69488899786851	0.91731706625691
C	1.09283778204099	4.20511762122532	2.10242342521071
C	1.40092929620755	5.49425131060093	2.66866739817214
C	0.53766429673687	6.59485211030720	2.44012649403856
C	-0.71960426906591	6.38275697087414	1.77387971984648
C	0.87058852149919	7.87982594918932	2.93787135113501
C	-0.02402678126037	8.98837452291100	2.71682769783103
C	2.07820443832800	8.06745767401837	3.65871944004581
C	2.43711553385163	9.38241753185518	4.12703143085661
C	2.92911140887176	6.95956277753086	3.91749616239173
C	4.14126612344414	7.14142082804311	4.67788574042929
C	2.58637439082373	5.67124348459821	3.42977173512896
C	3.44130782224125	4.54389058678439	3.70083964284664
H	4.91410017991940	11.03459069054808	5.80586851583723

reference

Total energy = -2396.274846 au

C	0.09256258758021	0.45288475438033	-0.52041461219398
C	1.19516338278184	1.11241985112517	0.32165183926250
C	2.54872336701549	1.01807974854462	0.00342516118411
C	3.55048627681308	1.61887581283551	0.78490431798404
C	4.96269540625969	1.50116342193835	0.42370338201107
C	5.36677965933579	0.80002194552799	-0.72433244517289
H	4.62888648114635	0.33094175549466	-1.37393261279002
H	8.72672067296739	1.16913824931920	-0.54763776433124
H	7.00430337975278	0.13886994117345	-1.96058871376363
H	2.83965844033232	0.45682945585270	-0.87909841611334
C	-0.67574502462473	-0.56183260217097	0.35493552151346
H	0.00283337387522	-1.34607367887524	0.73571202137885
H	-1.47149513265964	-1.05230299416406	-0.23513174625170
H	-1.15316558734969	-0.07662418534403	1.22380065720858
C	-0.88192325442823	1.54018951552302	-1.02477666569262
H	-1.35960758511404	2.08179448488105	-0.19026221960432
H	-1.68462800646086	1.08417320069443	-1.63276792244230
H	-0.35391434850619	2.28100003885863	-1.65154657949580
C	0.65807544087755	-0.29297925407780	-1.74063631709964
H	1.20030647052260	0.38645683295885	-2.42124369185779
H	-0.16882072604720	-0.74908883494149	-2.31303484128962
H	1.34548476356960	-1.10404052896240	-1.44344720677414
C	6.71064690517167	0.68863320814670	-1.06171671328626
C	7.68192552472729	1.27447982433157	-0.25788358353058
C	7.33203374868779	1.98719305107070	0.90045702977534
C	8.35042867918435	2.60281680353374	1.75086006471918
C	9.71649290886283	2.49638439825403	1.44032339790211
C	10.71014139511240	3.07058287104745	2.23181900722863
C	10.30193455616820	3.77202419951837	3.37033470324933

C	8.95627043385211	3.91090726803591	3.73124426325122
C	8.56180646807801	4.64970744346261	4.93083126382038
C	9.52146150207866	5.23919372128672	5.77049744485341
C	9.17587683261887	5.94703328738000	6.92029615405113
C	7.81490067741775	6.06209114866662	7.22088578652280
C	6.81388875349551	5.49869732743107	6.42082378168650
C	5.39668737621614	5.64145206928047	6.76123606611034
C	4.98746503163738	6.36181590423663	7.88941835950254
C	3.64213585974387	6.51410420839188	8.24078946065303
C	2.69170697714988	5.91229530107822	7.41832308581864
C	3.04164752882397	5.17827257134182	6.27232864491044
C	2.02070340699448	4.55799372270840	5.42913617689602
C	0.65448369593636	4.67236530590118	5.73744796992243
C	-0.34052907310916	4.09219047415727	4.95305795482068
C	0.06586848835060	3.37345286588419	3.82411626518476
C	1.41101087595680	3.22389984089991	3.46759803184696
C	1.80458288844176	2.46330504337220	2.27995499152529
C	0.85182846481257	1.84238510648651	1.46425330387980
H	-0.20154497218096	1.92482675702101	1.72475521249223
C	3.18379471923262	2.35080635550894	1.94526921324292
C	4.19273987633684	2.96681287301783	2.77305851069533
C	5.56613427511143	2.84262209071325	2.43127060965737
C	5.95452925130140	2.10821305003185	1.24936758845090
C	6.55796329138177	3.44400467743285	3.25422449669815
C	6.17623110794950	4.16817105683180	4.41482883483785
C	4.80208781641636	4.29568607639239	4.75283211526226
C	3.81081931158618	3.69486377959347	3.93261990090685
C	2.41523114328545	3.82560455714578	4.27730762658219
C	4.41285040207006	5.03722644720186	5.92847401094720
C	7.18419699413170	4.77259494901659	5.25367713413147
C	7.95372636733441	3.31886624680919	2.91146316120183
H	-0.70060229076326	2.91644385735134	3.20153931208897
C	-1.83611587092289	4.21610162621939	5.28025456423330
C	-2.43232937098450	2.80525863971455	5.48263243100173
H	-3.50994769657997	2.87452428494773	5.71907922559053
H	-1.93022077390387	2.28255104488875	6.31642155779261
H	-2.32649724654669	2.18055391436822	4.57895990714242
C	-2.08729611820411	5.03333322481675	6.55865304360090
H	-3.17259619184356	5.09435969858911	6.75260605759369
H	-1.70618501988618	6.06547909850897	6.46824633324625
H	-1.61591660091944	4.56823916931344	7.44200040853969
C	-2.55617743043701	4.91671178831246	4.10669718922713
H	-2.45175756720745	4.35065796795873	3.16502679253761
H	-2.14460006413314	5.92841256859928	3.94088845156391
H	-3.63589187016464	5.01534617284220	4.32218292643220
H	0.36115697428597	5.23394285828044	6.61909346746887
H	1.64147218872140	6.01665263655273	7.67285217012408
C	3.26725193966769	7.32314160404204	9.49144185946337
C	3.78145872505272	8.77100789419071	9.33222454620984
H	3.32960695668982	9.25300545924850	8.44678261399577
H	3.51979825825674	9.37200808778780	10.22237672973325
H	4.87822661460701	8.80713859653234	9.21386008289882
C	3.92115451628089	6.67602578241328	10.73238287003762
H	3.56814077730421	5.63773505374835	10.86554238406013

H	5.02153610501946	6.65167031803248	10.65189754270137
H	3.66335753432891	7.24667090408691	11.64328668535168
C	1.74694625289333	7.37283899656082	9.71902435548533
H	1.22043815403027	7.85223399033108	8.87541977592182
H	1.32124050352820	6.36448659535613	9.86288670662952
H	1.52631600476187	7.96069214257654	10.62730923921040
H	5.74077240839084	6.82697971385251	8.52210672355777
H	7.52932439633249	6.61042044597647	8.11639590487212
C	10.21910219587812	6.58380650277879	7.85030338648209
C	9.95518787751910	8.10223028773964	7.95322221414794
H	10.70152501328237	8.57691882350233	8.61617293763256
H	10.02297357001595	8.58138483755031	6.96008718491324
H	8.95482565173792	8.31909947210980	8.36575964349023
C	10.10333821293534	5.94321723297496	9.25140846316348
H	10.29126421627746	4.85580226261434	9.20142434045492
H	10.84346927988152	6.38921631938844	9.94088648162529
H	9.10150693272796	6.09353545619696	9.68958258257766
C	11.65625215281358	6.37776249430141	7.34283780655544
H	11.92110124381818	5.30775773052268	7.28156689558427
H	11.80874971341474	6.82814046741307	6.34635595377665
H	12.36733042399194	6.85713769538272	8.03843334944346
H	10.57254231629408	5.13776552712580	5.51778780019697
H	11.06679596801298	4.22592744185937	3.99696538228863
C	12.20631229888435	2.95849774342320	1.90241364947840
C	12.79296120095435	4.37479709846150	1.71005890670660
H	13.87096537277118	4.31434897390879	1.47298819424698
H	12.68285856935010	4.99183351792969	2.61843579755579
H	12.28725206816601	4.90019840850885	0.88015041917708
C	12.46212066832270	2.15207342471911	0.61821202392675
H	11.98844592457960	2.62088584992541	-0.26197410596682
H	12.08688290259976	1.11713058199917	0.70153826153346
H	13.54778889365100	2.09860023726877	0.42394502780000
C	12.93221819755874	2.25435107958879	3.07029024122013
H	14.01218421563875	2.16399452439316	2.85254643630663
H	12.52726281214226	1.23895243067983	3.22972853082679
H	12.82577978106460	2.81339136286241	4.01586368599510
H	10.01110830115364	1.94628360507733	0.55188156365701

5. X-ray structural data

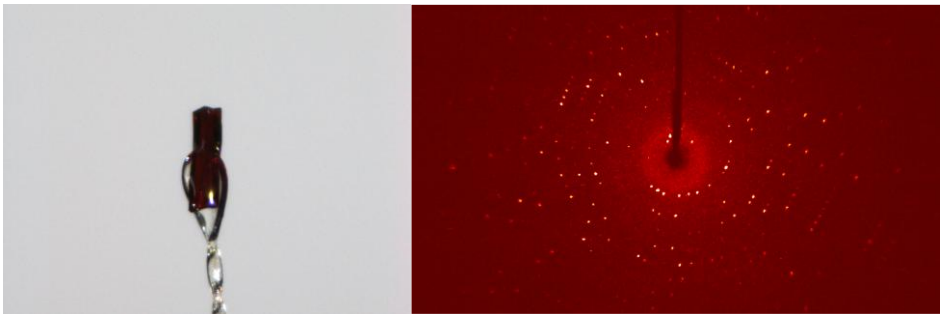

A suitable crystal for X-ray diffraction single crystal experiment (red board, dimensions = 0.040 x 0.100 x 0.390 mm) was selected and mounted with a cryoloop on the goniometer head of a D8 Venture (Bruker-AXS) diffractometer equipped with a CMOS-PHOTON70 detector, using Mo-K_α radiation (λ = 0.71073 Å, multilayer monochromator) at T = 150(2) K. Crystal structure has been described in monoclinic symmetry and *C2/c* (I.T.#15) centric space group (R_{int} = 0.0444; R_σ = 0.0452). Cell parameters have been refined as follows: *a* = 19.9437(10), *b* = 32.6613(17), *c* = 27.5799(14) Å, β = 130.259(2) °, V = 13709.8(12) Å^3. Number of formula unit *Z* is equal to 8 and calculated density ρ and absorption coefficient μ values are 1.185 g·cm^{-3} and 2.089 mm^{-1}, respectively. Crystal structure was solved by dual-space algorithm using SHELXT program,[59] and then refined with full-matrix least-squares methods based on F^2 (SHELXL program[60]). The contribution of the disordered solvents to the calculated structure factors was estimated following the BYPASS algorithm,[61] implemented as the SQUEEZE option in PLATON.[62] A new data set, free of solvent contribution, was then used in the final refinement. All non-hydrogen atoms were refined with anisotropic atomic displacement parameters. H atoms were finally included in their calculated positions and treated as riding on their parent atom with constrained thermal parameters. A final refinement on F2 with 15624 unique intensities and 726 parameters converged at $\omega R(F^2)$ = 0.0832 (R_F = 0.0318) for 12380 observed reflections with I > 2σ.

Table S10. Crystallographic data and structure refinement for **NG1**.

Empirical formula	$C_{76}H_{69}NO_2Pt$
Formula weight ($g \cdot mol^{-1}$)	1223.41
Temperature (K)	150(2)
Crystal system	Monoclinic
Space group	*C2/C*
a (Å)	19.9437(10)
b (Å)	32.6613(17)
c (Å)	27.5799(14)
α (°)	90
β (°)	130.259(2)
γ (°)	90
Volume ($Å^3$)	13709.8(12)
Z	8
$\rho_{calc.}$ ($g \cdot cm^{-3}$)	1.184
μ (mm^{-1})	2.089
F (000)	5000
Crystal size (mm^3)	0.04 × 0.10 × 0.39
Radiation type	Mo K_α (λ = 0.71073)
Θ range for data collection (°)	2.302 to 27.485
Index ranges	$-23 \le h \le 25$, $-42 \le k \le 42$, $-33 \le l \le 35$
Reflections collected	55031
Independent reflection	15624 [R_{int} = 0.0444, R_σ = 0.0452]
Data/restraints/parameters	15624/0/726
Goodness-of-fit on F^2	0.969
Final *R* indexes [$I \ge 2\sigma(I)$]	R_1 = 0.0318, ωR_2 = 0.0832
Final *R* indexes [all data]	R_1 = 0.0467, ωR_2 = 0.0915
Largest diff. peak/hole ($e \cdot Å^{-3}$)	1.756/−1.131

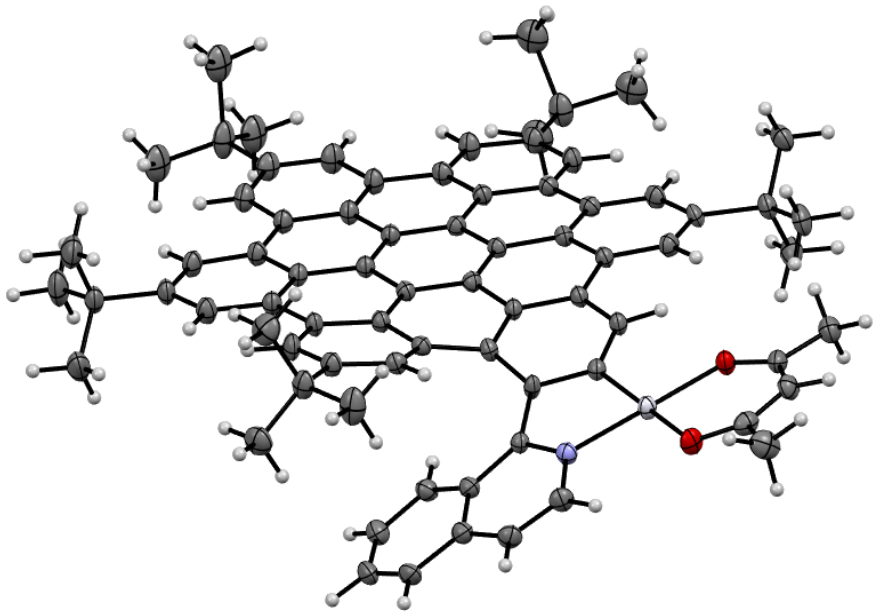

Figure S29. ORTEP view of the molecular structure of (*P*)-**NG1**, obtained from the analysis of a racemic crystal. Thermal ellipsoids are drawn at 50% probability level. Disorder is omitted for clarity.

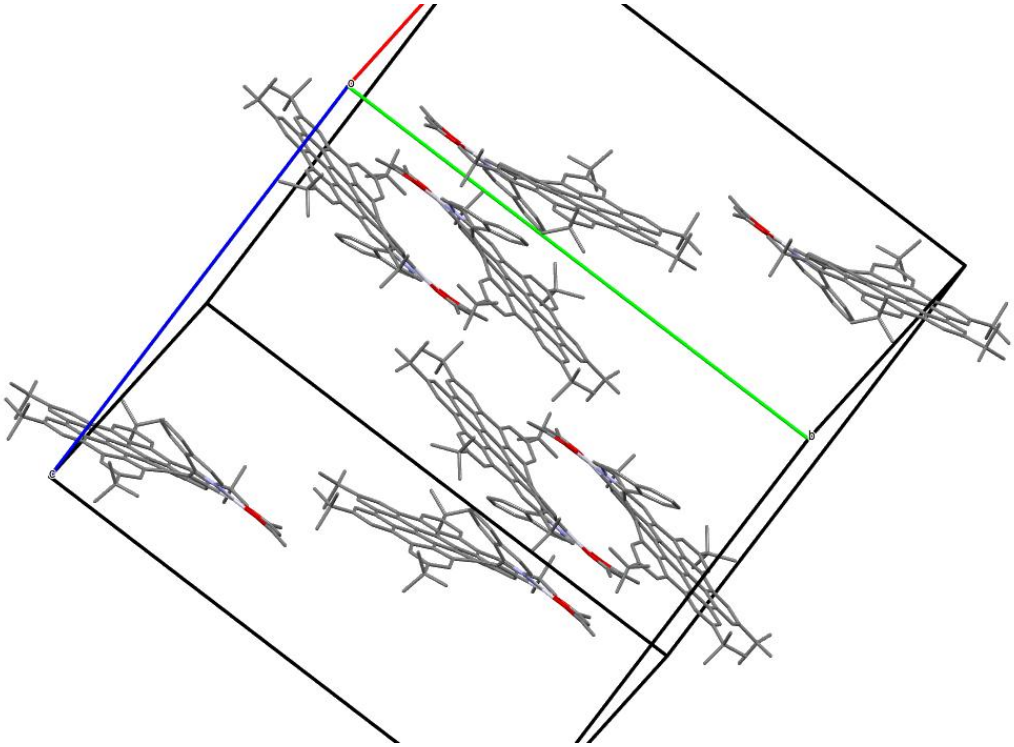

Figure S30. View of the molecular packing structure of **NG1**, obtained from the analysis of a racemic crystal. Disorder and hydrogen atoms are omitted for clarity.

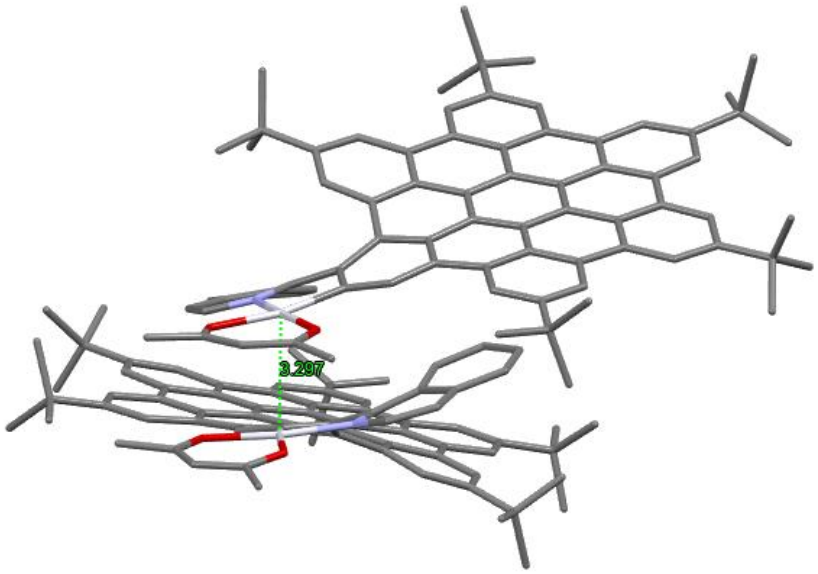

Figure S31. View of a homochiral dimer of **NG1** (here, from (*P*) enantiomers), formed at the solid state by Pt-Pt interactions (with an intermetallic distance of 3.297 Å) obtained from the analysis of a racemic crystal. Disorder and hydrogen atoms are omitted for clarity.

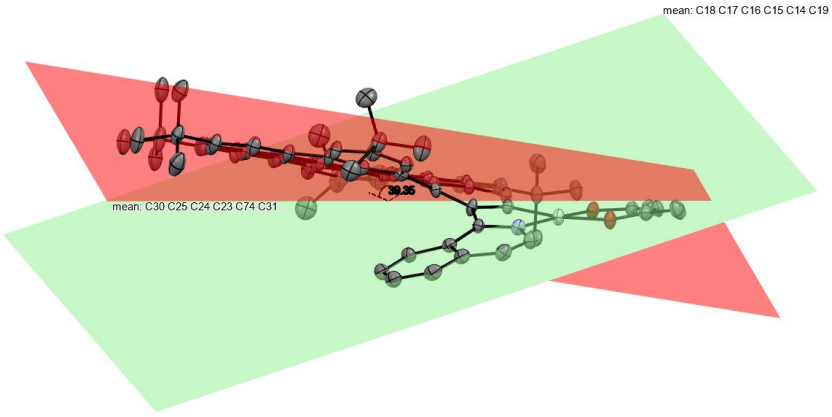

Figure S32. Measurement of the helicity (angle between the planes of the two terminal aryl groups composing the helix) on the ORTEP view of the molecular structure of (*P*)-**NG1**, obtained from the analysis of a racemic crystal. Thermal ellipsoids are drawn at 50% probability level. Disorder and hydrogen atoms are omitted for clarity.

6. NMR spectra

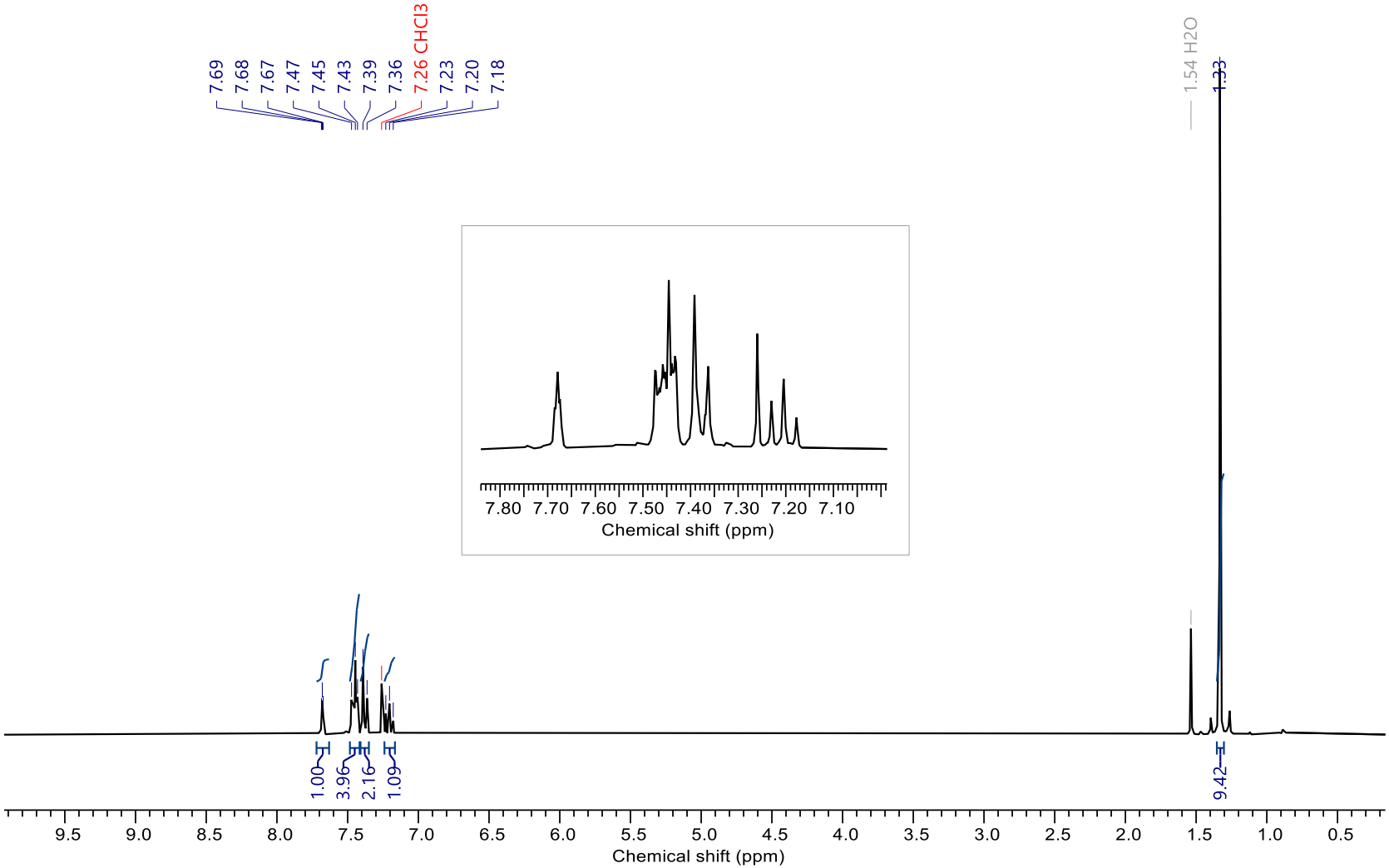

Figure S33. ^{1}H NMR spectrum of **1-bromo-3-((4-(*tert*-butyl)phenyl)ethynyl)benzene (1)** (300 MHz, $CDCl_3$, 298 K).

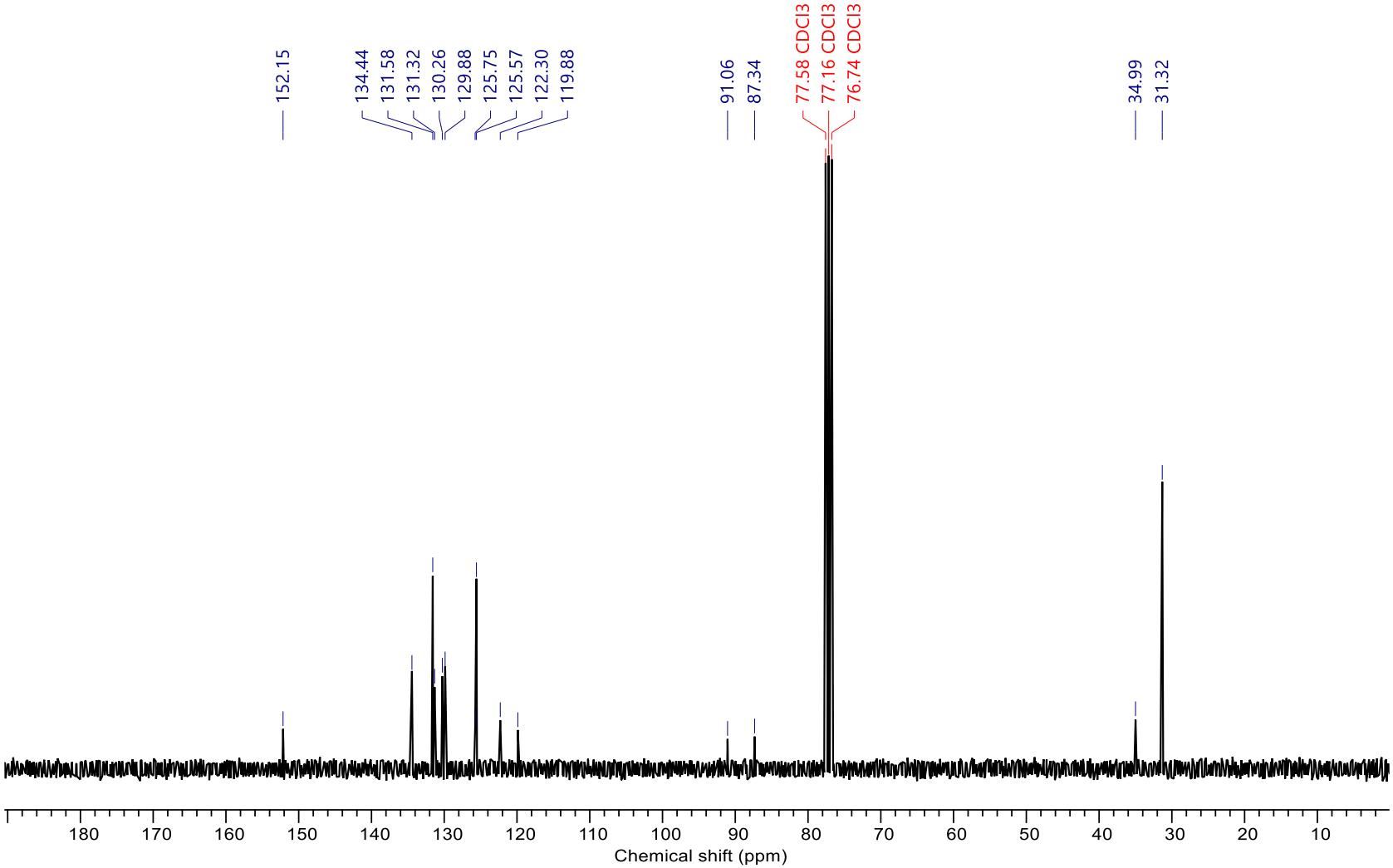

Figure S34. $^{13}C\{^{1}H\}$ NMR spectrum of **1-bromo-3-((4-(*tert*-butyl)phenyl)ethynyl)benzene (1)** (75 MHz, $CDCl_3$, 298 K).

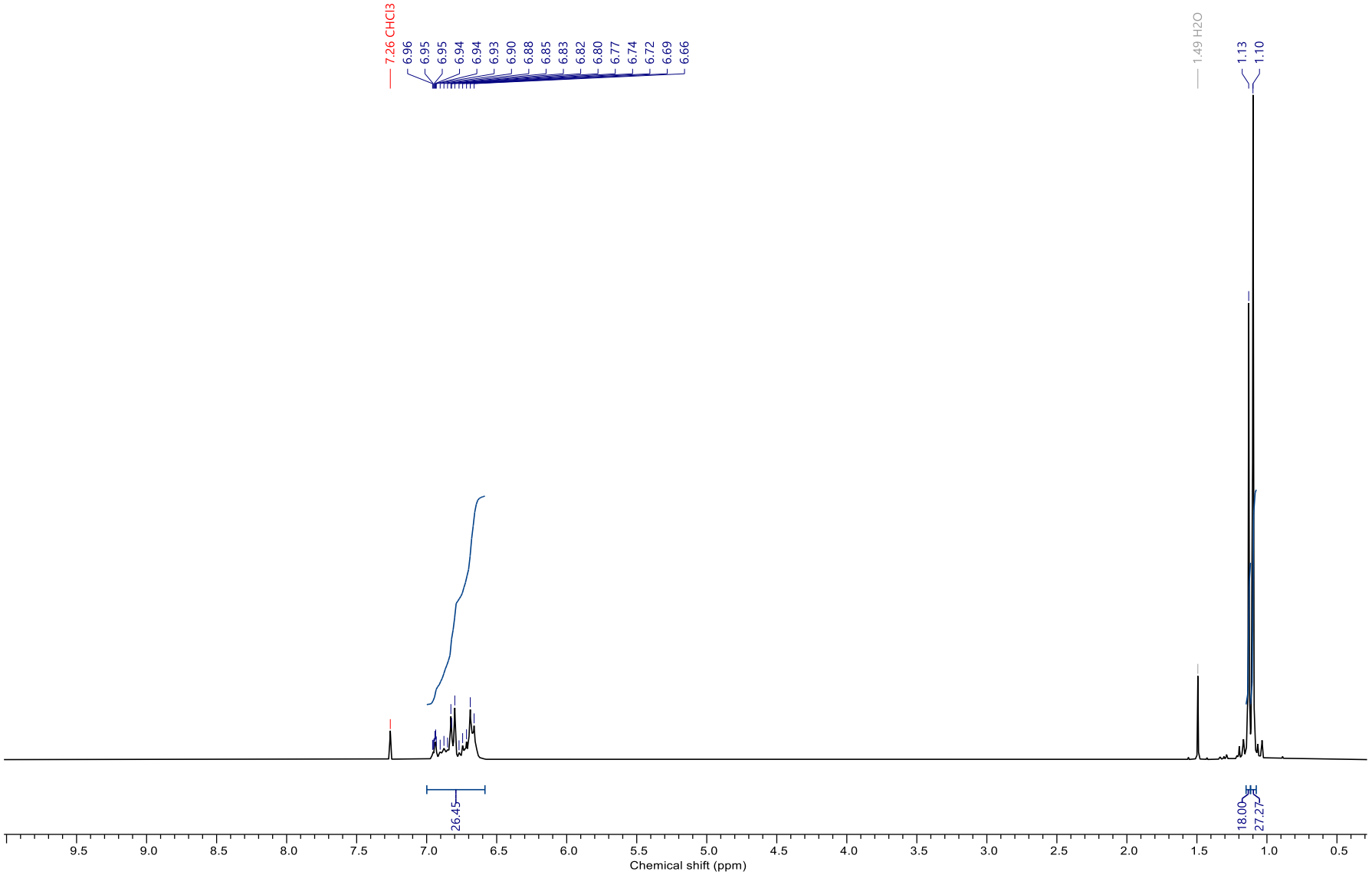

Figure S35. ^{1}H NMR spectrum of **3** (300 MHz, $CDCl_3$, 298 K).

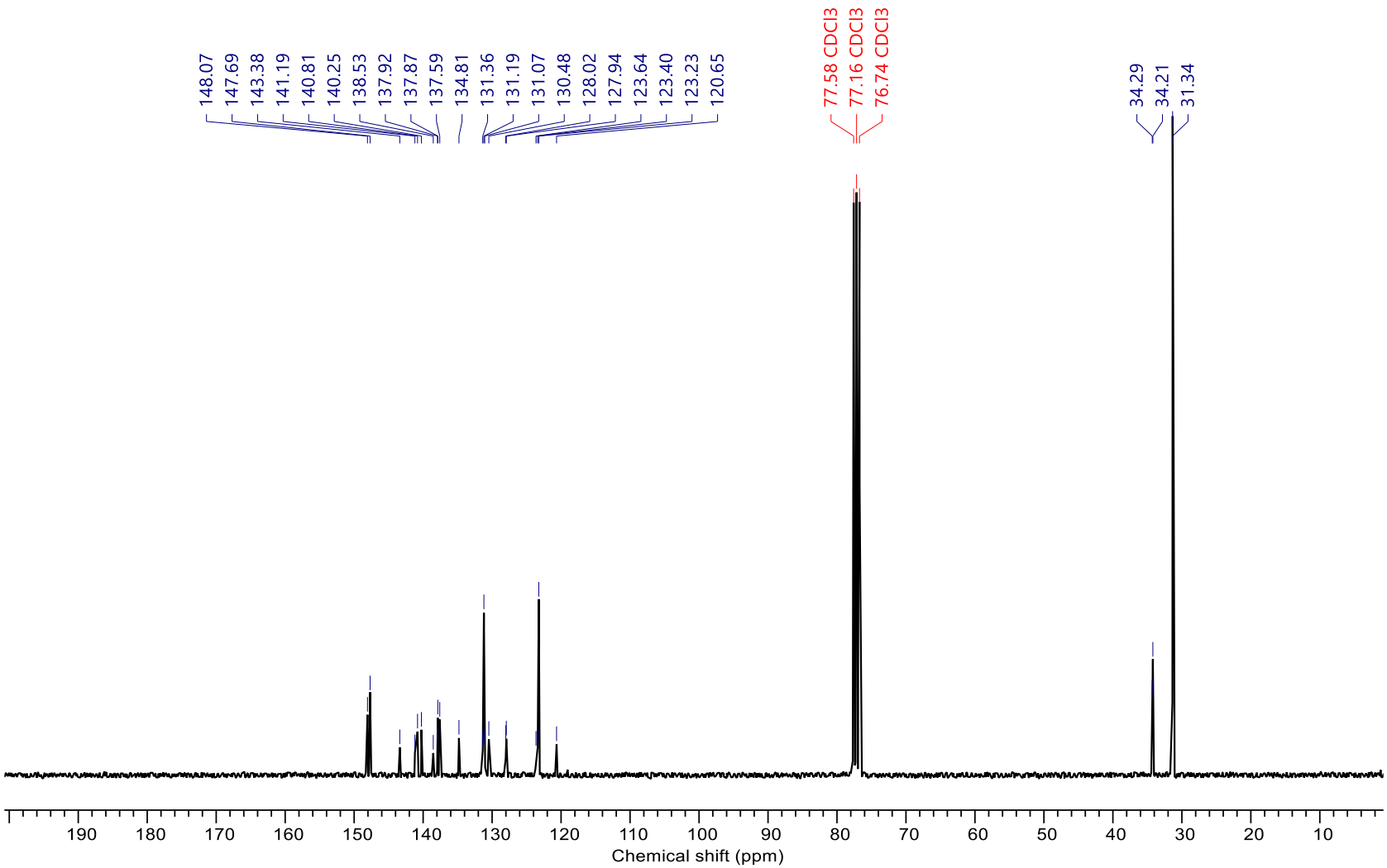

Figure S36. $^{13}C\{^{1}H\}$ NMR spectrum of **3** (75 MHz, $CDCl_3$, 298 K).

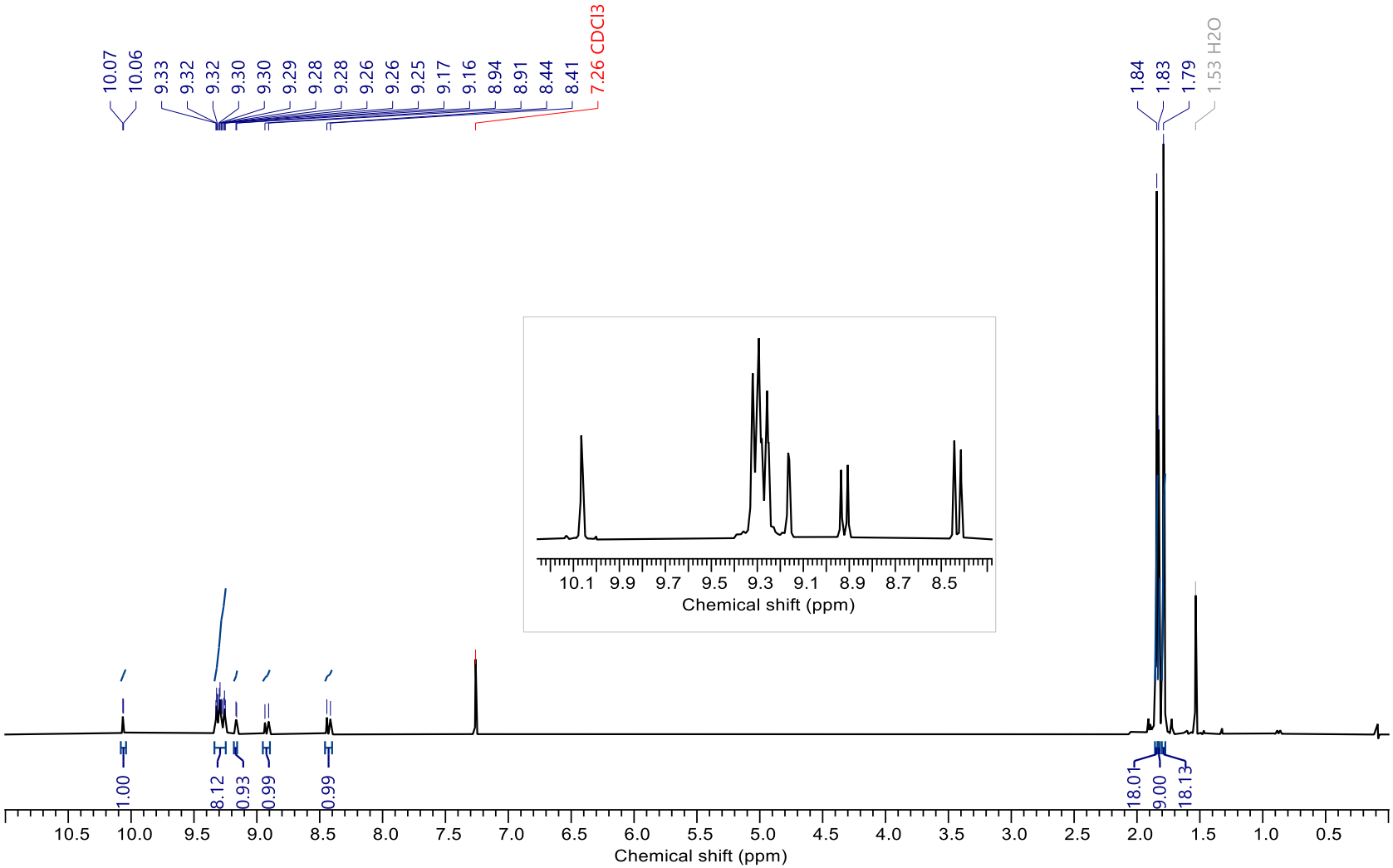

Figure S37. ^{1}H NMR spectrum of **4** (300 MHz, $CDCl_3$, 298 K).

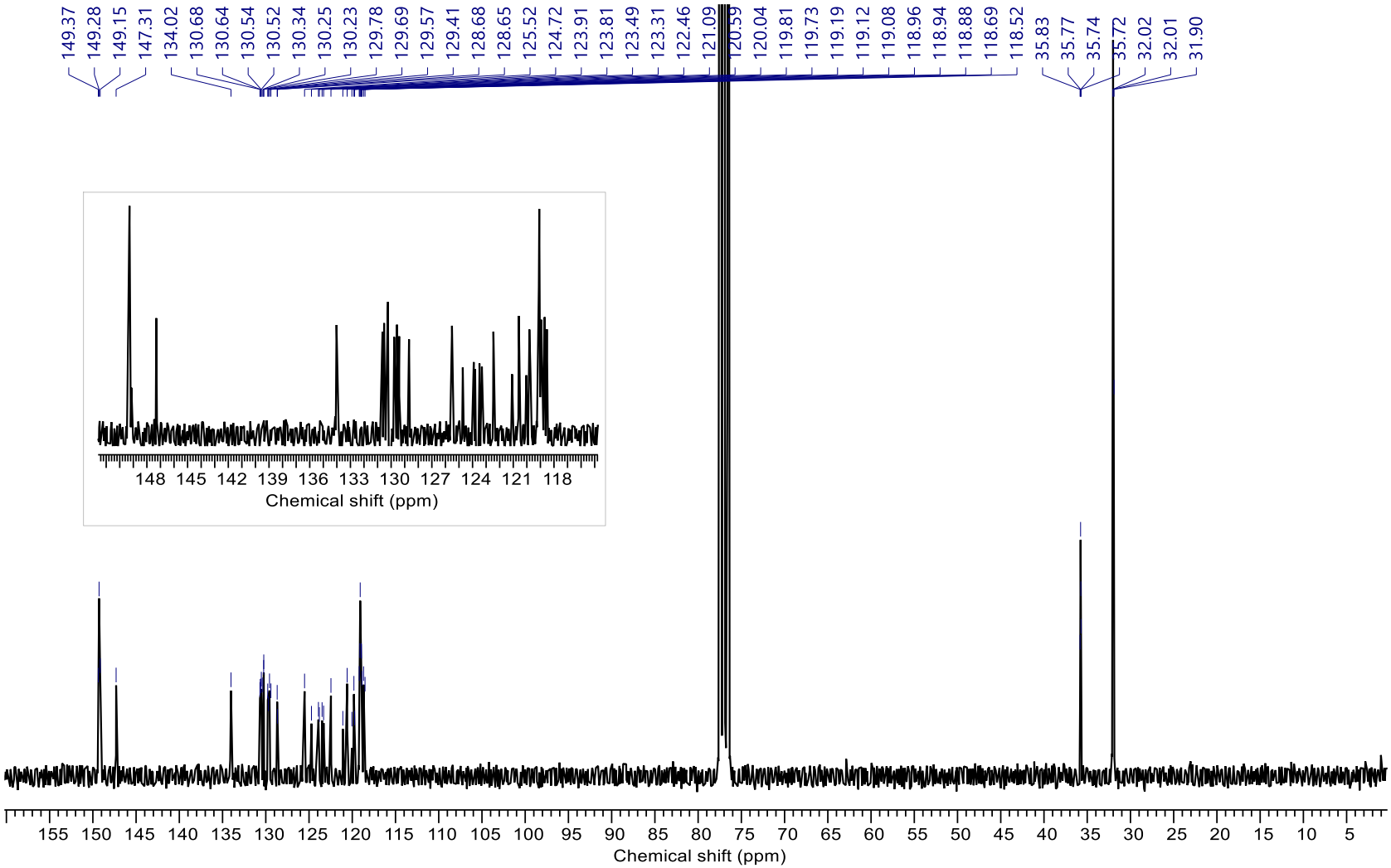

Figure S38. $^{13}C\{^{1}H\}$ NMR spectrum of **4** (75 MHz, $CDCl_3$, 298 K).

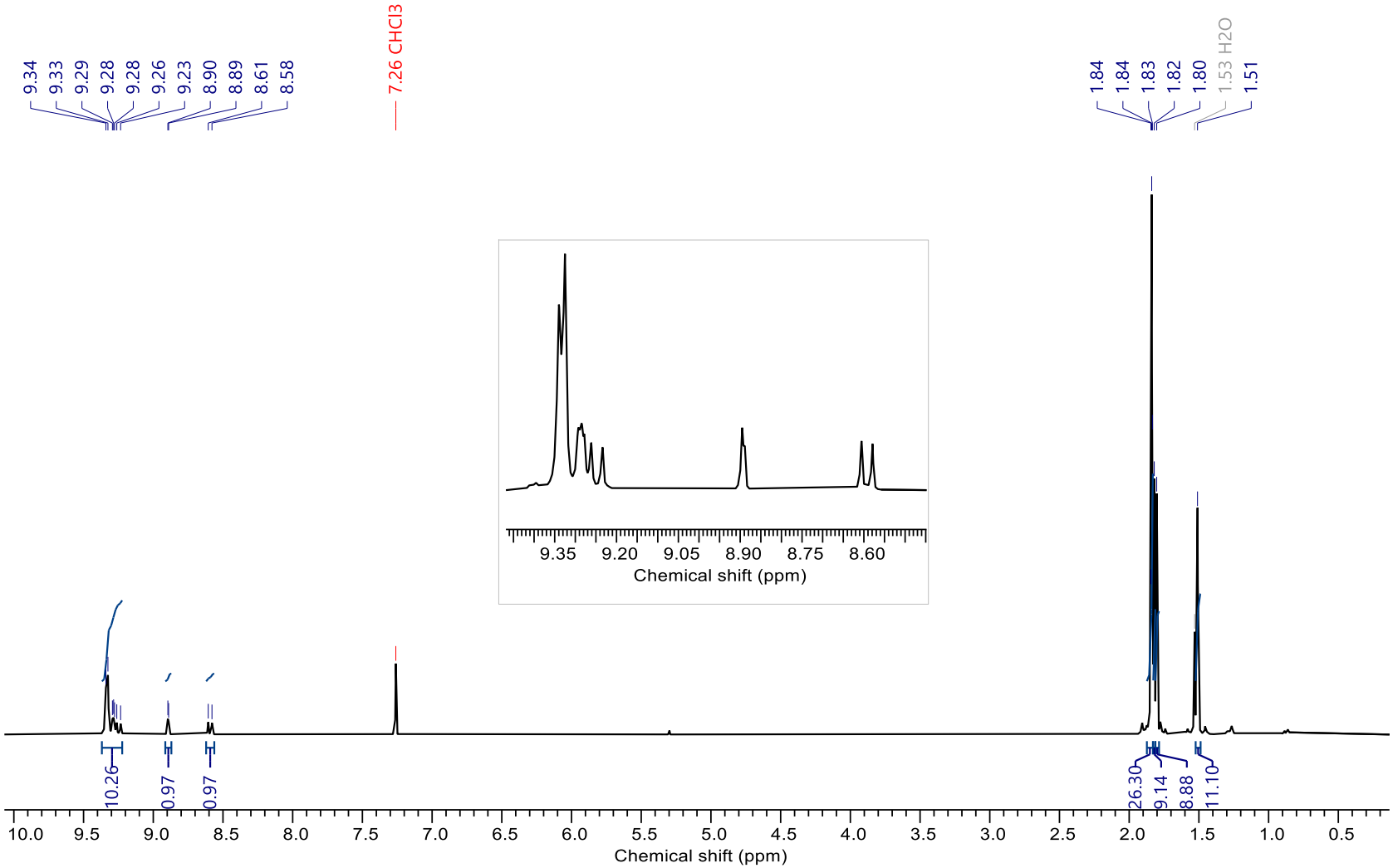

Figure S39. ^{1}H NMR spectrum of **5** (300 MHz, $CDCl_3$, 298 K).

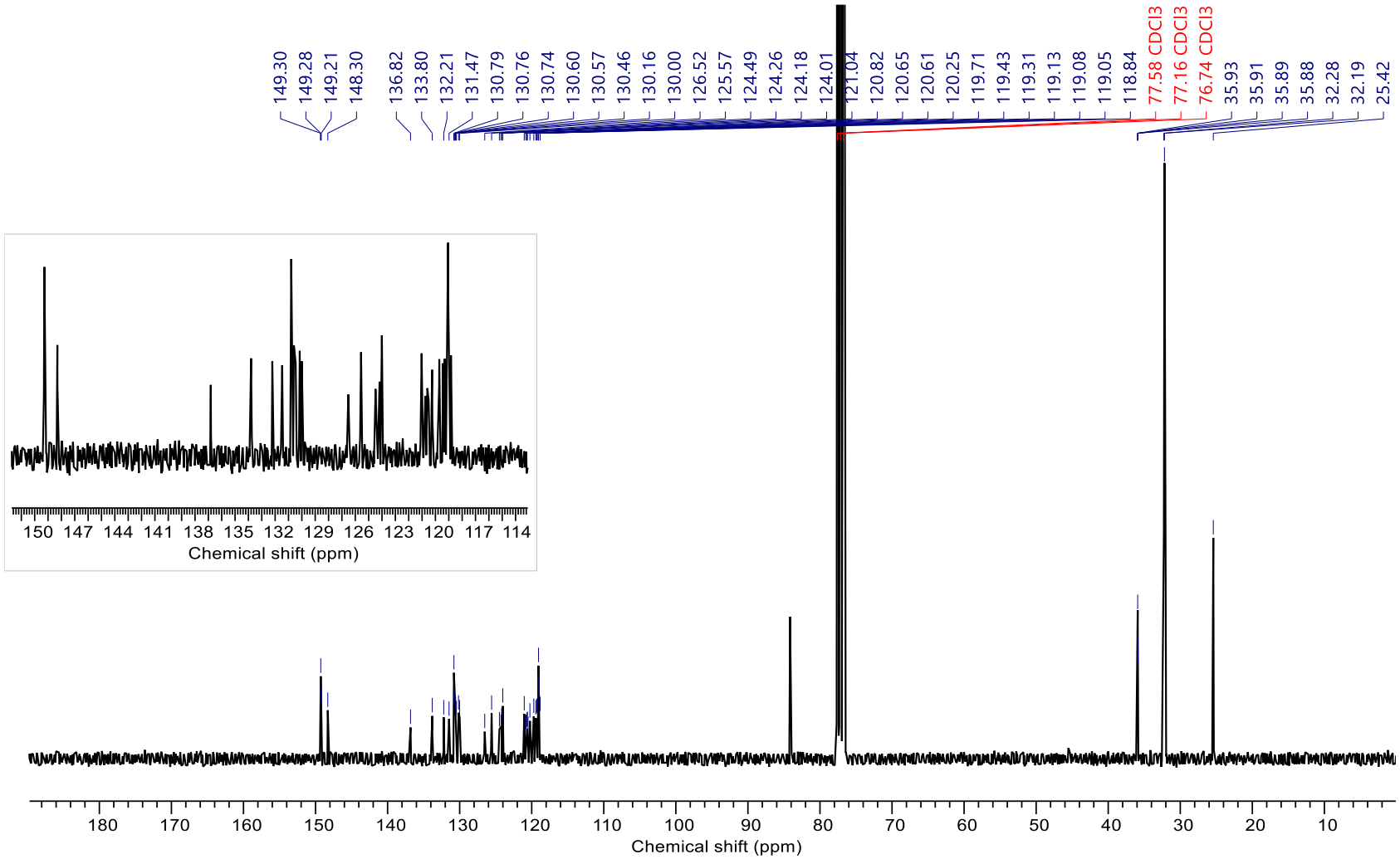

Figure S40. $^{13}C\{^{1}H\}$ NMR spectrum of **5** (75 MHz, $CDCl_3$, 298 K).

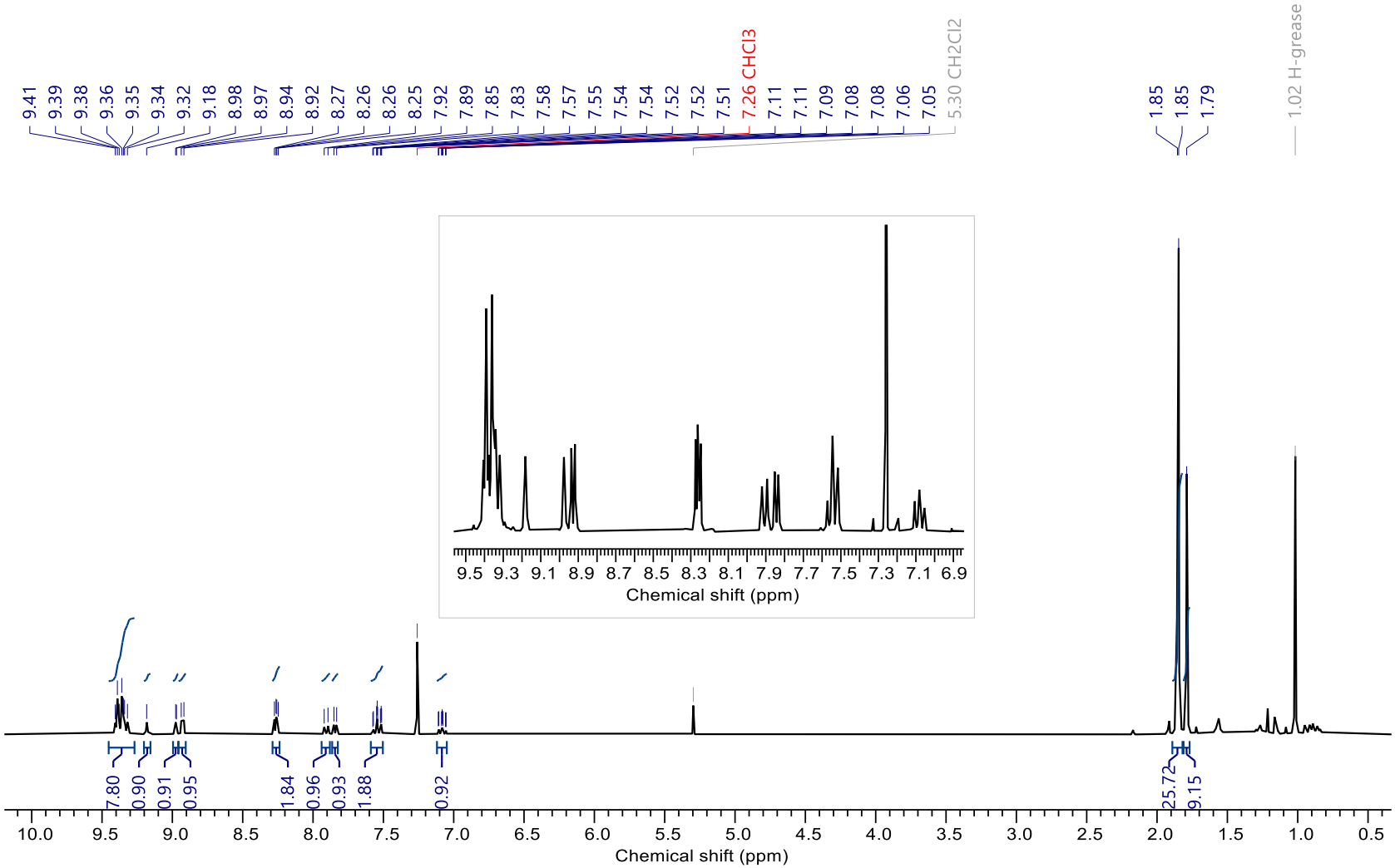

Figure S41. ^{1}H NMR spectrum of **7** (300 MHz, $CDCl_3$, 298 K).

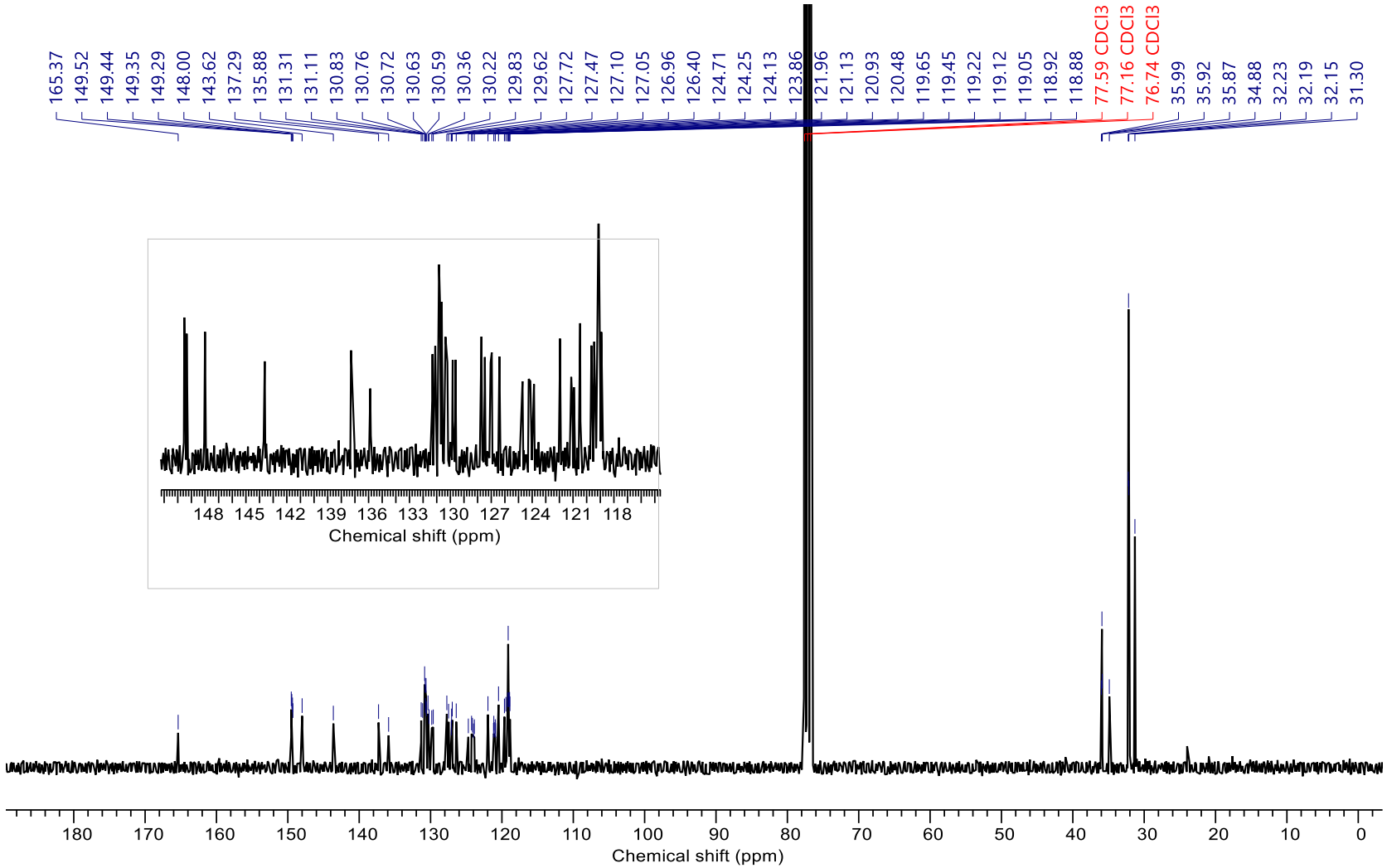

Figure S42. $^{13}C\{^{1}H\}$ NMR spectrum of **7** (75 MHz, $CDCl_3$, 298 K).

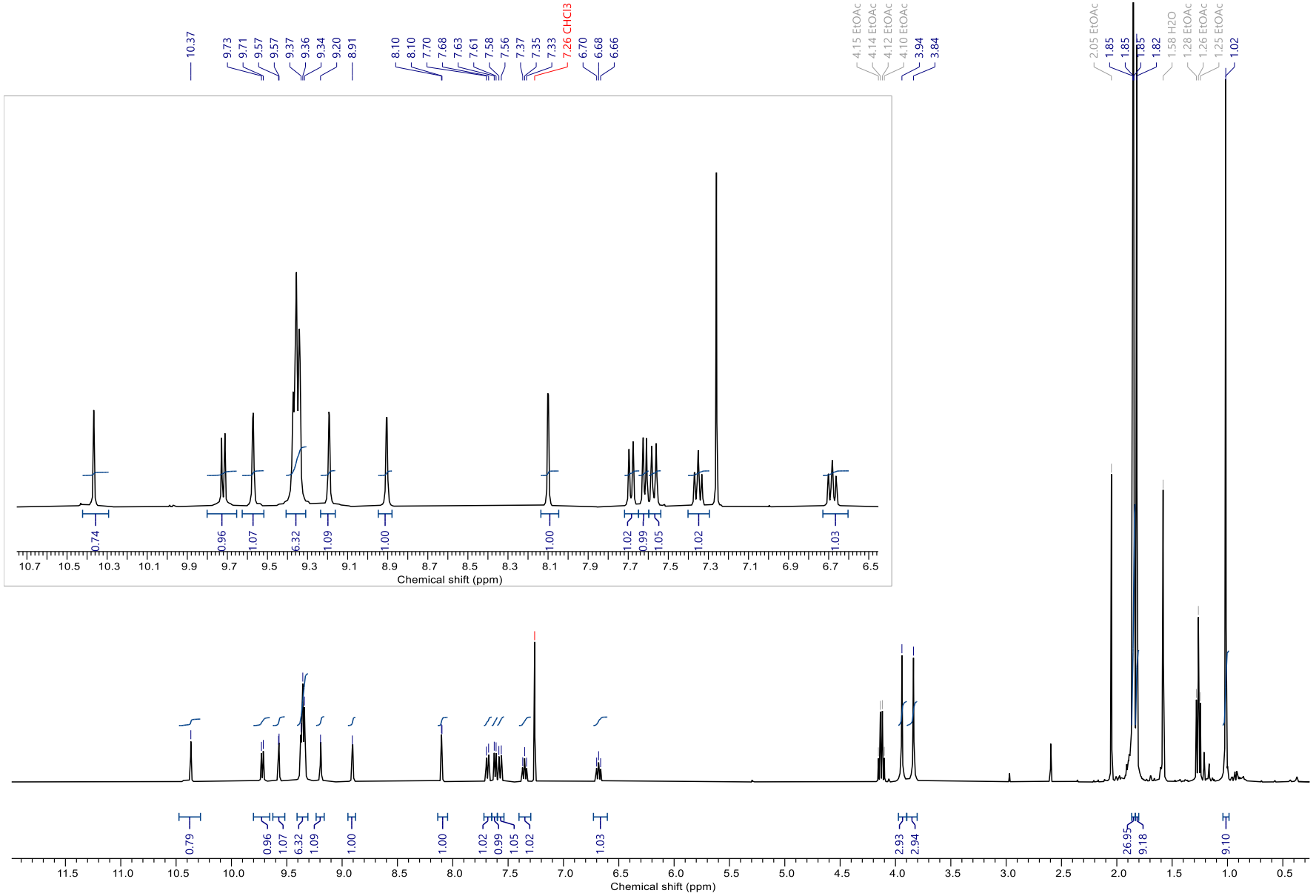

Figure S43. ^{1}H NMR spectrum of **8** (400 MHz, $CDCl_3$, 298 K).

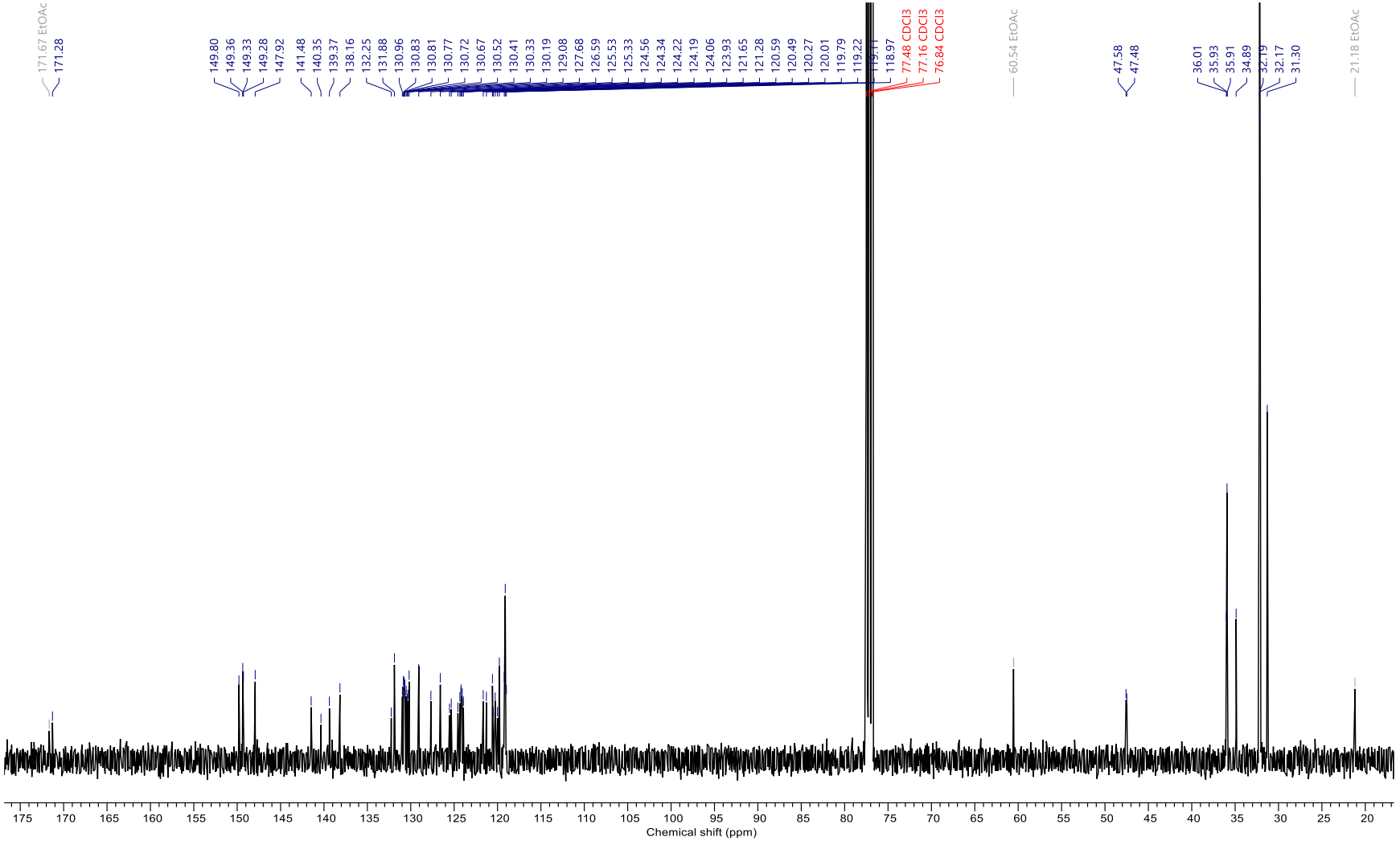

Figure S44. $^{13}C\{^{1}H\}$ NMR spectrum of **8** (101 MHz, $CDCl_3$, 298 K).

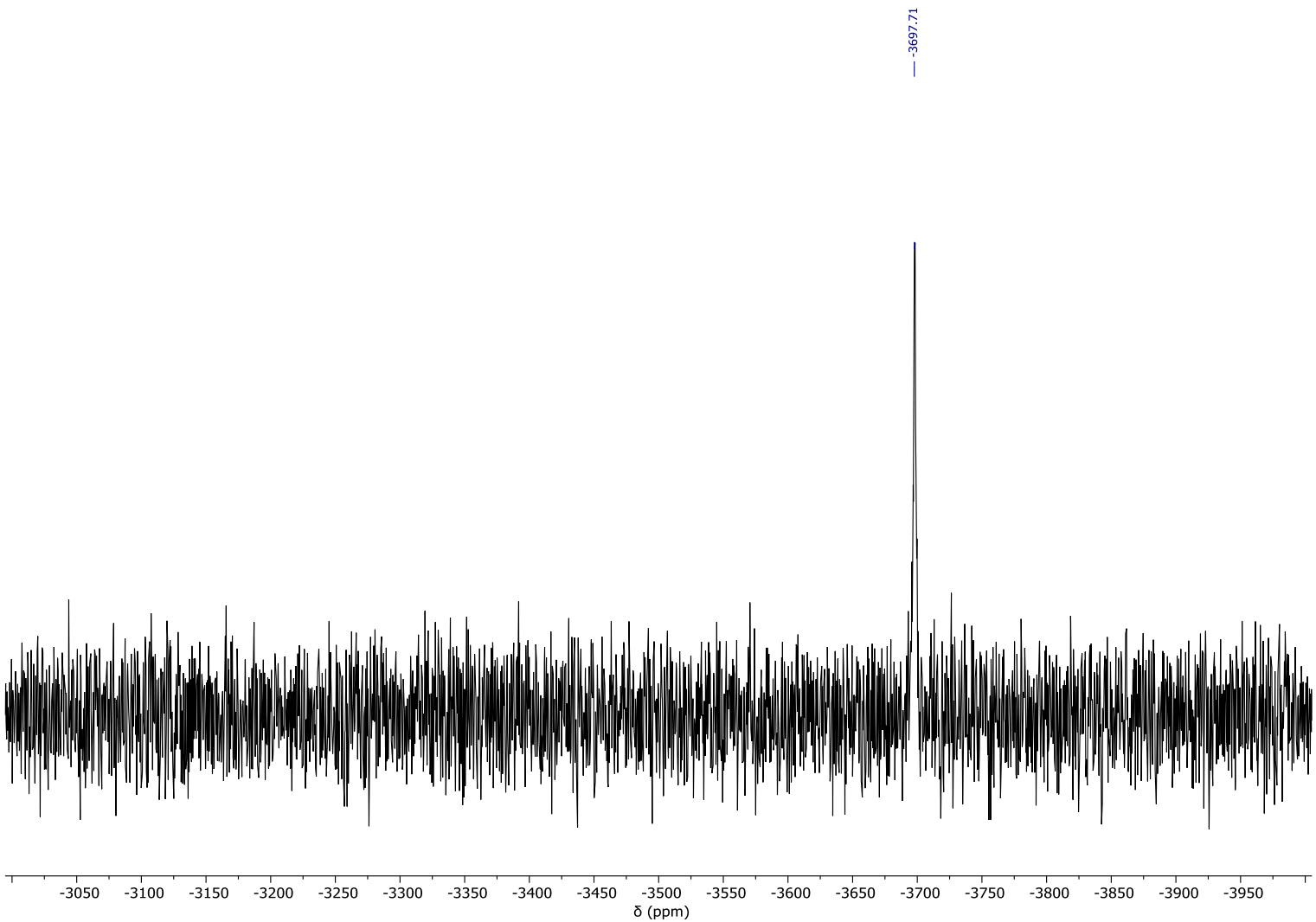

Figure S45. ^{195}Pt NMR spectrum of **8** (107 MHz, $CDCl_3$, 298 K).

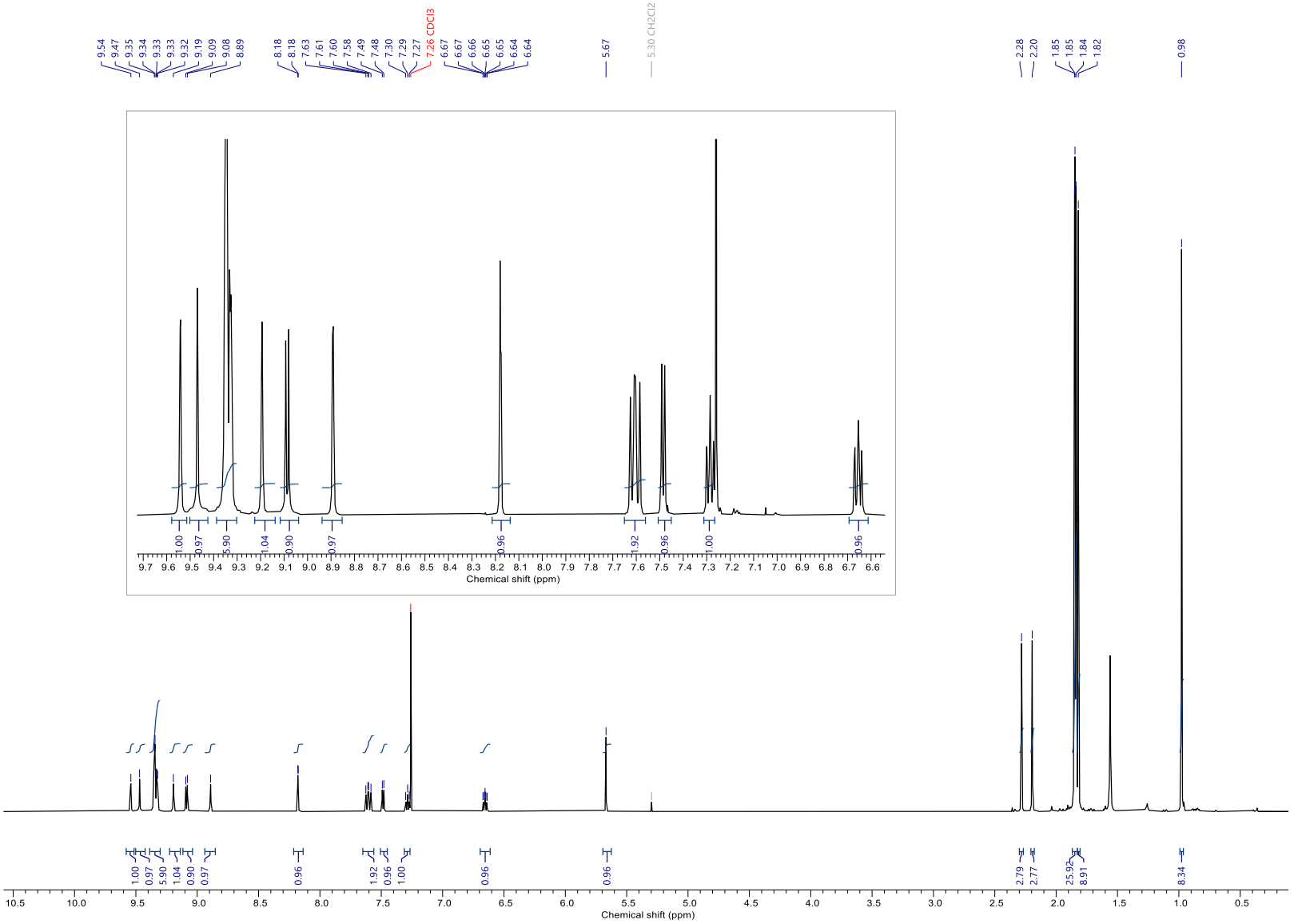

Figure S46. ^{1}H NMR spectrum of **NG1** (500 MHz, $CDCl_3$, 298 K).

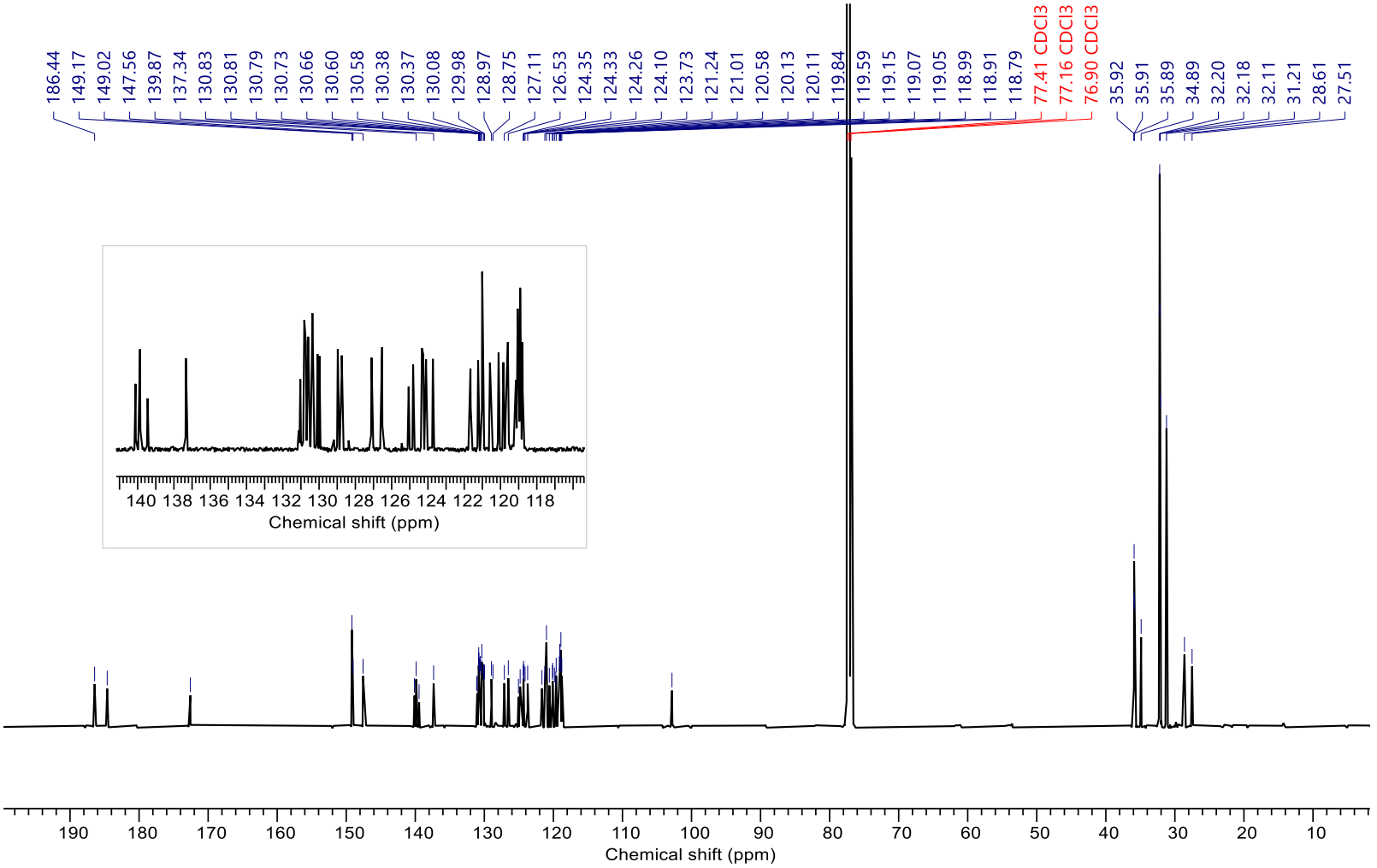

Figure S47. $^{13}C\{^{1}H\}$ NMR spectrum of **NG1** (126 MHz, $CDCl_3$, 298 K).

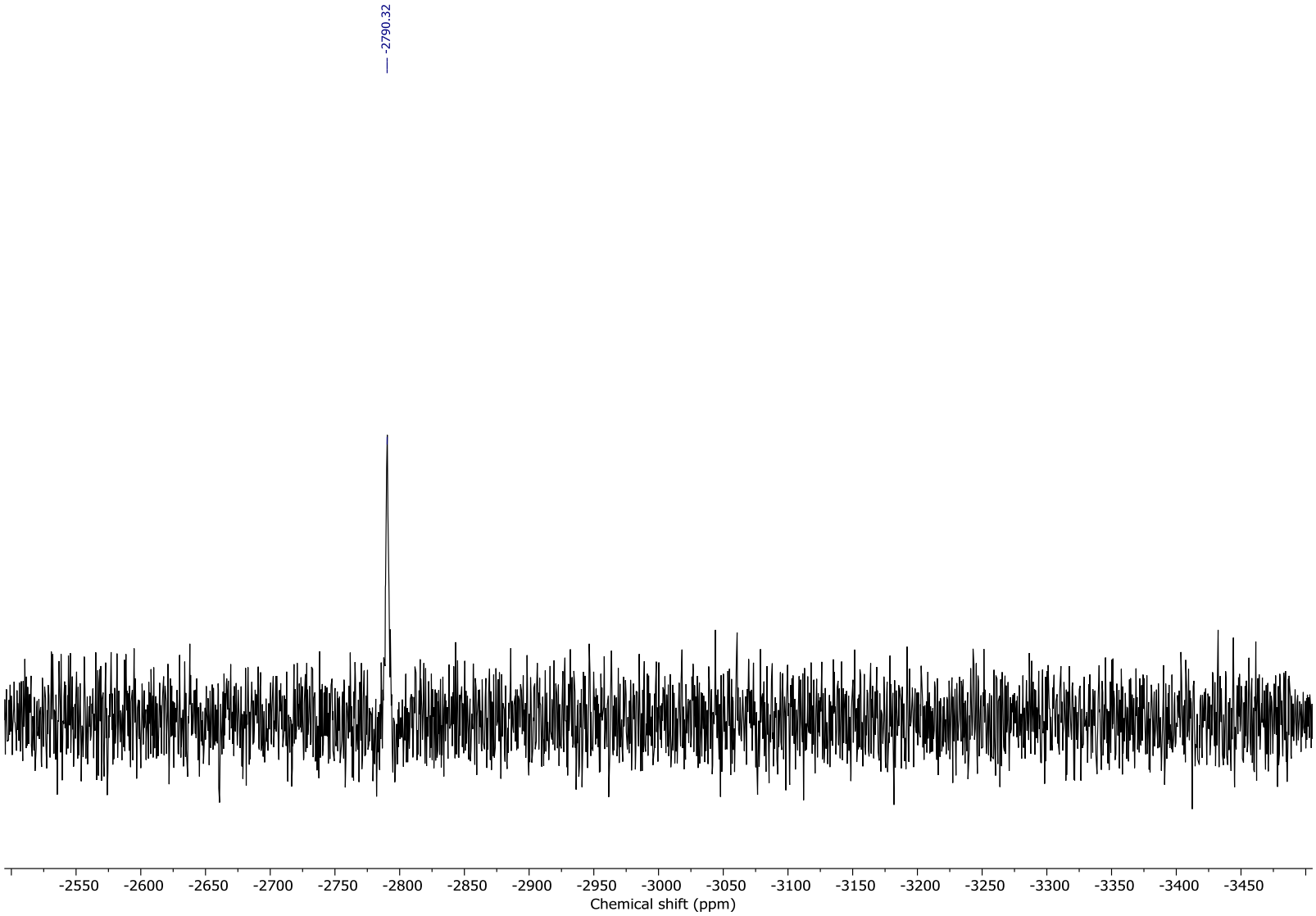

Figure S48. ^{195}Pt NMR spectrum of **NG1** (107 MHz, $CDCl_3$, 298 K).

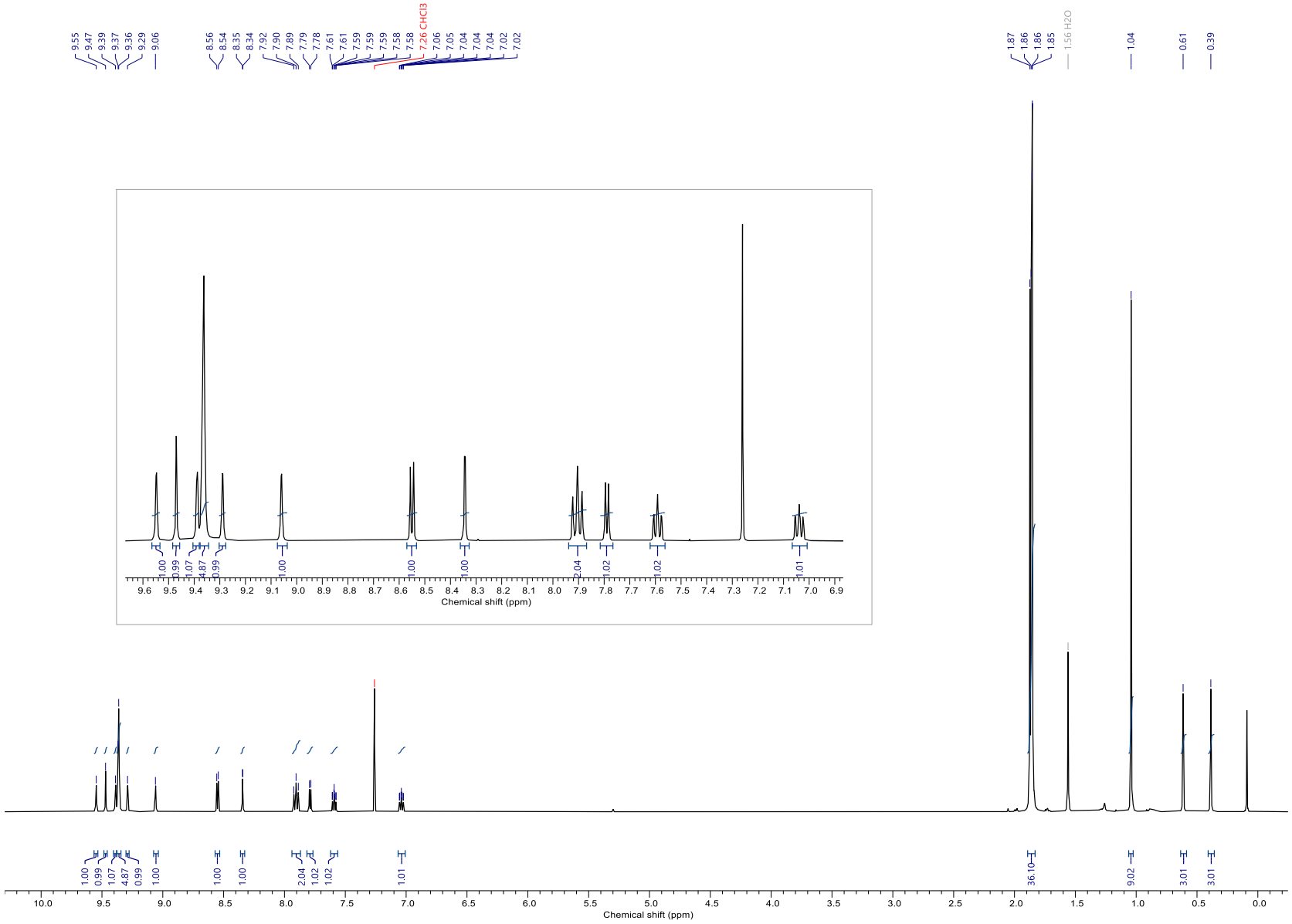

Figure S49. ^{1}H NMR spectrum of **NG2** (500 MHz, $CDCl_3$, 298 K).

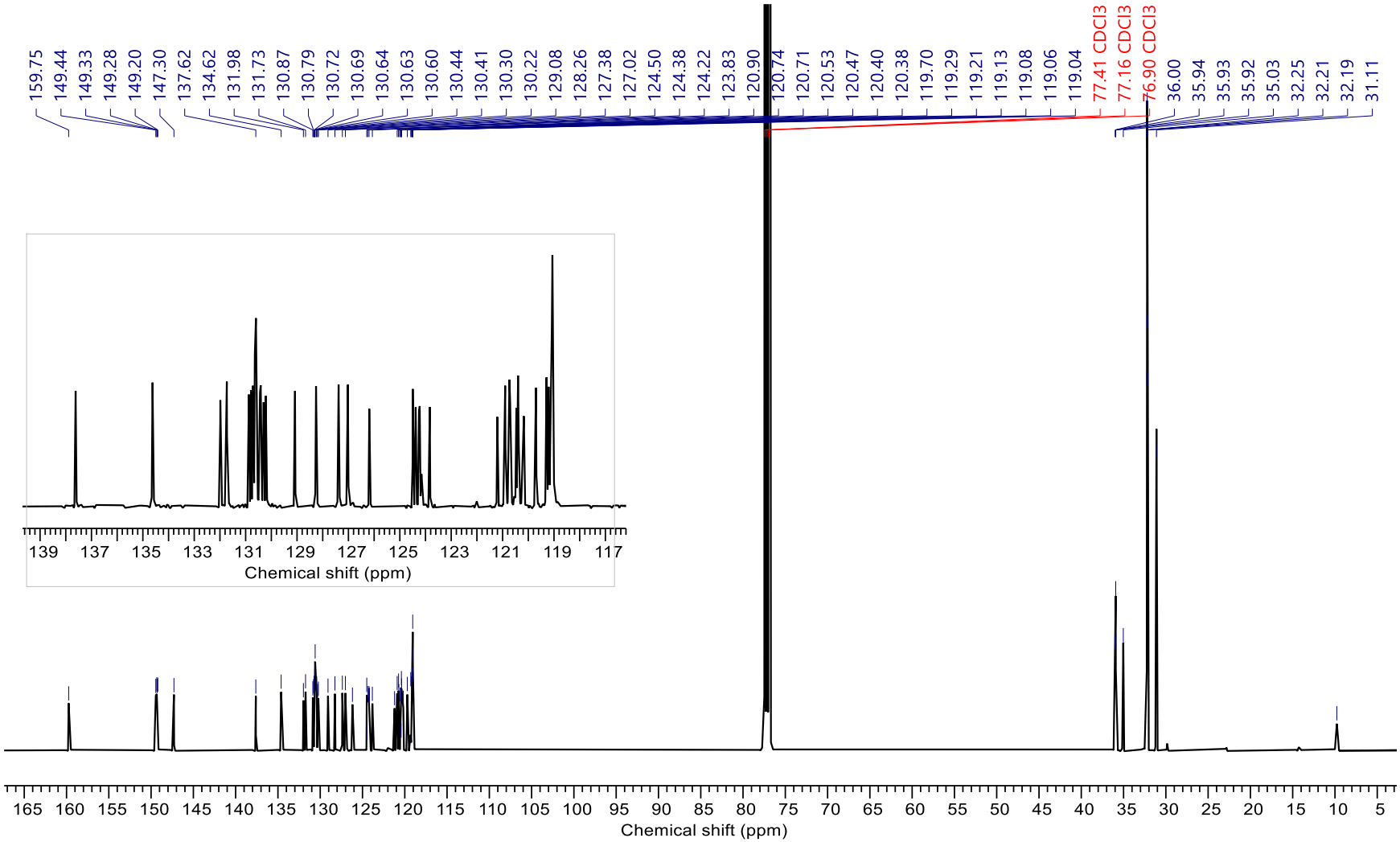

Figure S50. $^{13}C\{^{1}H\}$ NMR spectrum of **NG2** (126 MHz, $CDCl_3$, 298 K).

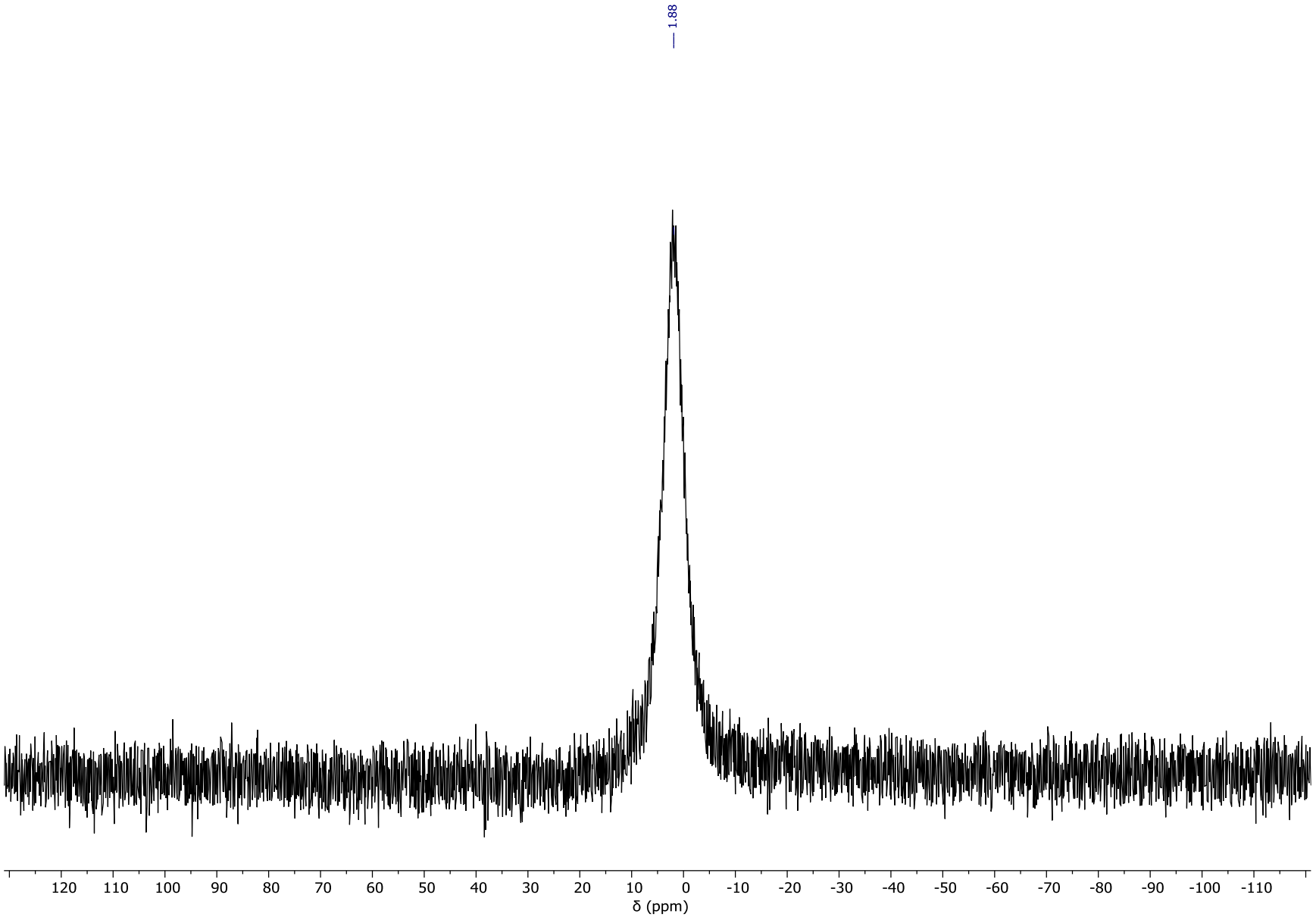

Figure S50. $^{11}B\{^{1}H\}$ NMR spectrum of **NG2** (193 MHz, $CDCl_3$, 300 K).

7. Chiral HPLC Analysis

7.1. Chiral separation of NG1

Analytical chiral HPLC separation for NG1

The sample was dissolved in dichloromethane, injected on Chiralpak IE column, eluted with heptane / dichloromethane (40/60) as mobile phase, and detected with an UV detector at 254 nm. The flow-rate was 1 mL/min.

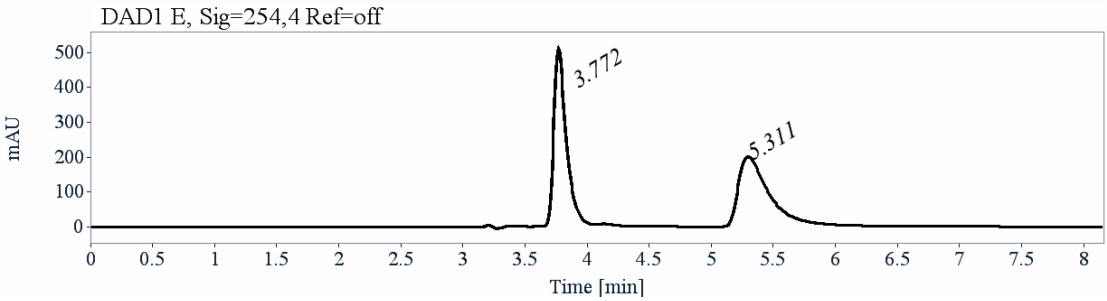

RT [min]	Enantio.	Area	Area%	Capacity Factor	Enantioselectivity	Resolution (USP)
3.77	*P*	3627	50.27	0.28	-	-
5.31	*M*	3588	49.73	0.80	2.87	5.16
Sum		7214	100.00	-	-	-

Preparative separation for NG1

• Sample preparation: About 37 mg of **NG1** are dissolved in 5 mL of a mixture of dichloromethane and hexane (40/60).
• Chromatographic conditions: Chiralpak IE (250 x 10 mm), hexane / dichloromethane (40/60) as mobile phase, flow-rate = 5 mL/min, UV detection at 300 nm.
• Injections (stacked): 20 times 250 μL, every 3 minutes.
• 18 mg of the first eluted enantiomer (*P*)-**NG1** with *ee* > 99%

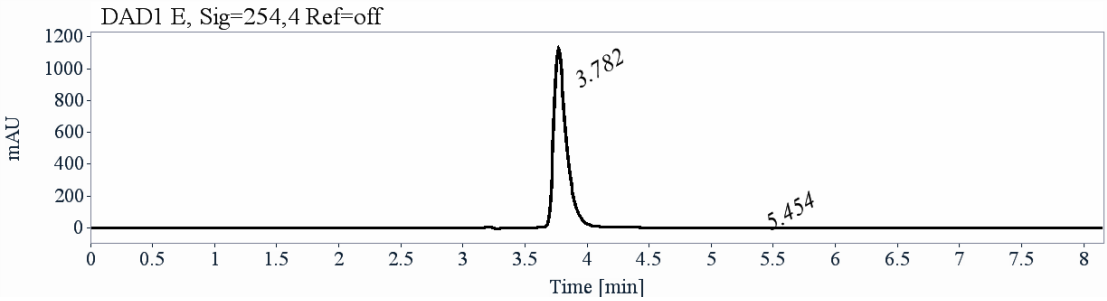

RT [min]	Enantio.	Area	Area%
3.78	*P*	8093	99.72
5.45	*M*	23	0.28
Sum		8116	100.00

• 18 mg of the second eluted enantiomer (*M*)-**NG1** with *ee* > 99%

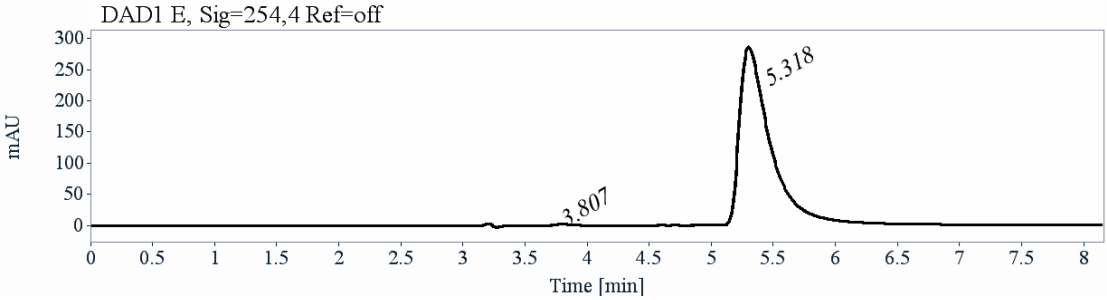

RT [min]	Enantio.	Area	Area%
3.81	*P*	19	0.38
5.32	*M*	5004	99.62
Sum		5023	100.00

7.2. Chiral separation of NG2

Analytical chiral HPLC separation for NG2

The sample was dissolved in dichloromethane, injected on Chiralpak IE column, eluted with heptane / dichloromethane (70/30) as mobile phase, and detected with an UV detector at 254 nm. The flow-rate was 1 mL/min.

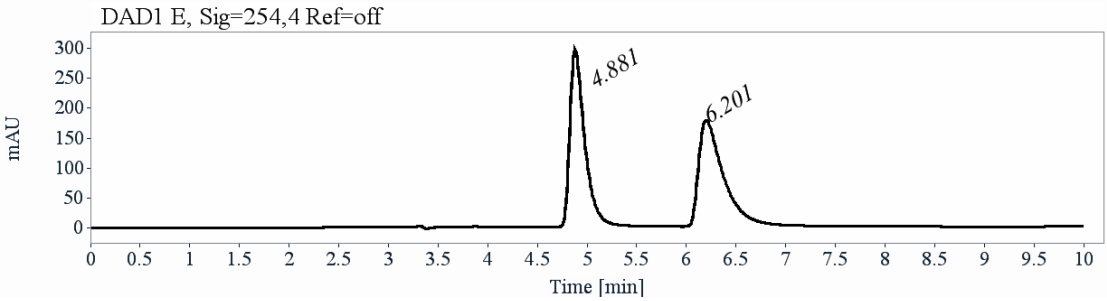

RT [min]	Enantio.	Area	Area%	Capacity Factor	Enantioselectivity	Resolution (USP)
4.88	*P*	3117	49.92	0.65	-	-
6.20	*M*	3127	50.08	1.10	1.68	3.85
Sum		6244	100.00	-	-	-

Preparative separation for NG2

• Sample preparation: About 44 mg of **NG2** are dissolved in 8 mL of a mixture of dichloromethane and hexane (50/50).
• Chromatographic conditions: Chiralpak IE (250 x 10 mm), hexane / dichloromethane (70/30) as mobile phase, flow-rate = 5 mL/min, UV detection at 300 nm.

• Injections (stacked): 40 times 200 μL, every 3.8 minutes.

• 20 mg of the first eluted enantiomer (*P*)-**NG2** with *ee* > 99%

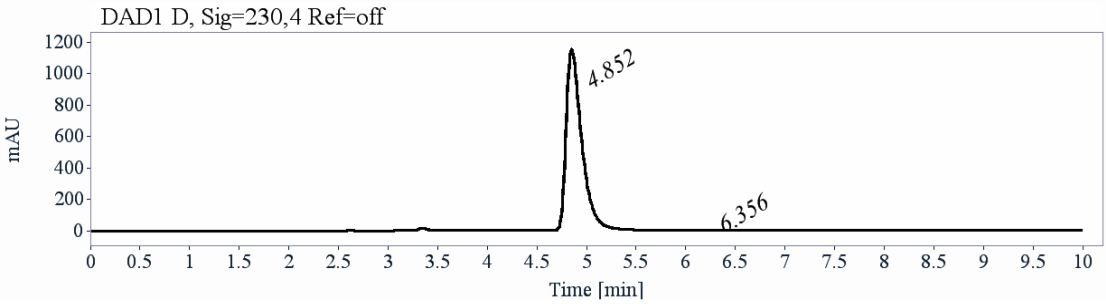

RT [min]	Enantio.	Area	Area%
4.85	*P*	12755	99.68
6.36	*M*	41	0.32
Sum		12796	100.00

• 20 mg of the second eluted enantiomer (*M*)-**NG2** with *ee* > 99%

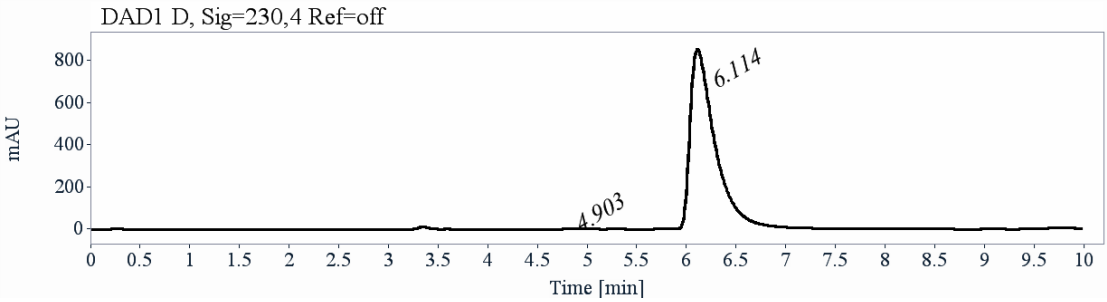

RT [min]	Enantio.	Area	Area%
4.90	*P*	36	0.24
6.11	*M*	14950	99.76
Sum		14986	100.00

7.3. Chiral separation of 8

Analytical chiral HPLC separation for 8

The sample was dissolved in a mixture of heptane, ethanol and dichloromethane, injected on Chiralpak IC column, eluted with heptane/ethanol/dichloromethane 85/5/10 as mobile phase, and detected with an UV detector at 230 nm. The flow-rate was 1 mL/min.

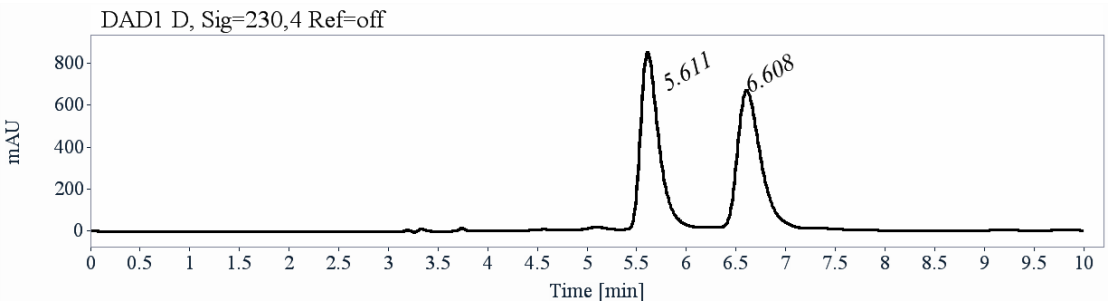

RT [min]	Enantio.	Area	Area%	Capacity Factor	Selectivity	Resolution (USP)
5.61	*M*	11089	49.36	0.90	-	-
6.61	*P*	11375	50.64	1.24	1.37	2.66
Sum		22464	100.00	-	-	-

Preparative separation for 8

• Sample preparation: About 39 mg of **8** are is dissolved in 4 mL of a mixture of hexane and dichloromethane (50/50).
• Chromatographic conditions: Chiralpak IC (250 x 10 mm), hexane / ethanol / dichloromethane 85/5/10 as mobile phase, flow-rate = 5 mL/min, UV detection at 254 nm.
• Injections (stacked): 135 times 30 μL, every 4.5 minutes.
• 16 mg of the first eluted enantiomer (*M*)-**8** with *ee* > 98%

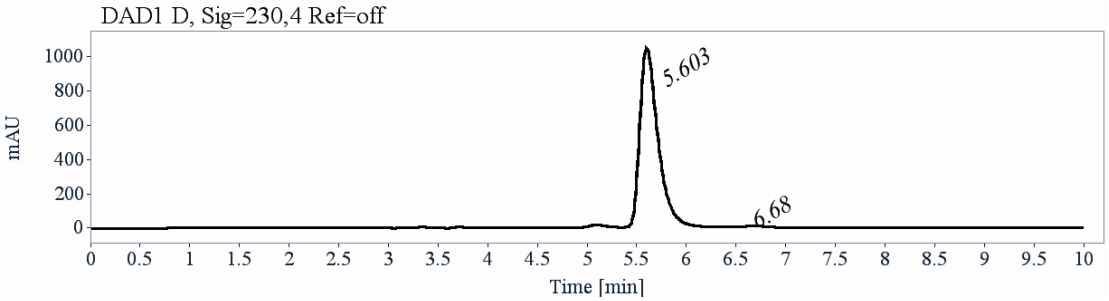

RT [min]	Enantio.	Area	Area%
5.60	*M*	13439	99.17
6.68	*P*	113	0.83
Sum		13552	100.00

• 16 mg of the second eluted enantiomer (*P*)-**8** with *ee* > 97%

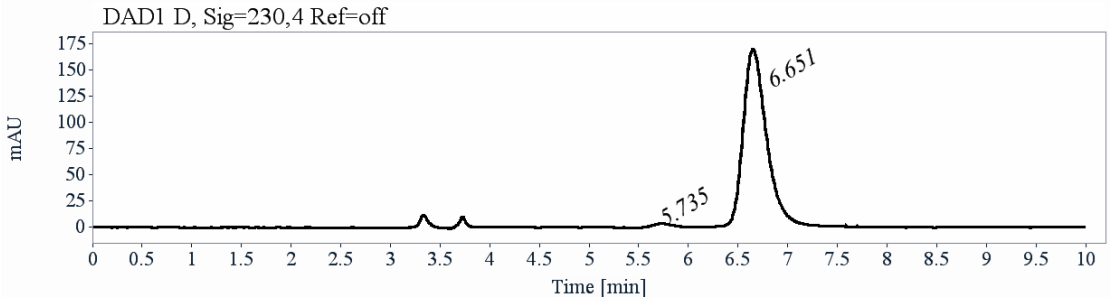

RT [min]	Enantio.	Area	Area%
5.73	*M*	43	1.46
6.65	*P*	2882	98.54
Sum		2924	100.00

8. References

1. N. Saleh, C. Shen and J. Crassous, *Chem. Sci.*, 2014, **5**, 3680–3694.
2. L. Norel, M. Rudolph, N. Vanthuyne, J. A. G. Williams, C. Lescop, C. Roussel, J. Autschbach, J. Crassous and R. Réau, *Angew. Chem. Int. Ed.*, 2010, **49**, 99–102.
3. Z.-P. Yan, X.-F. Luo, W.-Q. Liu, Z.-G. Wu, X. Liang, K. Liao, Y. Wang, Y.-X. Zheng, L. Zhou, J.-L. Zuo, Y. Pan and H. Zhang, *Chem. Eur. J.*, 2019, **25**, 5672–5676.
4. P. Vázquez-Domínguez, M. Horojat, E. Suits, F. J. F. de Córdova, N. Vanthuyne, D. Jacquemin, A. Ros and L. Favereau, *Mater. Chem. Front.*, 2024, **8**, 3799–3806.
5. T. Biet, T. Cauchy, Q. Sun, J. Ding, A. Hauser, P. Oulevey, T. Bürgi, D. Jacquemin, N. Vanthuyne, J. Crassous and N. Avarvari, *Chem. Commun.*, 2017, **53**, 9210–9213.
6. G. Fu, Y. He, W. Li, B. Wang, X. Lü, H. He and W.-Y. Wong, *J. Mater. Chem. C*, 2019, **7**, 13743–13747.
7. A. F. Palermo, B. S. Y. Chiu, P. Patel and S. A. L. Rousseaux, *J. Am. Chem. Soc.*, 2023, **145**, 24981–24989.
8. R. Nagpal, S. Arora, P. Ponnan, Kharu-Nisa, A. Dandia and S. M. Singh Chauhan, *ChemistrySelect*, 2019, **4**, 8444–8449.
9. F. Neese, *Wiley Interdiscip. Rev.: Comput. Mol. Sci.*, 2012, **2**, 73–78.
10. F. Neese, *Wiley Interdiscip. Rev.: Comput. Mol. Sci.*, 2025, **15**, e70019.
11. E. Caldeweyher, S. Ehlert, A. Hansen, H. Neugebauer, S. Spicher, C. Bannwarth and S. Grimme, *J. Chem. Phys.*, 2019, **150**, 154122.
12. V. Barone and M. Cossi, *J. Phys. Chem. A*, 1998, **102**, 1995–2001.
13. M. Garcia-Rates and F. Neese, *J. Comput. Chem.*, 2020, 41, 922–939.
14. A. D. Becke, *J. Chem. Phys.*, 1993, **98**, 5648–5652.
15. C. Lee, W. Yang and R. G. Parr, *Phys. Rev. B Condens. Matter.*, 1988, **37**, 785–789.
16. P. J. Stephens, F. J. Devlin, C. F. Chabalowski and M. J. Frisch, *J. Phys. Chem.*, 1994, **98**, 11623–11627.
17. A. Schäfer, C. Huber and R. Ahlrichs, *J. Chem. Phys.*, 1994, **100**, 5829–5835.
18. K. Eichkorn, F. Weigend, O. Treutler and R. Ahlrichs, *Theor. Chem. Acta.*, 1997, **97**, 119–124.
19. F. Weigend and R. Ahlrichs, *Phys. Chem. Chem. Phys.*, 2005, **7**, 3297–3305.
20. D. Andrae, U. Häußermann, M. Dolg, H. Stoll and H. Preuß, *Theoret. Chim. Acta*, 1990, **77**, 123–141.
21. M. Srebro-Hooper, J. Crassous and J. Autschbach, in *Helicenes: Synthesis, Properties and Applications*, John Wiley & Sons, Ltd, 2022, pp. 395–421.
22. M. Srebro-Hooper and J. Autschbach, *Annu. Rev. Phys. Chem.*, 2017, **68**, 399–420.
23. J. Autschbach, *Chirality*, 2009, **21**, E116–E152.
24. Gaussian 16, Revision C.01, Frisch, M. J.; Trucks, G. W.; Schlegel, H. B.; Scuseria, G. E.; Robb, M. A.; Cheeseman, J. R.; Scalmani, G.; Barone, V.; Petersson, G. A.; Nakatsuji, H.; Li, X.; Caricato, M.; Marenich, A. V.; Bloino, J.; Janesko, B. G.; Gomperts, R.; Mennucci, B.; Hratchian, H. P.; Ortiz, J. V.; Izmaylov, A. F.; Sonnenberg, J. L.; Williams-Young, D.; Ding, F.; Lipparini, F.; Egidi, F.; Goings, J.; Peng, B.; Petrone, A.; Henderson, T.; Ranasinghe, D.; Zakrzewski, V. G.; Gao, J.; Rega, N.; Zheng, G.; Liang, W.; Hada, M.; Ehara, M.; Toyota, K.; Fukuda, R.; Hasegawa, J.; Ishida, M.; Nakajima, T.; Honda, Y.; Kitao, O.; Nakai, H.; Vreven, T.; Throssell, K.; Montgomery, J. A., Jr.; Peralta, J. E.; Ogliaro, F.; Bearpark, M. J.; Heyd, J. J.; Brothers, E. N.; Kudin, K. N.; Staroverov, V. N.; Keith, T. A.; Kobayashi, R.; Normand, J.; Raghavachari, K.; Rendell, A. P.; Burant, J. C.; Iyengar, S. S.; Tomasi, J.; Cossi, M.; Millam, J. M.; Klene, M.; Adamo, C.; Cammi, R.; Ochterski, J. W.; Martin, R. L.; Morokuma, K.; Farkas, O.; Foresman, J. B.; Fox, D. J. Gaussian, Inc., Wallingford CT, 2016.
25. C. Adamo and V. Barone, *J. Chem. Phys.*, 1999, **110**, 6158–6170.
26. M. Ernzerhof and G. E. Scuseria, *J. Chem. Phys.*, 1999, **110**, 5029–5036.

27. M. Cossi, V. Barone, R. Cammi and J. Tomasi, *Chem. Phys. Lett.*, 1996, **255**, 327–335.
28. M. Cossi and V. Barone, *J. Chem. Phys.*, 2001, **115**, 4708–4717.
29. J. Autschbach, T. Ziegler, S. J. A. van Gisbergen and E. J. Baerends, *J. Chem. Phys.*, 2002, **116**, 6930–6940.
30. I. Tamm, *J. Phys. (USSR)*, 1945, **9**, 449.
31. S. M. Dancoff, *Phys. Rev.*, 1950, **78**, 382–385.
32. S. Hirata and M. Head-Gordon, *Chem. Phys. Lett.*, 1999, **314**, 291–299.
33. M. J. G. Peach, M. J. Williamson and D. J. Tozer, *J. Chem. Theory. Comput.*, 2011, **7**, 3578–3585.
34. M. J. G. Peach and D. J. Tozer, *J. Phys. Chem. A*, 2012, **116**, 9783–9789.
35. M. Peach, D. J. Tozer and N. Warner, *Mol. Phys.*, 2013, **111**, 1271–1274.
36. G. Scalmani, M. J. Frisch, B. Mennucci, J. Tomasi, R. Cammi and V. Barone, *J. Chem. Phys.*, 2006, **124**, 94107.
37. R. Cammi, B. Mennucci and J. Tomasi, *J. Phys. Chem. A*, 2000, **104**, 5631–5637.
38. G. te Velde, F. M. Bickelhaupt, E. J. Baerends, C. Fonseca Guerra, S. J. A. van Gisbergen, J. G. Snijders and T. Ziegler, *J. Comput. Chem.*, 2001, **22**, 931–967.
39. ADF 2025.1, SCM, Theoretical Chemistry, Vrije Universiteit, Amsterdam, The Netherlands, http://www.scm.com.
40. H. D. Ludowieg, M. Srebro-Hooper, J. Crassous and J. Autschbach, *ChemistryOpen*, 2022, **11**, e202200020.
41. E. Van Lenthe and E. J. Baerends, *Journal of Computational Chemistry*, 2003, **24**, 1142–1156.
42. C. C. Pye and T. Ziegler, *Theor. Chem. Acc.*, 1999, **101**, 396–408.
43. E. van Lenthe, E. J. Baerends and J. G. Snijders, *J. Chem. Phys.*, 1993, **99**, 4597–4610.
44. E. van Lenthe, E. J. Baerends and J. G. Snijders, *J. Chem. Phys.*, 1994, **101**, 9783–9792.
45. A. Rosa, E. J. Baerends, S. J. A. van Gisbergen, E. van Lenthe, J. A. Groeneveld and J. G. Snijders, *J. Am. Chem. Soc.*, 1999, **121**, 10356.
46. F. Wang, T. Ziegler, E. van Lenthe, S. van Gisbergen and E. J. Baerends, *J. Chem. Phys.*, 2005, **122**, 204103.
47. M. Sterzel and J. Autschbach, *Inorg. Chem.*, 2006, **45**, 3316–3324.
48. F. Gendron, B. Moore II, O. Cador, F. Pointillart, J. Autschbach and B. Le Guennic, *J. Chem. Theory Comput.*, 2019, **15**, 4140–4155.
49. Z. Chen, C. S. Wannere, C. Corminboeuf, R. Puchta and P. von R. Schleyer, *Chem. Rev.*, 2005, **105**, 3842–3888.
50. R. Gershoni-Poranne and A. Stanger, in *Aromaticity*, Elsevier, 2021, pp. 99–154.
51. D. Geuenich, K. Hess, F. Köhler and R. Herges, *Chem. Rev.*, 2005, **105**, 3758–3772.
52. R. Herges and D. Geuenich, *J. Phys. Chem. A*, 2001, **105**, 3214–3220.
53. I. Cernusak, P. W. Fowler and E. Steiner, *Mol. Phys.*, 2000, **98**, 945–953.
54. E. Steiner, P. W. Fowler and L. W. Jenneskens, *Angew. Chem.Int. Ed.*, 2001, **40**, 362–366.
55. H. Fallah-Bagher-Shaidaei, C. S. Wannere, C. Corminboeuf, R. Puchta and P. v. R. Schleyer, *Org. Lett.*, 2006, **8**, 863–866.
56. J. Stanojkovic, R. William, Z. Zhang, I. Fernández, J. Zhou, R. D. Webster and M. C. Stuparu, *Nat. Commun.*, 2023, **14**, 803.
57. H. Liu, J. Guo, T. Che, C. Ding, B. Xu and Q. Tan, *Angew. Chem. Int. Ed.*, 2025, **64**, e202506862.
58. Z.-L. Qiu, X.-W. Chen, Y.-D. Huang, R.-J. Wei, K.-S. Chu, X.-J. Zhao and Y.-Z. Tan, *Angew. Chem. Int. Ed.*, 2022, **61**, e202116955.
59. G. M. Sheldrick, *Acta Cryst. A*, 2015, **71**, 3–8.
60. G. M. Sheldrick, *Acta Cryst. C*, 2015, **71**, 3–8.
61. P. van der Sluis and A. L. Spek, *Acta Cryst. A*, 1990, **46**, 194–201.
62. A. L. Spek, *J. Appl. Cryst.*, 2003, **36**, 7–13.